YENİ FLORESAN PROBLARIN dsDNA İLE BAĞLANMA MEKANİZMALARI: SPEKTRAL LUMİNESANS YÖNTEMLERİ İLE ÇALIŞMALAR

THE MECHANISMS of NOVEL FLUORESCENT PROBES BINDING WITH dsDNA: STUDIES BY SPECTRAL-LUMINESCENT METHODS

NURİYE AKBAY

Submitted to Institute of Sciences of Hacettepe University

as a partial fulfillment to therequirements for the award of the degree of

DOCTOR OF PHILOSOPHY

in CHEMISTRY

2009

To institute for Graduate studies in Pure & Applied Sciences,

This study has been accepted as a THESIS OF DOCTOR OF PHILOSOPHY in CHEMISTRY DEPARTMENT by our examining committee.

Head ....

Prof. Dr. Sema BEKTAŞ

Advisor ....

Prof. Dr. Elmas GÖKOĞLU

Member ....

Prof. Dr. Kadir PEKMEZ

Member ....

Prof. Dr. Menemşe GÜMÜŞDERELİOĞLU

Member ....

Asst. Prof. Zeynel SEFEROĞLU

APPROVEMENT

This thesis has been accepted on 16 / 09 / 2009 by the above mentioned examining committee members through the Boards of Directors of the Institute for Graduate Studies in Pure and Applied Sciences.

.../.../2009

Prof. Dr. Erdem YAZGAN

Director of Graduates School of
Natural and Applied Sciences

THE MECHANISMS of NOVEL FLUORESCENT PROBES BINDING WITH dsDNA: STUDIES BY SPECTRAL-LUMINESCENT METHODS

Nuriye Akbay

ABSTRACT

Fluorescence spectroscopy is one of the most widely used spectroscopic techniques in the fields of gene expression, clinical chemistry, biochemistry and molecular biophysics today. The technique has become quite popular because of its acute sensitivity to changes in the structural and dynamic properties of biomolecules and biomolecular complexes. Fluorescent probes constitute an important field in fluorescence spectroscopy. In this thesis, interaction of two group fluorescent dyes with double stranded DNA (dsDNA) was investigated using fluorescence sensing and UV-visible absorption spectra.

In the first part studies of the interaction mode of monomer and two homodimer benzothiazole styryl dyes containing spermine-like linkage/tail group with the dsDNA are reported. For these dyes, equilibrium constant of dye binding to DNA (K_b), as well as the number of dsDNA base pairs occupied by one bound dye molecule (n) were determined. The data obtained show that the presence of spermine-like group containing quaternary nitrogen (Bos-5) results in increase of K_b value as compared to this of unsubstituted analogue (Sbt). Besides, for the dimer dyes containing benzothiazole styryl chromophores, the K_b value is either five times higher (DBos-13) or almost the same (DBsu-10) as compared to this of corresponding monomer Sbt, depending on the position in the benzothiazole ring where the linker is attached. Moreover, the n values for both dimers are significantly different as well, pointing to the bis-intercalative binding mechanism for DBos-13 and for the groovebinding one for DBsu-10.

In second part of the studies, we reported the syntheses and investigation of the modes of binding to dsDNA of the four ethidium derivatives (coded as *E2, E3, E4* and E5) and also effects of functional groups substitueted both amines at 3- and 8-positions on binding mechanisms. The Stern-Volmer quenching constants, binding constants, binding sites and the corresponding thermodynamic parameters ΔH, ΔS and ΔG were calculated at different temperatures. The results indicated the formation of *E2, E3, E4* and *E5*-DNA complexes and van der Waals interactions are the predominant intermolecular forces for *E2* and *E3* complexes and hydrophobic associations are the predominant for *E4* and *E5* complexes. The results of absorption, ionic strength and iodide ion quenching suggested that the interaction mode of E2 and *E3* with *ct*-DNA was intercalative binding like parent dye ethidium bromide. On the contrary *E4* and *E5* set out groove binding. The limit of detection (LOD) of *ct*-DNA were 7.49×10^{-8} (n=4), 4.18×10^{-8} M (n=7), 2.87×10^{-5} (n=5) and 7.23×10^{-6} M (n=6) in presence of *E2*, *E3*, *E4* and *E5* respectively.

Keywords: Styrylcyanine dyes, ethidium bromide, dsDNA, fluorescence quenching, *Stern-Volmer* equation, intercalation, groove binding.

YENİ FLORESAN PROBLARIN dsDNA İLE BAĞLANMA MEKANİZMALARI: SPEKTRAL LUMİNESANS YÖNTEMLERİ İLE ÇALIŞMALAR

Nuriye Akbay

ÖZ

Floresans spektroskopisi günümüzde genetik incelemeler, klinik kimya, biyokimya ve moleküler biyofizikte en fazla kullanılan spektroskopik yöntemlerden bir tanesidir. Biyomoleküllerin ve biyomoleküler komplekslerin gerek yapısal gerekse dinamik özelliklerindeki değişikliklere olan hızlı duyarlılığı nedeni ile bu tekniğin popüleritesi hızla artmaktadır. Floresant problar floresans spektroskopisinde önemli bir alanı işgal eder. Bu çalışmada iki boya grubunun çift sarmal DNA (dsDNA) ile etkileşimleri floresans izleme ve UV-görünür bölge absoprsiyon spektroskopisi ile incelendi.

Çalışmanın birinci bölümünde pozitif yüklü kuaterner amonyum grubu köprü/uç gruplar içeren monomer ve iki homodimer benzotiyazol stiril siyanin boyasının dsDNA ile etkileşim türü incelendi. Bu boyalar için bağlı bir boya molekülü tarafından kullanılan dsDNA baz çifti sayısı (n) yanısıra boyaların DNA ile bağlanma sabitleri (K_b) de bulundu. Elde edilen sonuçlar yapıda kuaterner azot içeren spermin-like grupların (Bos-5) bulunmasının fonksiyonel grup içermeyen analoglara (Sbt) göre Kb değerlerinde artışa neden olduğunu gösterdi. Bunun yanısıra benzotiyazol stiril kromoforları içeren dimer boyaların K_b değerlerinin çıkış monomeri ile karşılaştırıldığında bu monomerin K_b değerinin köprünün benzotiyazol halkasına bağlanma noktasına bağlı olarak beş katı (Dbos-13) veya hemen hemen aynısı (Dbsu-10) olduğu gözlendi. Buna ek olarak iki dimer için n değerleri Dbos-13 için bis-interkelasyonu işaret eden DBsu-10 için ise oluğa bağlanmayı işaret eden oldukça farklı sonuçlar verdi.

Çalışmanın ikinci bölümünde dört etidiyum türevinin (*E2, E3, E4* ve *E5* olarak kodlandı) sentezi, dsDNA ile bağlanma türleri ve aynı zamanda 3- ve 8- amino pozisyonlarındaki fonksiyonel grupların bağlanma mekanizmalarına etkileri incelendi. Stern-Volmer sönüm sabitleri, bağlanma sabitleri, bağlanma kısım sayıları ve ΔH, ΔS ve ΔG gibi ilgili termodinamik parametreler çeşitli sıcaklıklarda hesaplandı. Sonuçlar *E2, E3, E4* ve *E5*-DNA komplekslerinin oluştuğunu ve *E2* ile E3 kompleksleri için etkileşimin van der Waals kuvvetleri tarafından, *E4* ile *E5* komplekslerinde ise hidrofobik birleşmelerin baskın tür olduğunu gösterdi. Absorpsiyon, iyonik şiddet ve iyodür iyonu ile sönüm çalışmalarından elde edilen sonuçlar *E2* ve *E3*'ün dsDNA ile çıkış boyası etidiyum bromür gibi interkelasyon üzerinden bağlandığını gösterdi. Buna karşılık *E4* ve *E5* groove bağlanma gösterdi. dsDNA için gözlenebilirlik sınırı *E2*, *E3*, *E4* ve *E5* varlığında sırası ile 7.49×10^{-8} (n=4), 4.18×10^{-8} M (n=7), 2.87×10^{-5} (n=5) ve 7.23×10^{-6} M (n=6) olarak bulundu.

Anahtar kelimeler: Stiril siyanin boyaları, etidiyum bromür, dsDNA, floresans sönümü, *Stern-Volmer* eşitliği, interkelasyon, oluğa bağlanma.

ACKNOWLEDGEMENTS

First, I wish to express my deep appreciations to my thesis advisor, Prof.Dr. Elmas Gökoğlu, for her contribution to my educational and inner life. Heartfelt thanks to her for opening the door of sharing her scientific and mental experiences.

Mykhaylo Losytskyy deserves my special thank in my scientific life. His invaluable suggestions and limitless helpfulness opened a new door in my mind.

And also, I want to present my thanks to Asst. Prof. Zeynel Seferoğlu for his help during my studies.

I am indebted to my dear family, I am filled with gratefulness to them. Their corporality is not with me but we are always together in our minds. It is perfect feeling that to know somebody behinds you. To have this kind of mother and father is a pleasure, they provide a good balance of love and freedom to explore the avenues I desire by serving the constant help and encouragement. My sisters Dilek Akbay Gürer, Ebru Akbay and my brother Bekir Akbay, you shared my happiness to make it larger and my sadness to disappear it all the time.

Some people have special places in our hearts; Serpil Özkara Yavuz, İpek Özkan and Feyza Kalafat are three of them for me. You have registered places in my heart.

And also I want to present my thanks to my friends Yasemin Alfatlı, Ayşe Uzgören and Burcu Olanca for their friendship and full support during my studies.

This thesis was supported by The Scientific and Technological Research Council of Turkey (grant# 107T391) and Hacettepe University Scientific Research Unit (grant#07T06604001).

CONTENTS

LIST OF FIGURES

LIST OF TABLES

ABBREVIATIONS

EB	Ethidium bromide (*3,8-diamino-5-ethyl-6-phenylphenantridinium bromide*)
E2	3,8-Dibenzoylamino-5-ethyl-6-phenylphenantridinium chloride
E3	3,8-Diphenylacetylamino-5-ethyl-6-phenylphenantridinium chloride
E4	3,8-Diethylcarbamate-5-ethyl-6-phenylphenantridinium bromide
E5	3,8-Dimethylcarbamate-5-ethyl-6-phenylphenantridinium chloride
DNA	Deoxyribonucleic acid
BSA	Bovine serum albumin
HSA	Human serum albumin
Poly $(dA\text{-}dT)_2$	Poly(deoxyadenylic-thymidylic) acid sodium salt
Poly $(dG\text{-}dC)_2$	Poly(deoxyguanylic-deoxycytidylic) acid sodium salt

1. INTRODUCTION

The interaction studies between fluorescent dyes and DNA are significant for the design of new probes and the quantitative detection of nucleic acids. Many fluorescence assays have been reported for DNA measurement by using of fluorescent dyes, metal ions and metal complexes that exhibit fluorescence quenching or enhancement in the presence of DNA. The possible interaction models between these small molecules and DNA generally include the electrostatic or surface, the groove and the intercalative binding.

The styrylcyanines are among the fluorescent dyes widely used for biomolecules detection. Due to the ability of styrylcyanines to interact with DNA with up to hundred times fluorescent enhancement and ability to penetrate into the cell these dyes were proposed for intra cellular DNA imaging. Ethidium bromide (EB) is used as major intercalation agent for DNA in many years. It has been widely utilized in biochemical and biophysical applications as a fluorescent stain. In literature, novel ethidium derivatives have been proposed as DNA probes and compared their DNA affinity and toxicity with EB. They have been synthesized via amines at 3- and 8-positions or 6-position of phenyl ring. 5-substitued ethidium derivatives have also been synthesized recently.

In this thesis, the clarification of the interaction modes of benzothiazole styrylcyanine monomer and two various structure homodimers modified with spermine-like linkage/tail group and four new synthesized ethidium derivatives with the DNA are aimed. In first group study, the investigations of benzothiazole styrylcyanines-DNA complexes were based on fluorescence enhancement method. Calculation of the binding constants and the numbers of DNA base pairs occupied by one bound dye molecule were calculated from fluorescent titration curves. In second part, the interactions of DNA with ethidium derivatives were studied by fluorescence quenching method. The probable fluorescence quenching mechanisms of the derivatives by DNA were studied by means of Stern-Volmer modeling. The binding properties of DNA-dye complexes were investigated based UV–visible absorption spectra, ionic strength, iodide ion quenching and thermodynamic parameters.

2. GENERAL INFORMATION

Luminescence is the emission of light by a substance. It occurs when an electron returns to the electronic ground state from an excited state and loses its excess energy as a photon. Luminescence spectroscopy is a collective name given to *three* related spectroscopic techniques. They are fluorescence, phosphorescence and chemiluminescence.

Fluorescence and phosphorescence are alike in that excitation is brought about by absorption of photons. As a consequence, the two phenomena are often referred to by the more general term *photoluminescence.* The third type of luminescence, chemiluminescence occurs when a chemical reaction produces an electronically excited species which emits a photon in order to reach the ground state. One of the most attractive features of luminescence methods is their inherent sensitivity, large linear concentration ranges, with detection limits that are often one to three orders of magnitude lower than those encountered in absorption spectroscopy. Measurement of the intensity of photoluminescence or chemiluminescence permits the quantitative determination of a variety of important inorganic and organic species in trace amounts. Currently, the number of fluorimetric methods is far greater than the number of applications of phosphorescence and chemiluminescence procedures.

2.1. Phenomena of fluorescence

Fluorescence and phosphorescence depend on the nature of the excited state. In excited singlet states, the electron in the excited orbital is paired (of opposite spin) to the second electron in the ground-state orbital. Consequently, return to the ground state is spin-allowed and occurs rapidly by emission of a photon. The emission rates of fluorescence are typically 10^8 s^{-1}, so that a typical fluorescence lifetime is near 10 ns (10×10^{-9} s). The *lifetime* (τ) of a fluorophore is the average time between its return to the ground state. Phosphorescence is emission of light from triplet excited states, in which the electron in the excited orbital has the same spin orientation as the ground-state electron. Transitions to the ground state are forbidden and the emission rates are slow (10^3-100 s^{-1}), so that phosphorescence lifetimes are typically milliseconds to seconds. The processes which occur between the absorption and emission of light are illustrated by a Jablonski diagram (Figure 2.1).

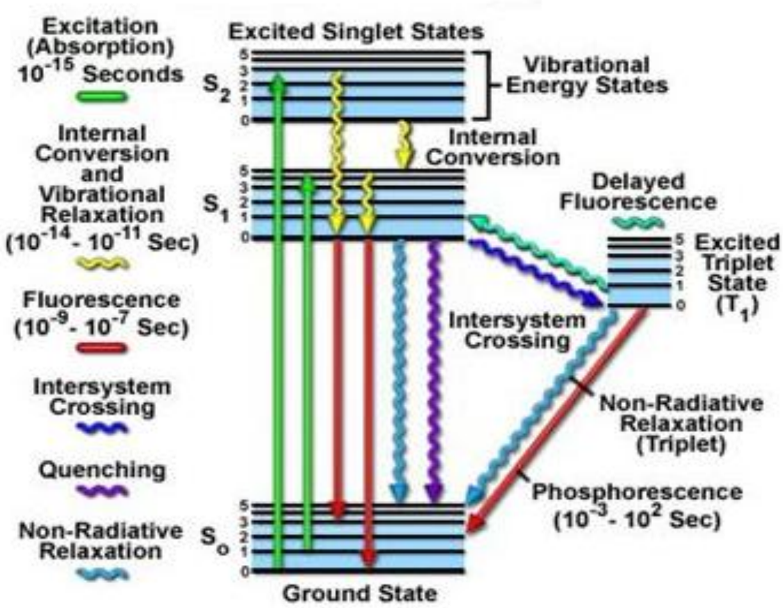

Figure 2.1. Jablonski diagram.

The singlet ground, first and second electronic states are depicted by S_o, S_1, and S_2 respectively. At each of these electronic energy levels, the fluorophores can exist in a number of vibrational energy levels, denoted by 0, 1, 2, etc. Examination of the Jablonski diagram reveals that the energy of the emission is typically less than that of absorption. Hence, fluorescence typically occurs at lower energies or longer wavelengths. This phenomenon is called *Stokes' Shift.* Fluorophores can display Stokes' shifts due to solvent effects, excited-state reactions, complex formation, and/or energy transfer (Lakowicz, 2006).

The *quantum yield (Q)* of molecular fluorescence is simply the ratio of the number of molecules that fluoresce to the total number of excited molecules (or the ratio of photons emitted to photons absorbed). The higher the value of Q, is the greater the fluorescence of a compound. Quantum efficiency of a non-fluorescent molecule is zero or close to zero that the fluorescence is not measurable. Highly fluorescent molecules such as, *fluorescein* have quantum efficiencies that approach unity under some conditions.

Any fluorescent molecule has two characteristic spectra;

- the excitation spectrum (the relative efficieny of different wavelengths of exciting radiation to cause fluorescence)
- the emission spectrum (the relative intensity of radiation emitted at various wavelengths).

The shape of the excitation spectrum should be identical with that of the absorption spectrum of the molecule and independent of the wavelength at which fluorescence is measured. Examination of the excitation spectrum indicates the positions of the absorption spectrum that give rise to fluorescence emission.

Fluorescence spectral data are generally presented as emission spectra. The emission, or fluorescence, spectrum of a compound results from the reemission of radiation absorbed by that molecule. The quantum efficiency and the shape of the emission spectrum are independent of the wavelength of the exciting radiation. If the exciting radiation is at a wavelength that differs from the wavelength of the absorption peak, less radiant energy will be absorbed and hence less will be emitted. A fluorescence spectrum is a plot of the fluorescence intensity versus wavelength (nanometers) or wavenumber (cm^{-1}). Emission spectra vary widely and are dependent upon the chemical structure of the fluorophore and the solvent in which it is dissolved. Fluorescence typically occurs from aromatic molecules.

Many fluorophores are encountered in daily life. The green or red-orange glow sometimes seen in antifreeze is due to trace quantities of fluorescein or rhodamine, respectively. Polynuclear aromatic hydrocarbons, such as anthracene and perylene, are also fluorescent, and the emission from such species is used for environmental monitoring of oil pollution. Some substituted organic compounds are also fluorescent. For example, 1,4-bis(5-phenyloxazol-2-yl) benzene (POPOP) is used in scintillation counting (Rosenzweig and Yeung, 1994), and acridine orange is often used as a DNA stain. Coumarins are also highly fluorescent and are often used as fluorogenic probes in enzyme assays, such as enzyme-linked immunosorbent assays (ELISA). In this case the parent molecule is typically umbelliferyl phosphate, which is nonfluorescent. A highly fluorescent product is obtained by the hydrolysis of the 7-hydroxylphosphate with alkaline phosphatase.

2.2. Quenching of Fluorescence

Fluorescence quenching refers to any process which *decreases* the *flourescence intensity* of a sample. A variety of molecular interactions can result in quenching. These include;

- excited-state reactions
- molecular rearrangements
- energy transfer
- ground-state complex formation
- collisional quenching

Quenching phenomena is concerned primarly with quenching resulting from collisional encounters between the fluorophore and quencher, which is called *collisional* or *dynamic quenching*. Fluorophores can form nonfluorescent complexes with quenchers. This process is referred to as *static quenching* since it occurs in the ground state and does not rely on diffusion or molecular collisions. Static quenching is a frequent complicating factor in the analysis of quenching data, but it can also be a valuable source of information about binding between the flourescent sample and the quencher.In addition to the processes described above, apperent quenching can occur due to the optical properties of the sample. For example, high optical densities or turbidity can result in decreased fluorescence intensities. This is a trivial type of quenching which contains little molecular information.

Collisional quenching of fluorescence is described by the Stern-Volmer equation,

$$F_0/ F = 1 + k_q \tau_0[Q] = 1 + K_D[Q]$$

In this equation, F_0 and F are the fluorescence intensities in the absence and the presence of quencher respectively, k_q is the bimolecular quenching constant, τ_0 is the lifetime of the fluorophore in the absence of quencher, and [Q] is the concentration of the quencher. The Stern-Volmer quenching constant is given by $k_q\tau_0$. If the quenching is known to be dynamic, the Stern-Volmer constant will be represented by K_D. Otherwise, this constant will be described as K_{SV}.

Quenching data are usually represented as plots of F_0/F versus [Q]. This is because F_0/F is expected linearly dependent upon the concentration of the quencher. A plot of F_0/F versus [Q] yields an intercept of 1 on the y-axis and a slope equal to K_D. A linear Stern-Volmer plot is generally indicative of a single class of fluorophores, all equally accessible to quencher.

It is important to recognize that observation of a linear Stern-Volmer plot does not prove that collisional quenching of fluorescence has occured. Static quenching also results in linear Stern-Volmer plots. Static and dynamic quenching can be distinguished by their differing dependence on temperature and viscosity or preferably by lifetime measurements. Higher temperatures result in faster diffusion and hence larger amounts of collisional quenching. Higher temperatures will typically result in dissociation of weakly bond complexes, and hence smaller amounts of *static quenching*.

Another type of quenching is due to *heavy atoms* such as iodine and bromine. Halogenated compounds such as trichloroethanol and bromo-benzene also act as collisional quenchers. Quenching by the larger halogens such as bromine and iodine may be a result of intersystem crossing to an excited triplet state, promoted by spin-orbit coupling of the excited (singlet) fluorophore and the halogen. Since emission from the triplet state is slow, the triplet emission is highly quenched by other processes.

Fluorescence quenching has been widely studied both as a fundamental phenomenon and as a source of information about biochemical systems. The biochemical applications of quenching are due to the intrinsic role of molecular interactions in quenching phenomena. Both static and dynamic quenching requires molecular contact between the fluorophore and quencher. In general quenching occurs without any permanent change in the molecules, that is, without a photochemical reaction. In the case of static quenching, a complex is formed between the fluorophore and the quencher, and this complex is nonfluoroscent.

2.2.1 Quenchers of fluorescence

A wide variety of substances act as quenchers of fluorescence. One of the best-known collisional quenchers is molecular oxygen, which quenches almost all known fluorophores. Depending upon the sample under investigation, it is frequently necessary to remove dissolved oxygen to obtain reliable measurements of the fluorescence yields or lifetimes. The paramagnetic oxygen causes the fluorophore to undergo intersystem crossing to the triplet state. In fluid solutions the long-lived triplets are completely quenched, so that phosphorescence is not observed. Aromatic and aliphatic amines are also efficient quenchers of most unsubstituted aromatic hydrocarbons. For example, anthracene fluorescence is effectively quenched by diethylaniline. In this instance the mechanism of quenching is the formation of an excited charge-transfer complex. The excited-state fluorophore accepts an electron from the amine.

2.3. Fluorescent probes

The function of a major part of the genome is still unknown and the relationship between enzymes, hormones, signalling substances and various small molecules is still rather limited. In order to fully understand genetic disorders and to treat them successfully more information of recognition of DNA by proteins, transcription factors, drugs and other small molecules is required. The advancements in bioscience during the last century would not have been possible without simple methods for detecting and visualization of biomolecules such as DNA and enzymes; this is usually achieved by the use of fluorescent or highly coloured chromophores or fluorophores.

Fluorophores can be broadly divided into two main classes; *intrinsic* and *extrinsic*. Intrinsic fluorophores are those that occur naturally (Figure 2.2). Intrinsic protein fluorescence originates with the aromatic amino acids tryptophan (trp), tyrosine (try), and phenylalanine (phe).

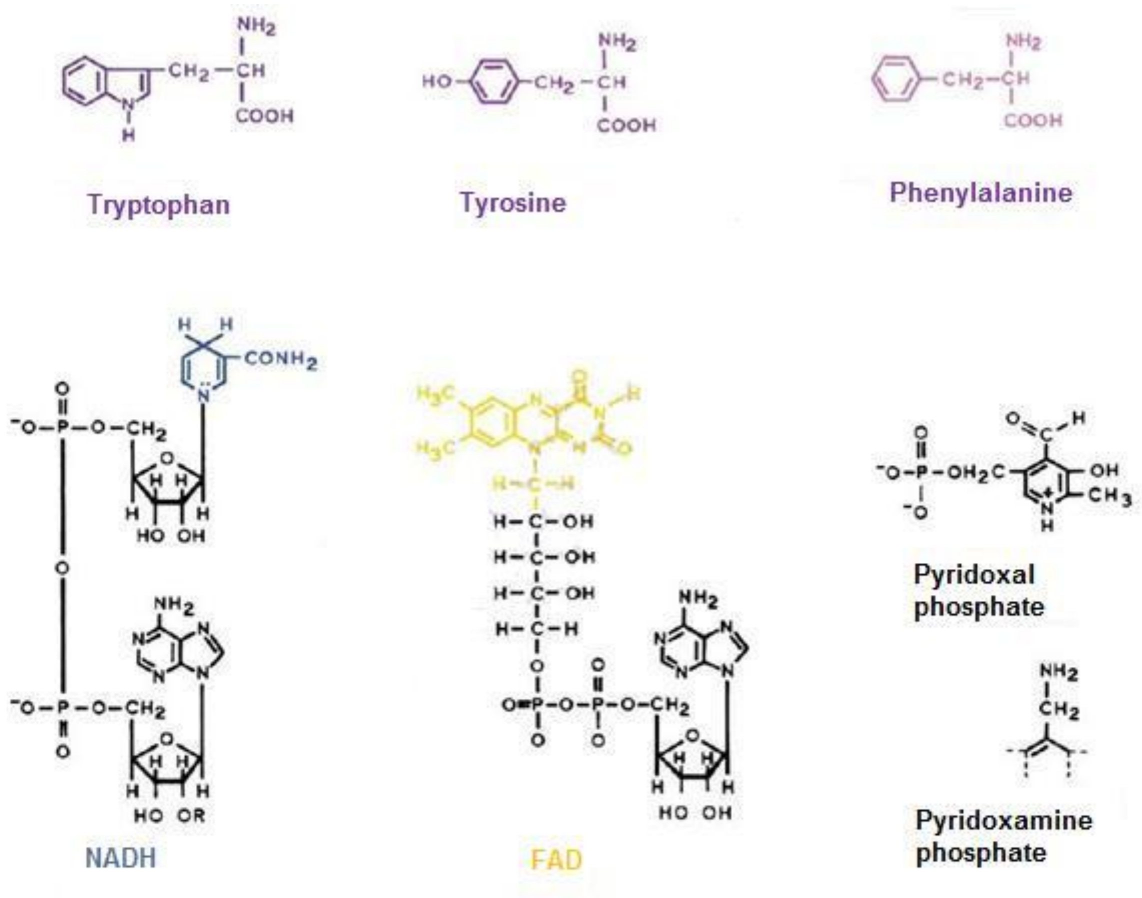

Figure 2.2. Intrinsic biochemical fluorophores.

Extrinsic fluorophores frequently the molecules of interest are nonfluorescent, or the intrinsic fluorescence is not adequate for the desired experiment. In these cases useful fluorescence is obtained by *labelling* the molecule with extrinsic probes (Figure 2.3). For proteins it is frequently desirable to label them with chromophores with longer excitation and emission wavelength than the aromatic amino acids. Then the labeled protein can be studied in the presence of other unlabeled proteins.

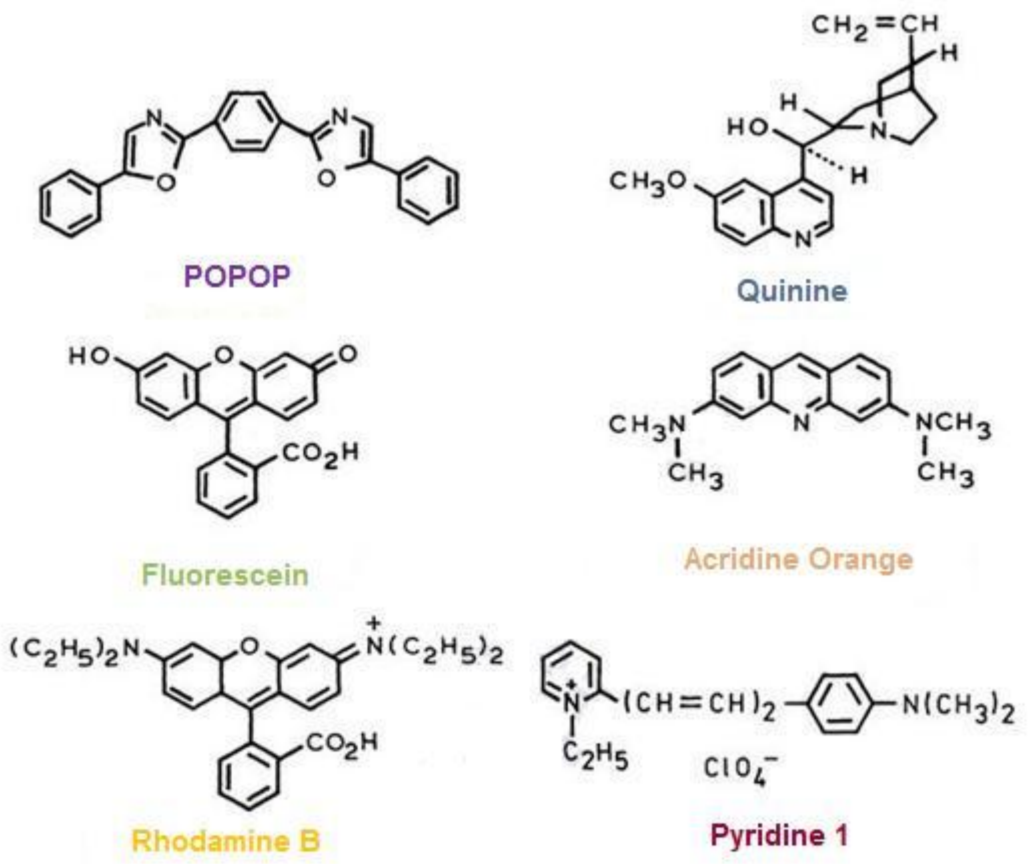

Figure 2.3. Structures of typical florescence probes.

2.4. DNA Probes

The recognition of a DNA molecule can, on the one hand, be general for any individual nucleotide or sequence. At the other extreme, it can be highly specific, solely recognizing a defined sequence within a genome. The term genome describes the entire collection of genes within an organism that provides all of the information required for organisms that respire, synthesize materials, and reproduce-as well as all of the other functions to maintain life. DNA, or deoxyribonucleic acid, is the actual substance constituting the genes. Figure 2.4 presents the primary constituents of the nucleic acids: heterocyclic amines known as purines and pyrimidines and a five carbon sugar, either ribose or 2-deoxyribose. Figure 2.5 represents a portion of a nucleic acid chain and shows how the constituents are joined together by phosphate groups. The combination of a phosphate group, a sugar and a heterocyclic amine is called a nucleotide (Petrucci, et.al., 1997).

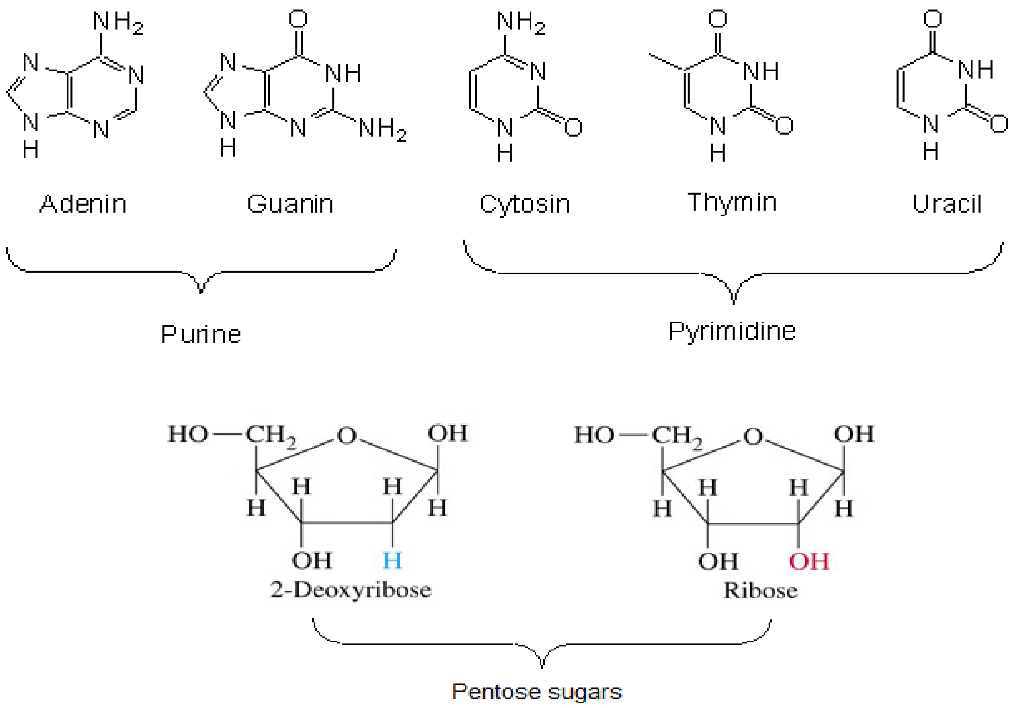

Figure 2.4. Constituents of nucleic acids.

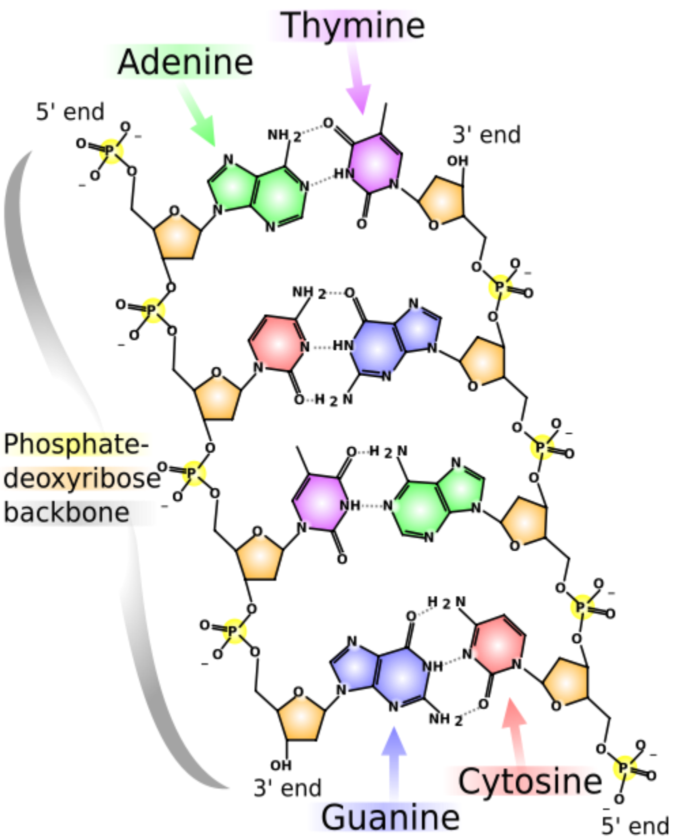

Figure 2.5. A portion of a nucleic acid chain.

In recent years there has been growing interest in the using of small molecules, such as proteins, synthetic organic molecules, small fluorescent dyes, and ions for DNA studies. Considerable interests have been focused on the binding of small molecules. While very weak intrinsic emission has been observed from unlabeled DNA, this emission is too weak and too far in the UV for practical applications. Fortunately, there are numerous probes that spontaneously bind to DNA and display enhanced emission.

One of the most widely used dyes is ethidium bromide (EB). EB is weakly fluorescent in water, and its intensity increases about 30-fould upon binding to DNA. The lifetime of EB is about 1.7 ns in water, and increases to about 20 ns upon binding to double-helical DNA. In recent years improved DNA dyes have been developed that bind to DNA with high affinity. Representative DNA probes are shown in Figure 2.6.

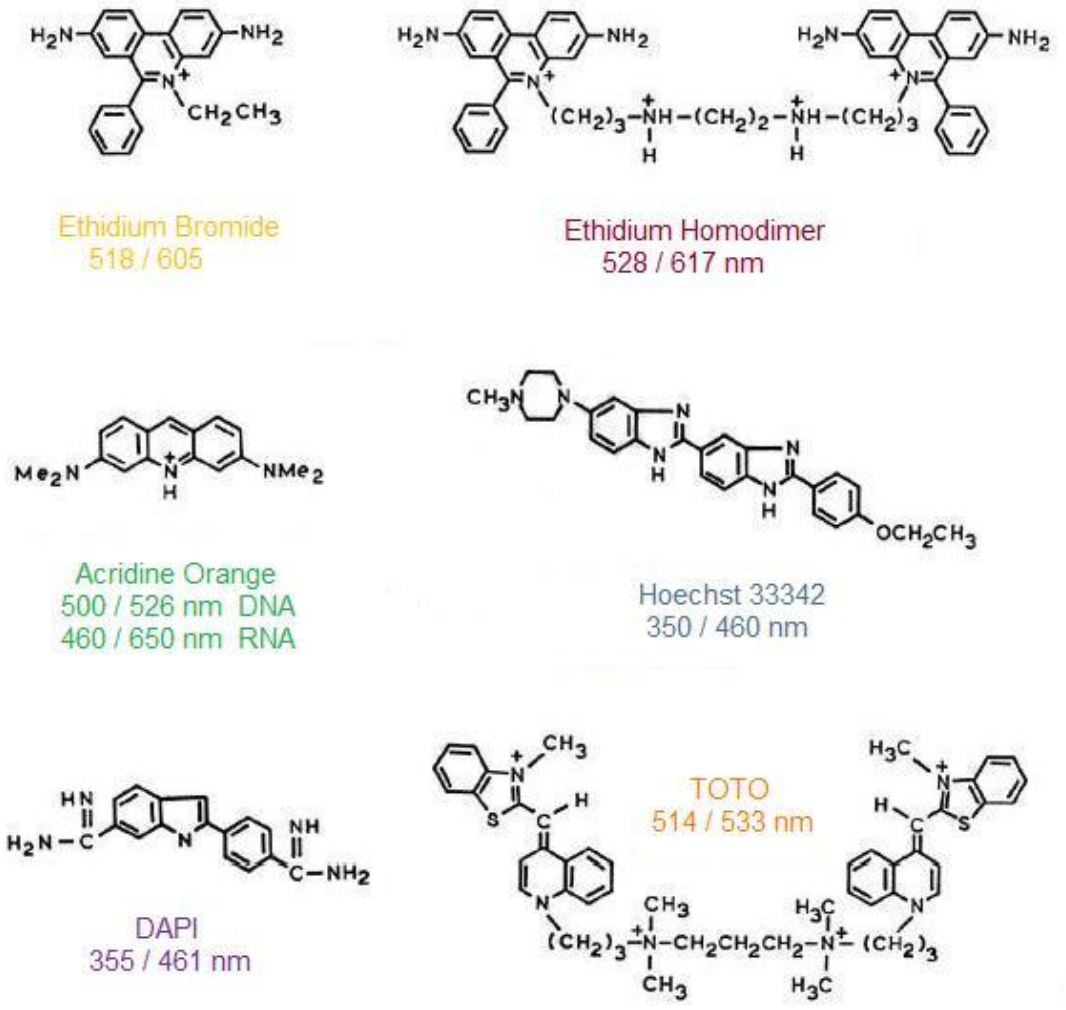

Figure 2.6. Representative DNA probes. Excitation and emission wavelengths refer to DNA-bound dye.

A group of fluorescent DNA probes is cyanine dyes. Cyanine dyes can be divided into two groups, the symmetrical and the asymmetrical dyes. The symmetrical cyanine dyes consist of two benzazole groups, whereas the asymmetrical have one benzazole group and one quinoline or pyridine group. Asymmetric cyanine dyes have become very popular lately due to their extraordinary increase in fluorescence upon binding to DNA. The fluorescence of the asymmetric cyanine dye Thiazole Orange (TO) increases 3000 times when binding to RNA. Subsequently, Rye *et al.* reproduced these tests and showed that TO have the same increase in fluorescence when binding to DNA. A similar dye Oxazole Yellow (YO) was shown to have similar spectral properties. To increase the affinity for DNA Glazer and co-workers developed the dimeric asymmetrical cyanine dyes TOTO and YOYO. These dyes have a quadratic increase in affinity compared to the monomer forms (Göransson, et.al., 2005).

The small molecules can reversibly bind to DNA by three main modes:

(1) intercalative binding;

(2) major or minor groove-binding;

(3) external binding.

Intercalative binding: there are a large number of antibiotics, antibacterial, and anti-tumor drugs that are characterized by the possession of an extended planar heteroatomic ring system (chromophore). This essential structural feature is a chromophore of typically three fused six-membered rings in size, which is approximately the same size as a base pair itself. The intercalation hypothesis, originally proposed that the planar chromophore of the drug molecule becomes inserted in between adjacent base pairs in an intercalative manner (Figure 2.7).

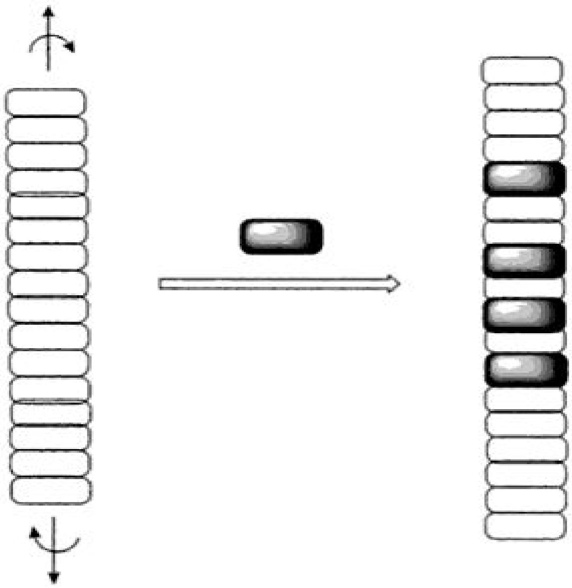

Figure 2.7. A schematic view of intercalation.

The probe chromophore is stabilized by polarization forces and van der Waals dispersion interactions between its planar group and the base pairs surrounding it. Optimal attractive interactions occur when the intercalating chromophore has polarized character, incorporating one or more hetero-atoms such as nitrogen. Electron deficiency is also important, and a formal cationic charge is common (e.g. in the acridines). Intercalation results in an extension of the double helix by 3.4 Å per bound probe molecule, together with changes in helical twist (unwinding) for the base pairs at and adjacent to each binding site. The base pairs either side of an intercalated molecule thus increase in separation from 3.4 Å to 6.8 Å. The maximum number of drug molecules which can be bound to a DNA duplex is one for every three base pairs that is every other potential site becomes occupied at probe saturation. So the immediate base pair step either of a binding site cannot bind a probe molecule. This is neighbor-exclusion principle, which originates from the interpretation of solution binding data, but is based on the structural constraints forced on backbone geometry by intercalation.

DNA-intercalator recognition itself is essentially sequence- neutral, although, base pair satcking/ unstacking requirements usually result in a small preference for a GC sequence step at the binding site. The 'simple intercalators' consist solely or priamarily of an intercalating chromophore, often carrying a positive charge on the ring system- for example, proflavine and ethidium bromide. The GC sequence preference at the drug binding sites is generally obeyed both for these simple intercalators and for the complex ones such as daunomycin and its analogues. More complex intercalators have attached groups such as side chins, sugar rings or peptide units. These groups reside in a DNA groove, where they are stabilized by van der Waals interactions, and can hydrogen-bond to adjacent bases, providing sequence-specific direct readout. Yet more complex is the drug molecules typified by the echinomycin and triostin family of anti-tumuor antibiotics, which have two intercalating chromophores linked together by cyclic oligopeptides. These molecules intercalate such that the two chromophores, whose planes are separated by a distance of 10.2 Å (i.e. three base pairs), can simultaneously bind at sites separated by two intervening base pairs. This mode is termed as bis-intercalation (Figure 2.8.).

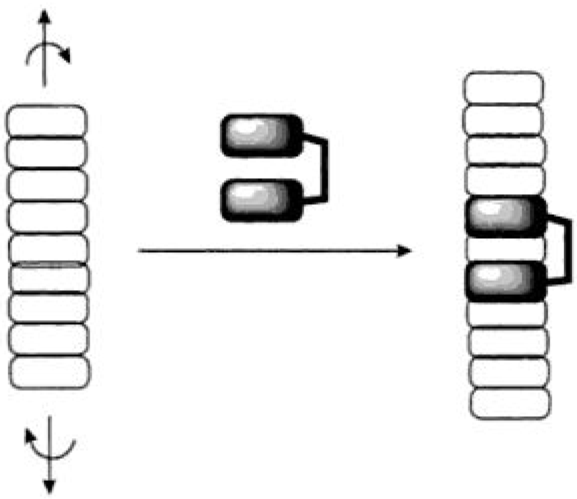

Figure 2.8. A schematic view of bis-intercalation.

Groove binding: A large and chemically diverse family of compounds can be classified as DNA groove-binders. Many show biological activity and several of find medicinal use as anti-parasitic or anti-viral agents. They generally show a preference for binding to AT regions of DNA. By contrast to intercalating molecules, they do not significantly perturb DNA structure. They bind exclusively in the minor groove of DNA duplexes. Groove binding ligands are also attracting increasing interest as starting-points for the design of sequence-specific molecules capable of the recognition of unique sequences within a genome. The common structural characteristics shared by most minor-groove binding molecules are:

- positive charge(s)
- linked rather than fused aromatic and/ or heteroaromatic rings
- an approximately crescent shape in three dimensions.

Typically, the ligand is bound in the AT region, with the aromatic groups of the ligand lying between and parallel to the two sugar-phosphate backbones (Figure 2.9). There is little change to the structure of the DNA upon groove binding. The groove tends to be exceptionally narrow in this region, and the backbones and groove floor are in close van der Waals contact with the ligand. Groove interaction involves the concave curvature of the inner surface of the bound molecule complementing that of the convex surface of the floor of the DNA minor groove itself. Thus a GC sequence with an exocyclic $-NH_2$ amino group of guanine protruding into the groove will hinder the effective binding of a molecule with a smooth concave inner surface (Neidle, 2002). This surface matching has been termed ‘isohelicity’ since both the drug inner surface and the floor of the minor groove have twists in their curvature as a result of the helical nature of the DNA double helix. Isohelicity has been found to be useful concept in the design of novel groove-binding agents.

Although a lot of publication, focused on interaction of small molecules with nucleic acids, take place in the literature, enlightened mechanisms are not sufficient. Yarmoluk’s Group (Kovalska, et.al., 2006) searchs and develops novel highly efficient fluorescent probes for biology and medicine by using the an original approach , called "lead dye" method, to design of fluorescent probes with required properties. Their investigation of 6,6’-disubstitution of benzothiazole trimethine cyanines showed that the incorporation of methyl-, 2-hydroxyethyl-, dimethyl- ,diethyl- and benzoyl-amino substituents into the 6,6’-positions of the dyes benzothiazole heterocycles leads to the increase in dyes tendency to form H-aggregates both in the solution and in the presence of biological molecules.Their results point out 6,6’-disubstituted trimethine cyanines the high preference of fluorescent complex formation with dsDNA as compared to RNA and BSA. According to this results this study propose a way for the designing of dyes selective to dsDNA by insertion of methyl-, dimethyl-, diethyl- and benzoyl amino substituents into 6,6’ –positions.

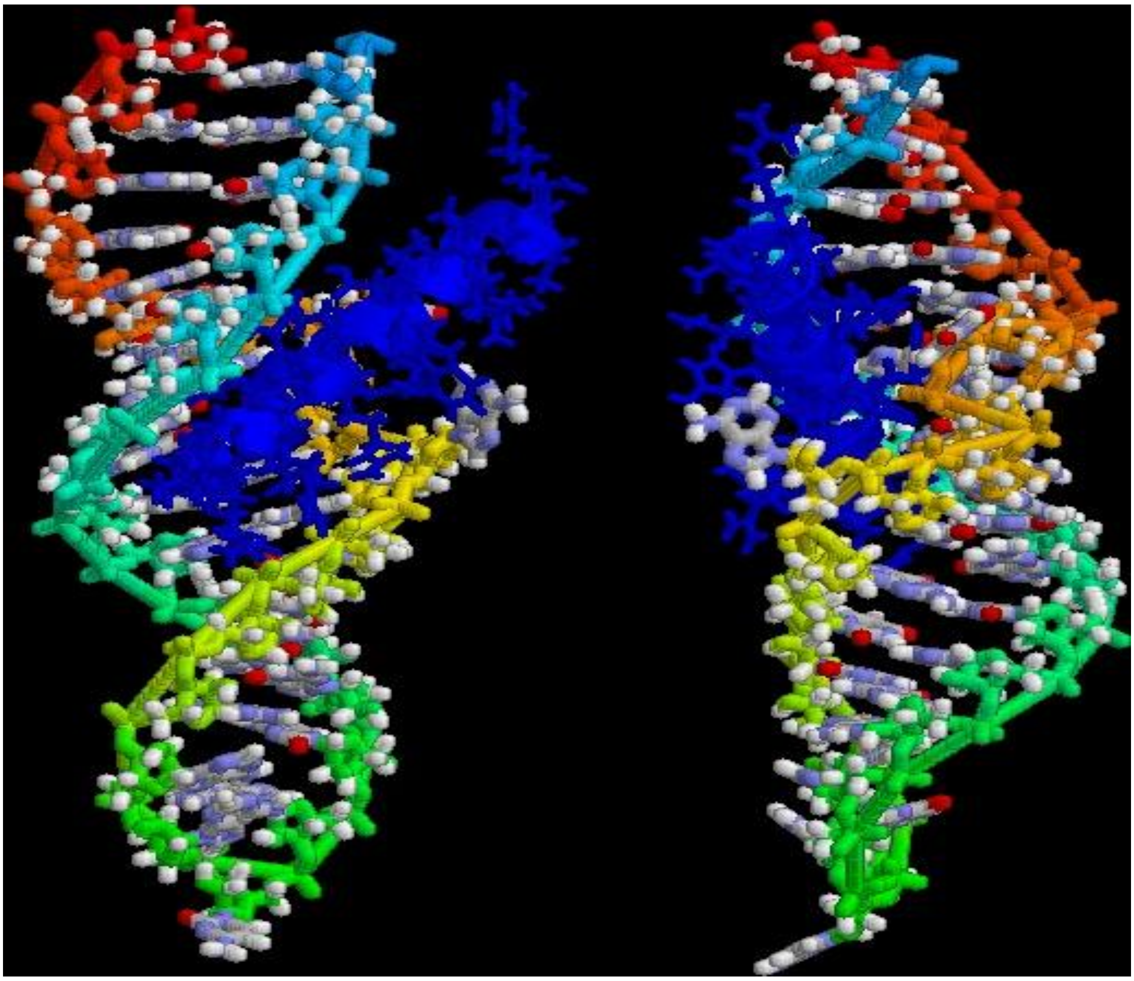

Figure 2.9. A schematic view of groove binding.

For today styrylcyanines are among the fluorescent dyes widely used for biomolecules detection. These dyes are successfully applied as sensitive probes for unspecific fluorescent detection of proteins in gels. Due to the ability of styrylcyanines to interact with DNA with up to hundred times fluorescent enhancement and ability to penetrate into cell these dyes were proposed for intra cellular DNA imaging. Kovalska et.al. (2005) analyzed the spectral-luminescent properties of series of homodimer styryls containing (p-dimethylaminostyryl) pyridinium template with aliphatic linkage groups in the presence of various biopolymers. This study found out the strong dependence of spectral-luminescent properties of homodimers on the length of the linkage group. Because of the DNA-binding affinity of (p-dimethylaminostyryl)-pyridinium homodimers with long linkage group significantly exceeds that of parent monomer that is known as fluorescent dye for DNA analysis these homodimers offered as sensitive, DNA specific probes.

Functional groups used to modify the best known fluorescent probes play key role at the interaction mechanisms of these new probes with the nucleic acids. Garbett et.al. (2004) underlined that there has been considerable work directed toward the elucidation of the thermodynamic, kinetic, and structural properties of dye-DNA complexes but there are still a lot of unanswered questions. One of them is the role of 3- and 8- amino substituents of EB in directing the energetics of the DNA binding process. This group investigates the EB and its three analogues to find out the 3- and 8- amino susbtituents of ethidium on the energetic contributions and concominant fluorescent properties upon DNA complex formation. As a result, decrease in binding affinities by an order of magnitude upon the removal of either the 3- or 8-amino substituent, with a further order-of-magnitude decrease in the absence of both amino groups are reported. It is also point out the thermodynamic binding mechanism changes from enthalpy-driven for the parent ethidium to entropy driven when both amino groups are removed. Upon DNA binding, fluorescence enhancement is observed in the presence of either or both of the amino groups, likely because of more efficient fluorescence quenching through solvent interactions of free amino groups than when buried within the intercalation site. The des-amino ethidium analog exhibits fluorescence quenching upon binding, consistent with less efficient quenching of the chromophore through interactions with solvent than within the intercalation site. Determination of the quantum efficiencies suggests distinct differences in the environments of the 3- and 8-amino substituents within the DNA binding site.

Effects of quenchers and ionic strength on dye-DNA systems are important parameters to identify the interaction mode in the meaning of groove binding or intercalative binding. Kumar et al. investigated salt effect on groove binding of a styrylcyanine dye to the DNA double helix. They found out that the addition of NaCl to the free probe, in the absence of DNA, had little or no effect on the fluorescence yield of the dye. However, in the presence of ct-DNA, they obtained the quenching plots and K_{sv} value as 18.5 M^{-1}. Since the fluorescence from the free probe was not quenched by salt, they concluded that quenching in the presence of DNA was due to the release of the dye from DNA grooves (Kumar, et.al., 1993). And this study reported that the strong dependence of the binding on the ionic strength indicates that binding is predominantly controlled by electrostatic interactions and these observations are consistent with groove binding rather than intercalation into the helix.

Iodide ion is a dynamic, or collision, fluorescence quencher for the small fluorescent molecules. Because of this property in almost all studies iodide ion quenching effect is investigated. Guo et.al. (2007) also performed these quenching experiments to further deduce the interaction mode of the fluorescence probe OPSA with ct-DNA. They explained that when small molecule intercalates to DNA base pairs, owing to the electrostatic repelling between ct-DNA phosphate backbone and the iodide anions, the iodide anions are difficult to collide with the small molecules, which lead to a decrease in fluorescent quenching. On the other hand, surface-binding mode between small molecule and DNA cannot afford a protection surrounding for the small molecule and iodide anions with the presence and absence of DNA will be equal. When the interaction mode belongs to groove binding, the small molecules will be partly protected by DNA, and iodide anions can partly quench its fluorescence.

2.5. Serum Albumins

Serum albumins are the major soluble protein constituents of circulatory system constituting 52% of the protein composition and possess many physiological and pharmacological functions. Albumins have significant contribution to colloid osmotic blood pressure and aid in the transport, distribution and metabolism of fatty acids, amino acids, steroids, metal ions and a variety of drugs. Changes in blood albumin levels can be caused by a number of disorders, including liver disease, nephrotic syndrome, neoplasia, severe dehydration etc. Protein intrinsic fluorescence is due to aromatic amino acid residues such as tryptophan, tyrosine and phenylalanine.

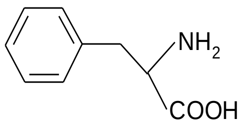

Phenylalanine
Phe

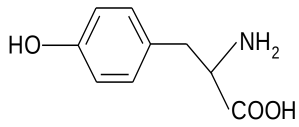

Tyrosine
Tyr

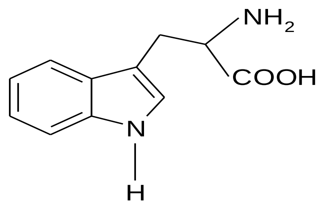

Tryptophan
Trp

Bovine serum albumin (BSA) and human serum albumin (HSA), two of the most extensively studied serum albumins, have similar structure. The main difference between these two serum albumins is the fluorophore–tryptophan number. BSA has two tryptophan residues that possess intrinsic fluorescence: Trp-212 is located within a hydrophobic binding pocket of the protein and Trp-134 is located on the surface of the molecule. However HSA has only one tryptophan residue Trp-214.

Generally, when the excitation wavelength of serum albumins is selected at 280 nm, the fluorescence was produced from the tryptophan and tyrosine residues. However, their fluorescence spectra were different for the emission maximum of tryptophan and tyrosine residues occurred near 350 nm and 303 nm respectively. According to the wavelength at which the maximum fluorescence intensity decreases we can know which residue is located in or near the binding position.

Quenching measurement of albumin fluorescence is an important method to investigate the interactions of compounds with serum albumins (Zhou, et.al., 2007; Shaikh, et.al., 2007; Akbay, et.al, 2009). It can reveal the accessibility of quenchers to albumin's fluorophore groups, help understand binding mechanisms of albumins with compounds, and provide clues to the essential of the binding phenomenon.

3. EXPERIMENTAL

3.1. Instrumentation

The fluorescence measurements were performed on *Cary Eclipse fluorescence (Australia)* and *Hıtachı F-4500* spectrofluorometers equipped with a 150 W xenon lamp source and quartz cells of 1 cm path length. The absorption spectra were performed on *Specord M 40* and *Shimadzu UV-1700(PharmaSpec)* UV-Vıs spectrophotometers equipped with quartz cells. pH measurements were carried out by a *NeoMet (pH-220L)* pH meter.

In characterization studies, IR spectra were recorded with *Mattson 1000 FTIR spectrometer* with KBr. Proton NMR spectra were obtained with *Bruker 400 MHz Ultra Shielded NMR* spectrometer. Mass spectra were recorded with *Agilent 1100 MSD* instrument. Elemental analyses were recorded on *Elementar Analysensysteme GmbH* (varioMICRO CHNS).

3.2. Reagents and preparation of solutions

Ethidium bromide (EB; *3,8-diamino-5-ethyl-6-phenylphenantridinium bromide)* was purchased from Sigma. Dimethylsulfoxide (DMSO) and tris-(oxymethyl-) amino methane hydrochloride (Tris) were used without purification. 0.05 M Tris-HCl solution (pH 8.0) was used as a buffer in all experiments.

The stock solution of calf thymus deoxyribonucleic acid (*DNA*, double stranded, type I, sodium salt, Sigma) were prepared in Tris-HCl buffer solution at pH 8.0 and stored in refrigerator at 4ºC until used. DNA concentrations were determined by absorption spectroscopy using the molar coefficient ($M^{-1}cm^{-1}$) of 6600 at the wavelength of 260 nm. Purity of DNA was checked by monitoring the ratio of the absorbance at 260 to that at 280 nm. The solution gave a ratio of A_{260}/A_{280}>1.8, indicating that DNA was sufficiently free from protein. The concentration of DNA stock solution in Tris-HCl was 6×10^{-3} M b.p. (moles of base pairs per liter). Poly$(dA\text{-}dT)_2$ and poly$(dG\text{-}dC)_2$ were purchased from Sigma.

The stock solutions of all cyanine and synthesized ethidium dyes were prepared in DMSO as 2.0×10^{-3} M and stored in refrigerator at 4ºC until used. The all aqueous solutions used in the experiments were prepared daily from the stock solutions by appropriate dilution in doubly distilled water.

3.3. Experimental studies of benzothiazole styrylcyanine derivatives

In the first part, this group of experiments were studied with Yarmoluk Fluorescent Probes Design Group in Kiev, Ukraine. Four benzothiazole styrylcyanine derivatives were used in this group studies. They were synthesized by Yarmoluk's Group (Kovalska,et al., 2005; Balanda, et al., 2006). Their chemical structures and abbreviated names (Bos-5, Sbt, DBos-13, DBsu-10) are given in Figure 3.1.

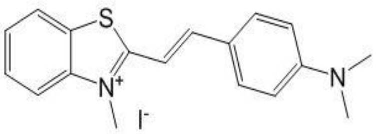

Sbt

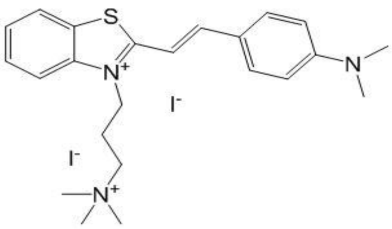

Bos-5

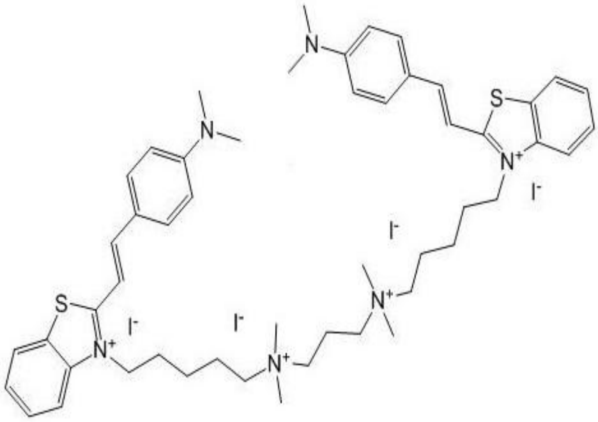

Dbos13

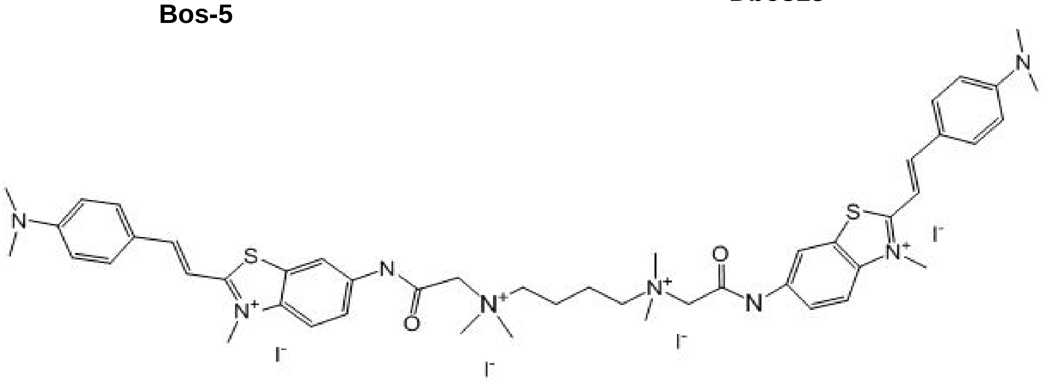

DBsu10

Figure 3.1. Chemical structures of four benzothiazole styrylcyanine derivatives.

3.3.1. Procedure

5×10^{-6} M Sbt, Bos-5, DBos-13, and DBsu-10 were titrated by DNA. Aliquots (5-325 μL) of the DNA stock solutions were added to the 5×10^{-6} M dye in buffer solution to obtain the mixing dye-base pair (dye-b.p.) ratios from 1:2.4 to 1:228. To avoid the dissolving the DNA stock solution contained 5×10^{-6} M dye as well. Also all absorption measurements were carried out at the dye concentration 5×10^{-6} M (Akbay, et.al., 2008).

3.4. Experimental studies of ethidium derivatives

In the second part, this group experiments were studied in our photochemistry laboratories. The new ethidium derivatives were synthesized by binding functional groups to the both amines at the 3- and 8-positions of EB. Several ethidium derivatives were obtained using different functional groups. And the four of the most sensitive ethidium derivatives were chosen from these dyes which have the affinity to *DNA*.

3.4.1. Syntheses and characterization of four ethidium derivatives

The four new ethidium derivatives, coded as *E2*, *E3*, *E4, E5,* were synthesized by binding functional groups to the both amines at the 3- and 8-positions of EB (Figure 3.2). They were characterized by IR, UV, MS, ^{1}H-NMR and elemental analysis.

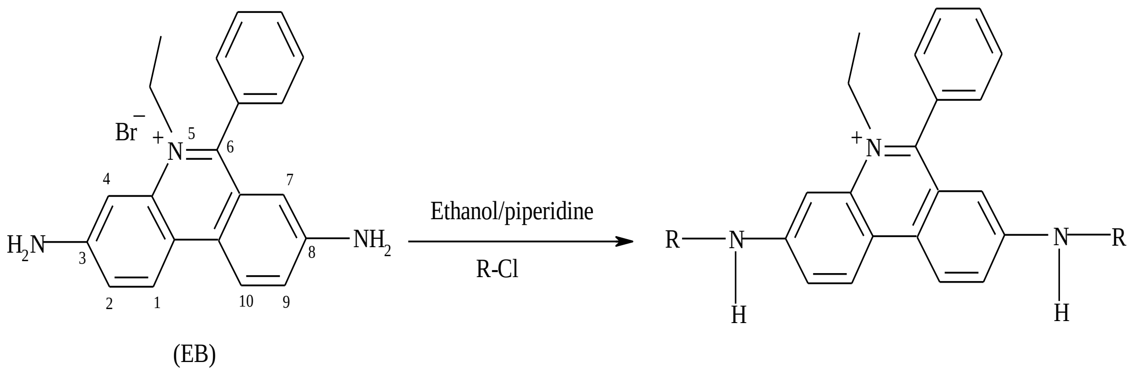

Figure 3.2. Syntheses of ethidium derivatives from EB.

Dye	R-Cl	
E2	PhCOCl	(benzoyl chloride)
E3	$PhCH_2COCl$	(phenylacetyl chloride)
E4	CH_3CH_2OCOCl	(ethyl chloroformate)
E5	CH_3OCOCl	(methyl chloroformate)

3,8-Dibenzoylamino-5-ethyl-6-phenylphenantridinium chloride (*E2*)

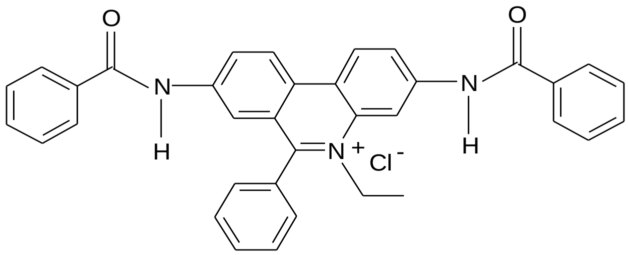

EB (197 mg, 0.5 mmol) was dissolved in mixture of absolute ethanol (30 mL) and piperidine (5 mL). The solution was cooled in salt/ice bath and followed by dropwise addition of benzoyl chloride (5 mmol, 0.4 mL) in 5 mL ethanol under constant stirring. The reaction mixture was heated at reflux on a steam bath for 1 h and then stirred at room temperature for 4 h. The residue was filtered, washed with water and then ether. The pure product was obtained on crystallization from ethanol gave as a yellow solid. Yield: 237 mg (91 %), m.p: 306-308 ^{o}C. Rf: 0.61 (40% methanol/ethyl acetate).

IR (KBr, cm^{-1}) 3408 (-NH), 3052 (aromatic C-H), 2951 (aliphatic C-H), 1657 (C=O, amide), 1599 (C=N), 1543 (C=C).

^{1}H NMR (DMSO-d_6, δ): 11.11 (b, -N_3H), 10.85 (b, -N_8H), 9.22 (m, 2H), 9.18 (d, 1H), 8.70 (dd, 1H), 8.55 (dd, 1H), 8.20 (s, 1H), 8.09 (d, 2H), 7.91 (d, 2H), 7.83 (m, 5H), 7.68 (d, 1H), 7.60 (m, 3H), 7.50 (m, 2H), 4.70 (2H, q, -N-$\underline{CH_2}$-CH_3), 1.58 (3H, t, -N-CH_2-$\underline{CH_3}$) (Figure 3.3).

^{13}C NMR (DMSO-d_6, δ, ppm): 166.9, 166.7, 163.9, 142.5, 140.3, 134.5, 134.1, 132.8, 132.5, 131.8, 131.1, 130.8, 129.8, 129.1, 128.6, 128.3, 126.2, 125.6, 123.9, 123.6, 122.3, 120.7, 109.6, 50.9, 14.4 (see appendix 1).

Elemental analysis (CHNS) Anal. Calcd. for $C_{35}H_{28}N_3O_2Cl$: C, 75.25; H, 5.01; N, 7.52. Found: C, 75.16; H, 4.98; N, 7.61.

MS (electron impact, m/z, 100 ev): 522.2 (100.0 %) $(M-35.5)^+$.

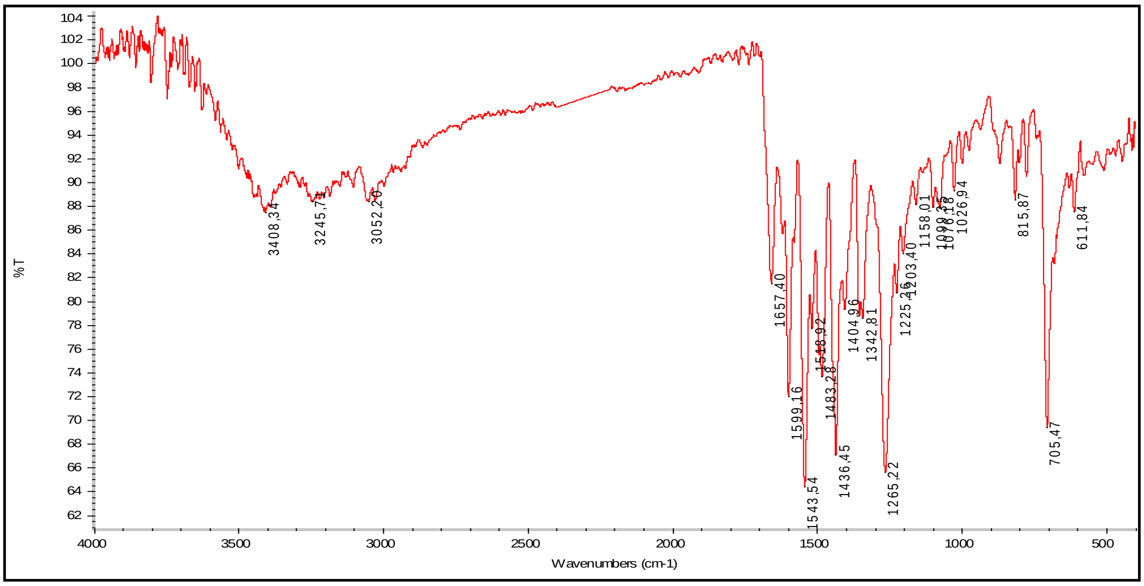

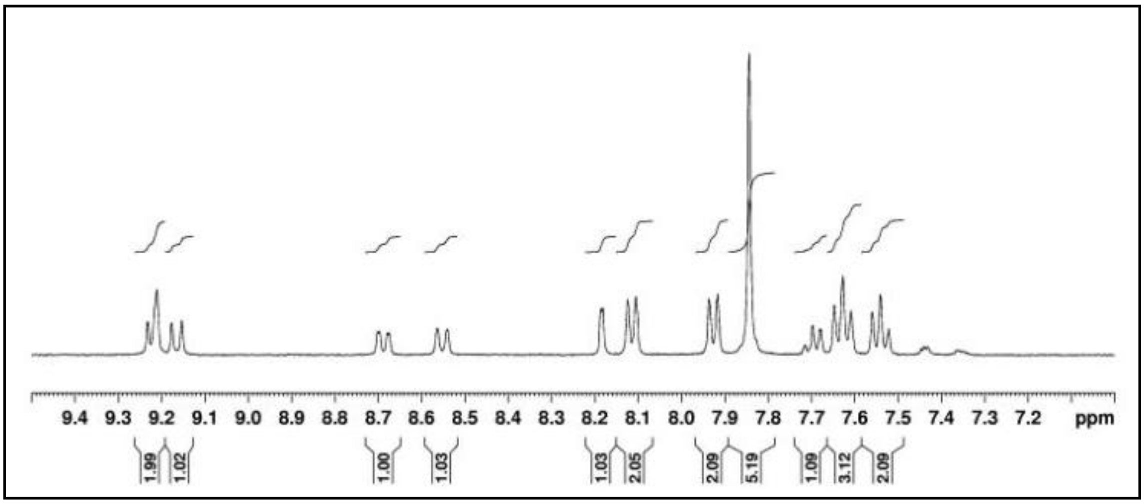

Figure 3.3. IR and 1H NMR spectra of *E2*.

3,8-Diphenylacetylamino-5-ethyl-6-phenylphenantridinium chloride (*E3*)

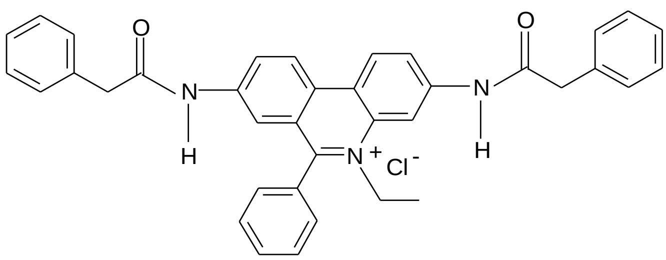

EB (197 mg, 0.5 mmol) was dissolved in mixture of absolute ethanol (30 mL) and piperidine (5 mL). The solution was cooled in salt/ice bath and followed by dropwise addition of phenylacetyl chloride (5 mmol, 0.5 mL) in 5 mL ethanol under constant stirring. The reaction mixture was heated at reflux on a steam bath for 1 h. and then stirred at room temperature 3 h. The residue was filtered, washed with water and then ether. The pure product was obtained on crystallization from ethanol gave as a yellow solid. Yield: 266 mg (87 %), m.p: 276-278 ^{o}C. Rf: 0.57 (40% methanol/ethyl acetate).

IR (KBr, cm^{-1}) 3454 (-NH), 3032 (aromatic C-H), 2949 (aliphatic C-H), 1676 (C=O, amide), 1627 (C=N), 1599 (C=C).

^{1}*H NMR* (DMSO-d$_6$, δ): 11.20 (b, -N$_3$H), 10.80 (b, -N$_8$H), 9.13 (d, 1H), 9.10 (d, 1H), 9.06 (d, 1H), 8.42 (dd, 1H), 8.20 (dd, 1H), 8.0 (m, 1H), 7.78 (m, 5H), 7.40-7.30 (m, 10H) 4.60 (2H, q, -N-$\underline{CH_2}$-CH$_3$), 3.83 (s, 2H), 3.64 (s, 2H), 1.50 (3H, t, -N-CH$_2$-$\underline{CH_3}$) (Figure 3.4).

^{13}*C NMR* (DMSO-d$_6$, δ, ppm): 171.0, 170.4, 163.7, 142.3, 140.1, 135.7, 134.1, 131.8, 130.8, 129.8, 128.8, 127.2, 125.7, 124.0, 122.6, 122.0, 119.3, 108.2, 43.8, 43.6, 14.3 (see appendix 2).

Elemental analysis (CHNS) Anal. Calcd. for $C_{37}H_{32}N_3O_2Cl$: C, 75.74; H, 5.46; N, 7.17. Found: C, 75.62; H, 5.52; N, 7.07.

MS (electron impact, m/z, 100 ev): 550.2 (100.0 %) (M-35.5)$^{+}$.

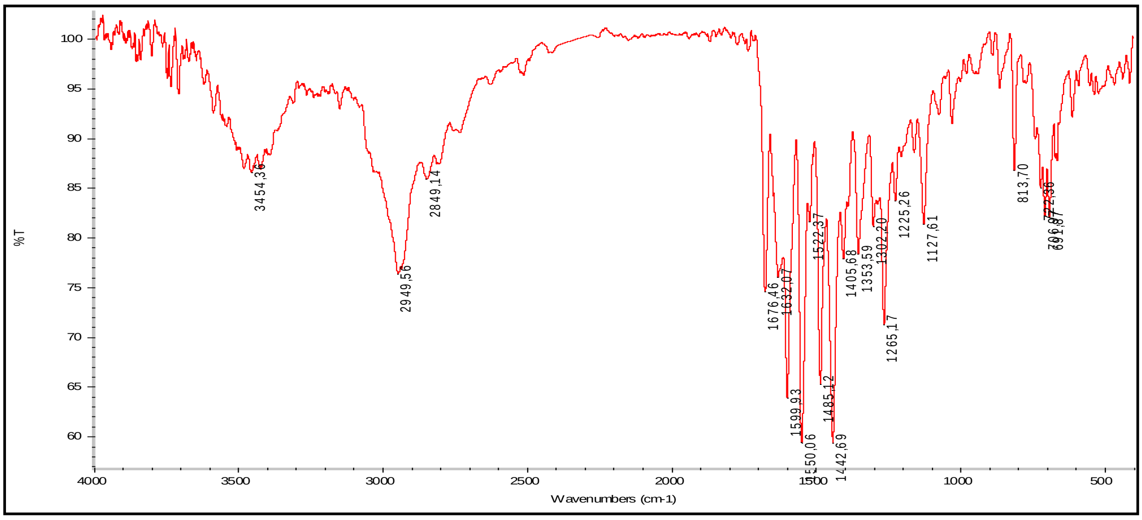

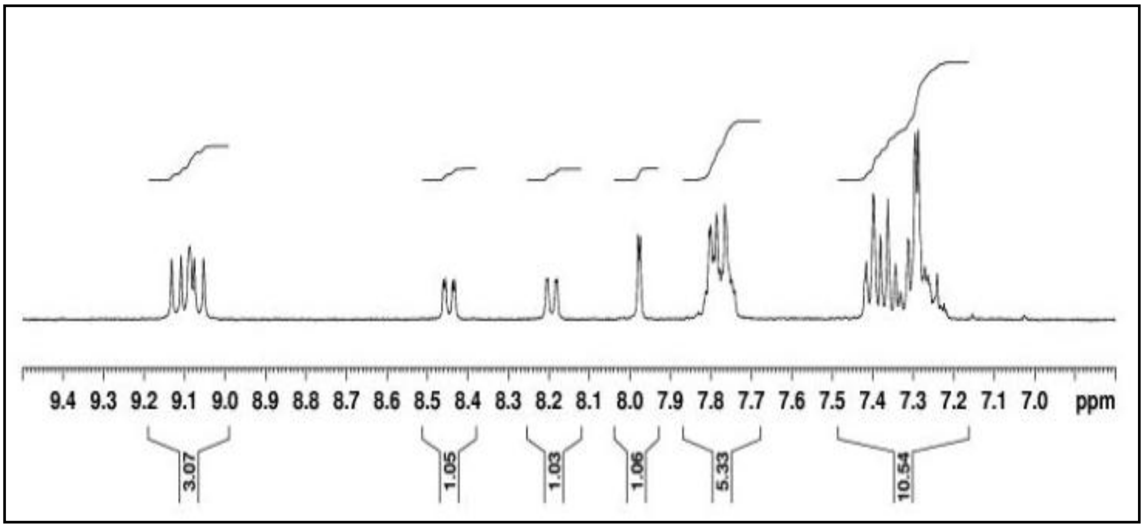

Figure 3.4. IR and ^{1}H NMR spectra of *E3*.

3,8-Diethylcarbamate-5-ethyl-6-phenylphenantridinium bromide (*E4*)

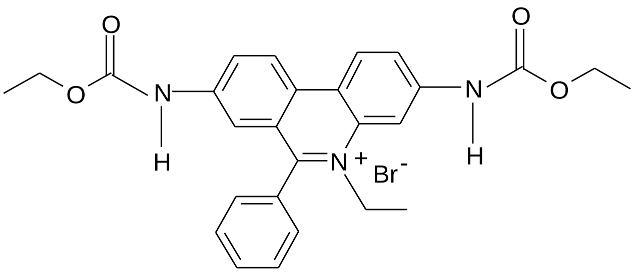

EB (197 mg, 0.5 mmol) was dissolved in mixture of absolute ethanol (30 mL) and piperidine (5 mL. The solution was cooled in salt/ice bath and followed by dropwise addition of ethyl chloroformate (5 mmol, 0.5 mL) in 5 mL ethanol under constant stirring. The reaction mixture was heated at reflux on a steam bath for 1 h and then stirred at room temperature 4 h. The residue was filtered, washed with water and then ether. The pure product was obtained on crystallization from ethanol gave as a orange solid. Yield: 182 mg (68 %), m.p: 257-258 ^oC. Rf: 0.64 (40% methanol/ethyl acetate).

IR (KBr, cm^{-1}): 3417 (-NH), 3112, 3068 (aromatic -H), 2984 (aliphatic -H), 1719 (C=O), 1622 (C=N), 1524 (C=C), 1231 (C-0).

^{1}H NMR (DMSO-d_6, δ): 10.58 (b, -NH), 10.27 (b, -NH), 9.10 (d, 1H), 9.0 (d, 1H), 8.80 (m, 1H), 8.25 (d, 1H), 8.10 (d, 1H), 7.80 (m, 6H), 4.64 (2H, q, -N-$\underline{CH_2}$-CH_3), 4.21 (2H, q, 0=C-0-$\underline{CH_2}$-CH_3), 4.10 (2H, q, 0=C-0-$\underline{CH_2}$-CH_3), 1.53 (2H, q, -N-CH_2-$\underline{CH_3}$), 1.30 (3H, q, 0=C-0-CH_2-$\underline{CH_3}$), 1.20 (2H, q, 0=C-0-CH_2-$\underline{CH_3}$) (Figure 3.5).

^{13}C NMR (DMSO-d_6, δ, ppm): 163.4, 154.1, 153.8, 142.6, 140.2, 134.1, 131.8, 131.6, 130.3, 129.7, 129.0, 128.6, 126.1, 125.7, 123.9, 121.9, 121.4, 117.8, 106.9, 61.5, 61.2, 60.2, 50.8, 14.8, 14.5, 14.2 (see appendix 3).

Elemental analysis (CHNS) Anal. Calcd. For $C_{27}H_{28}N_3O_4Br$: C, 60.22; H, 5.20; N, 7.81. Found: C, 59.89; H, 5.48; N, 7.88 %.

MS (electron impact, m/z, 100 ev): 459.2 (28.9 %) $(M-79)^+$, 458.2 (100 %) $(M-80)^+$, 386.1 (64.2 %) $(M-153)^+$.

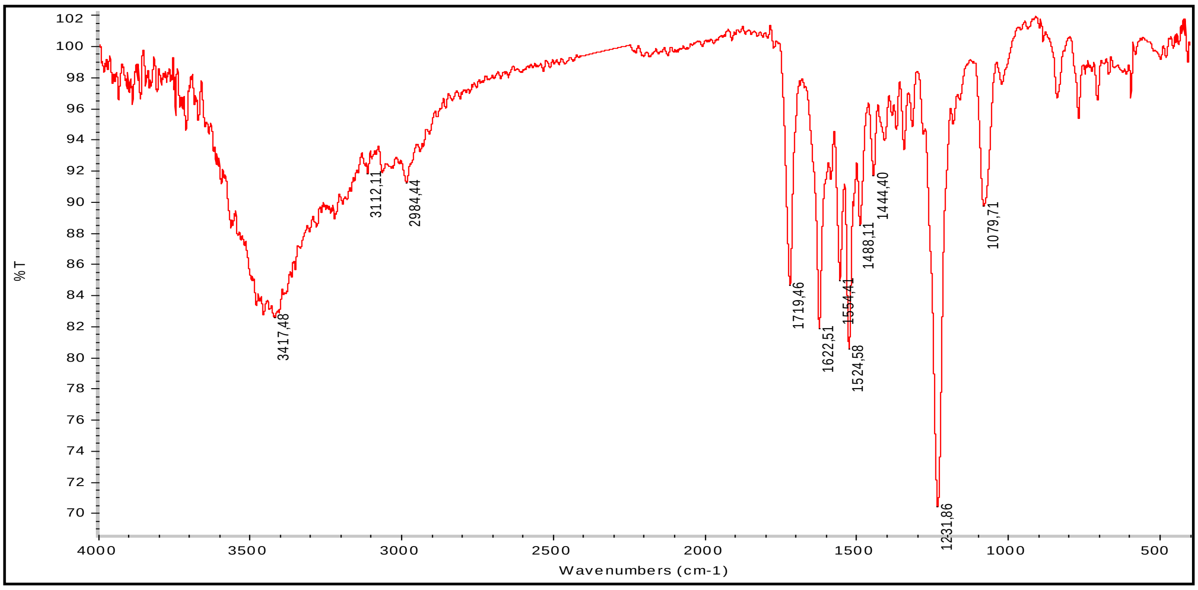

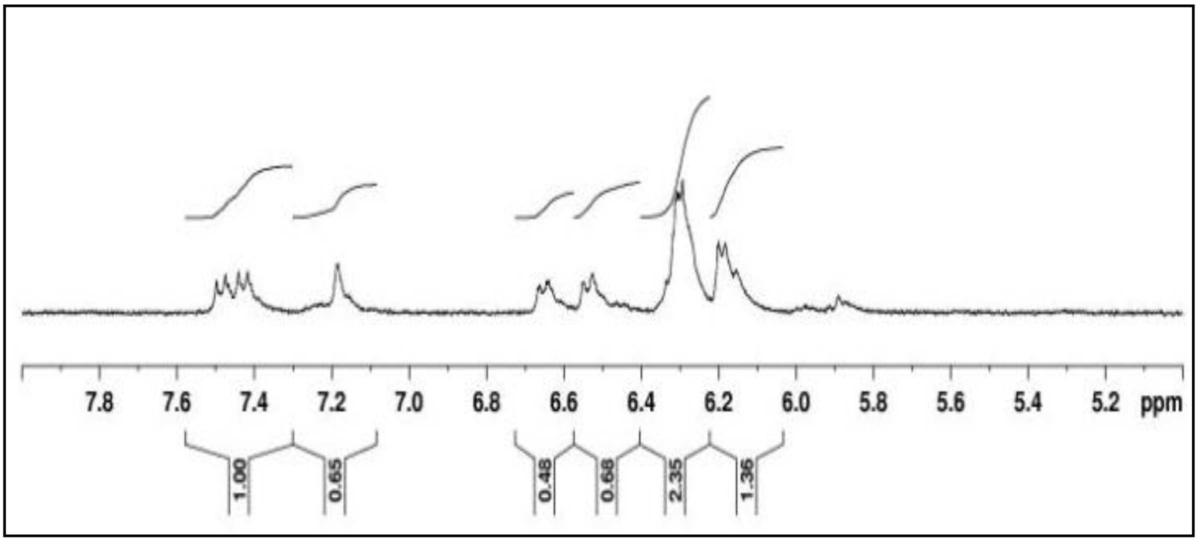

Figure 3.5. IR and 1H NMR spectra of *E4*.

3,8-Dimethylcarbamate-5-ethyl-6-phenylphenantridinium chloride (*E5*)

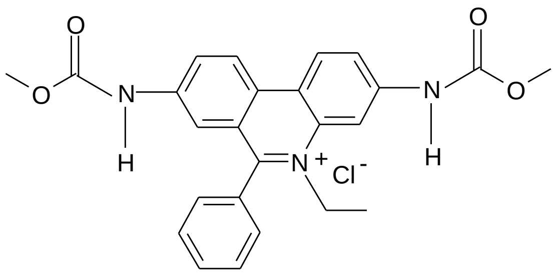

EB (197 mg, 0.5 mmol) was dissolved in mixture of absolute ethanol (30 mL) and piperidine (5 mL). The solution was cooled in salt/ice bath and followed by dropwise addition of methyl chloroformate (5 mmol, 0.4 mL) in 5 mL ethanol under constant stirring. Then the mixture was stirred 1 day at room temperature. The resulting solid was filtered, washed with water and then ether. The pure product was obtained on crystallization from ethanol gave as a orange solid. Yield: 110 mg (51 %), m.p: 336-338^{o}C. Rf: 0.53 (40% methanol/ethyl acetate).

IR (KBr, cm^{-1}) 3422 (-NH), 3175 (aromatic -H), 2949 (aliphatic -H), 1730 (C=O), 1622 (C=N), 1581, 1525 (C=C), 1223, 1240 (C-0).

^{1}H NMR (DMSO-d_6, δ): 10.63 (b, -NH), 10.32 (b, -NH), 9.10 (d, 1H), 9.0 (d, 1H), 8.78 (s, 1H), 8.22 (m, 1H), 8.09 (m, 1H), 7.82-7.70 (m, 6H), 4.62 (2H, q, -N-$\underline{CH_2}$-CH_3), 3.80 (3H, s, 0=C-0-CH_3, 3.63 (3H, s, 0=C-0-CH_3), 1.53 (3H, t, -N-CH_2-$\underline{CH_3}$) (Figure 3.6).

^{13}C NMR (DMSO-d_6, δ, ppm): 163.5, 154.6, 154.2, 142.5, 140.2, 134.1, 131.8, 131.6, 130.4, 129.7, 129.0, 128.7, 128.5, 126.1, 125.7, 124.0, 121.9, 121.5, 117.8, 107.0, 52.6, 50.4, 14.2, 14.0 (see appendix 4).

Elemental analysis (CHNS) Anal. Calcd. For $C_{25}H_{24}N_3O_4Cl$: C, 64.44; H, 5.15; N, 9.02 Found: C, 64.01; H, 5.27; N, 9.17 %.

MS (electron impact, m/z, 100 ev): 430.2 (100.0 %) (M-35.5)$^+$, 372.2 (7.0 %) (M-93)$^+$.

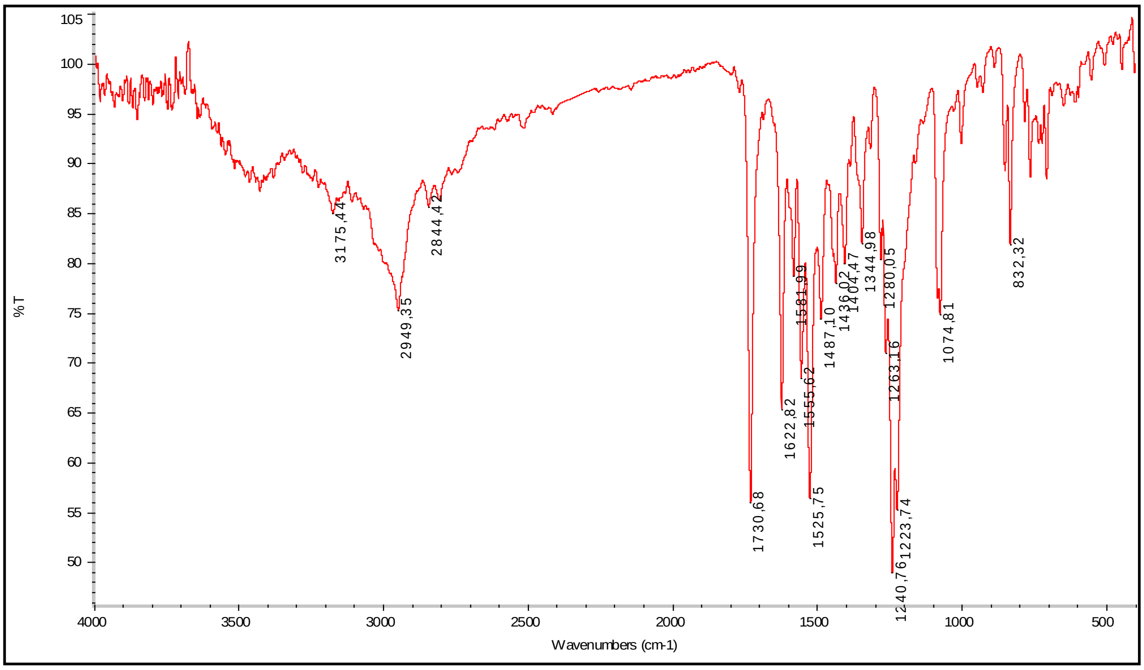

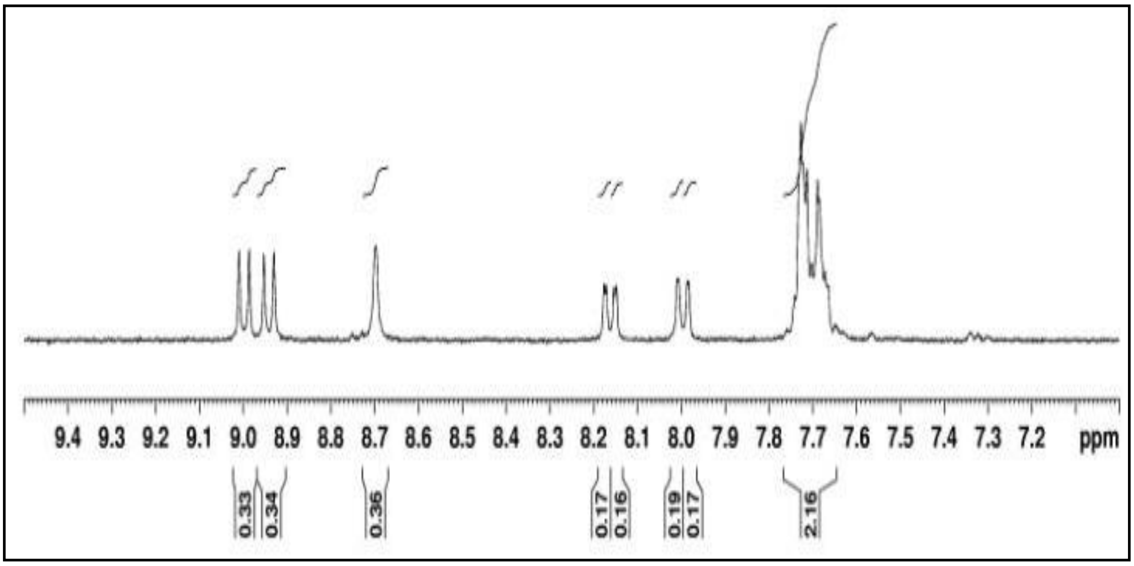

Figure 3.6. IR and ¹H NMR spectra of *E5*.

3.4.2. Procedure

The four compounds exhibited good fluorescent property. Table 3.1.gives fluorescence excitation and emission wavelengths of them in Tris HCl at pH 8.0.

Table 3.1. Fluorescence spectral characteristics of four ethidium derivatives.

Compound	λ_{ex} (nm)	λ_{em} (nm)
E2	313	519
E3	304	517
E4	300	527
E5	300	525

Fluorimetric titration method based on the fluorescence quenching of working molecules by DNA in all experimental studies was used. Fluorescence titrations were performed in a 1 cm quartz cuvette by successive addition of DNA solution to 5.0×10^{-6} M dye solutions in buffer. Their fluorescence intensities decreased regularly with increase of concentration of DNA.

The titration data were analyzed according to Stern-Volmer equation and interaction types of DNA with the four ethidium derivatives were investigated. The Stern-Volmer quenching constants, binding constants, binding sites and the corresponding thermodynamic parameters ΔH, ΔS and ΔG were calculated at different temperatures. In addition, the binding properties of DNA-derivatives were investigated based UV–visible absorption spectra, ionic strength and iodide ion quenching.

n4. RESULTS AND DISCUSSION

4.1. Studies of benzothiazole styrylcyanine derivatives

This group of study was aimed on the clarification of the interaction mode of benzothiazole styrylcyanine monomer and two various structure homodimers modified with spermine-like linkage/tail group (Figure 3.1) with DNA. For this purpose the specificity of the dyes binding to poly(dA-dT)$_2$ and poly(dG-dC)$_2$ polynucleotides was studied. Calculation of the binding constants and the numbers of DNA base pairs occupied by one bound dye molecule were carried out basing on the results of fluorescent titration. Non-substituted benzothiazole styryl dye Sbt (Figure 3.1) was used for the comparison that allowed us to estimate influence of the presence of spermine-like substituents on dye-DNA affinity. Dependence of dye-DNA binding mode on the position of linkage group connecting two chromophores of homodimer was studied.

4.1.1. Determination of the binding constant and the number of DNA base pairs occupied by one bound dye molecule (K_b, n)

The binding constant, K_b, indicates the stability of ligand-DNA complex. This is a useful measure to describe the strength of binding (or affinity) between DNA and their ligands. In the case there is the following equilibrium in the solution:

$$\text{dye} + \text{DNA} \leftrightarrow \text{dye-DNA} \qquad (1)$$

the law of mass action has the following form (McGheen and von Hippel, 1974):

$$\frac{C_{bd}}{C_{fDNA} \times C_{fd}} = K_b \qquad (2)$$

C_{bd}, C_{fd} and C_{fDNA} being concentrations of the dye bound to DNA, dye in free form and DNA binding sites unoccupied by dye molecules, respectively. One of the most difficult points in the K_b study is the determination of C_{fDNA}, taking into account the fact that the dye could occupy several DNA base pairs upon binding. McGhee and von Hippel reported a detailed theoretical study of ligand-DNA interactions accounting for the about mentioned difficulty, which have advantages over linear Scathard plots. In the case of the single mode of ligand-DNA interaction and non-cooperative binding (i.e., neighboring ligands do not influence one another), the following expression of the mass action law (2) was obtained (McGhee and von Hippel, 1974).

$$\frac{v}{L} = K_b(1-nv)\left(\frac{1-nv}{1-(n-1)v}\right)^{n-1} \qquad (3)$$

where L is the free ligand concentration, υ is the binding density (i.e. the number of the bound dye molecules per one DNA base pair), n is the number of DNA base pairs occupied by one bound dye molecule, and K_b is binding constant. Assuming only one type interaction between dye-DNA binding being non-cooperative, K_b and n values can be calculated from fluorimetric titration curves by modifying the formula (Eq. 3). Since the DNA presence sharply increases the dye fluorescence intensity, intrinsic fluorescence of free dye is neglected. Thus the percent of the bound dye value;

$$\frac{C_{bd}}{C_{dye}} = \frac{I}{I_{\max}} \qquad (4)$$

where C_{dye} is the total dye concentration, C_b is the concentration of bound dye to DNA, the maximum value of the fluorescence intensity (I_{max}) is obtained all the dye molecules are bound. Substituting equation (4) into equation (3), we can write the required expression to calculate K_b and n, as;

$$I_{\max} - I = \frac{I}{C_{DNA}K_b} \frac{\left(1-\left[(n-1)\frac{I}{I_{\max}}\frac{C_{dye}}{C_{DNA}}\right]\right)^{n-1}}{\left(1-\left[n\frac{I}{I_{\max}}\frac{C_{dye}}{C_{DNA}}\right]\right)^{n}} \qquad (5)$$

Therefore, we can plot fluorescence intensity as a function of the dye and DNA concentrations:

$$Y = I_{\max} - \frac{X}{C_{dye}K_b} \frac{\left(1 - \left[(n-1)\frac{X}{I_{\max}}\right]\right)^{n-1}}{\left(1 - n\frac{X}{I_{\max}}\right)^{n}} \qquad (6)$$

where Y=I and X=I×C_{dye} / C_{DNA}. Therefore, K_b, n and I_{max} values can be calculated as approximation parameters of fitting by the Eq. 6 the experimentally obtained data plotted as the dependence of Y on X. For the homodimer dyes, the calculation was performed with respect to the whole homodimer molecule.

4.1.2. The effect of interaction with DNA on the absorption and fluorescence spectra of dyes

The characteristics of absorption, fluorescence excitation and emission spectra of the studied dyes in aqueous buffer solution and in the presence of nucleic acids are summarized in Table 4.1. In absorption spectra of studied monomer styryls in Tris HCl buffer were comprised of only band corresponding to the dye monomer maximum. The maxima of absorption spectra for the dyes are located at 512 and 529 nm for Sbt and Bos-5, respectively. Absorption maxima for these dyes in the presence of DNA are shifted to the long wavelength region on 20-30 nm comparing with maxima in buffer and correspond to the dye monomer bound to DNA. Absorption spectra of these two dyes have the similar shape.

In absorption spectra of homodimer styryls dominating bands are blue-shifted as compared to that of the parent monomer Sbt; these bands are settled at 491 and 469 for DBos-13 and DBsu-10, respectively. Basing on the results (Tokar, et.al., 2006; Zeena and George Thomas, 2001) where the dimers with the same chromophore were regarded, it showed that mentioned absorption bands belong to H-aggregates of the dimer dyes. For homodimers DBos-13 and DBsu-10 the changes in absorption spectra caused by DNA presence are different. In the presence of DNA absorption band of DBos-13 was strongly red-shifted (491 nm for free dye and 554 nm for dye-DNA complex), corresponding to the dye monomers bound to DNA. For DBsu-10 H-aggregates band is shifted to the short wavelength region on 9 nm relative to the corresponding band of dye in buffer. Basing on the shift of the H-aggregate band caused by DNA presence, one can conclude that the aggregates are formed on the DNA molecule. The increasing concentration of DNA results in a decrease of the H-aggregates absorption band intensity and an increase in band of the dye molecules bound to DNA in monomer form.

Table 4.1. Characteristics of absorption spectra of styrylcyanine dyes in buffer and in complexes with DNA (6.0×10^{-4} M)

Dye	Free dye				In DNA presence				
	λ_{abs}	λ_{ex}	λ_{em}	I	λ_{abs}	λ_{ex}	λ_{em}	I	I/I_0
Sbt	512	525	593	17.9	541	555	603	1633.3	91.2
Bos-5	529	542	598	20.1	559	568	608	2005.9	99.8
DBos-13	491	540	596	1.5	554	560	606	1899	1266
DBsu-10	469	560	613	9.1	460	555	610	1253.6	137.8

4.1.3. Monomer dyes

Two styrylcyanines unsubstituted (Sbt) and modified with spermine-like tail group (Bos-5), were studied in comparison to characterize stability of monomeric dye-DNA complex and to study the influence of mentioned above substituent on affinity of DNA-dye complexes.

Absorption and fluorescence spectra of the dyes in presence of different DNA concentrations were studied. The absorption spectra of the both dyes in presence of 0-6.0×10^{-4} M DNA (Figures 4.1 and 4.2) consist of the two bands corresponding to the non-bound (maxima at 510 nm for Sbt and at 530 nm for Bos-5) and DNA-bound (542 nm for Sbt and at 558 nm for Bos-5) monomer forms of dye.

Since for both Sbt and Bos-5 the absorption spectra of the dye in presence of different DNA concentrations cross near the isobestic point, one can generally consider the equilibrium between the nonbound and DNA bound dye molecules in monomer form in the solution:

$$\text{dye} + \text{DNA} \leftrightarrow \text{dye-DNA} \qquad (1)$$

The parameters of the equilibrium (1) could then be found using the equation developed by McGhee and von Hippel.

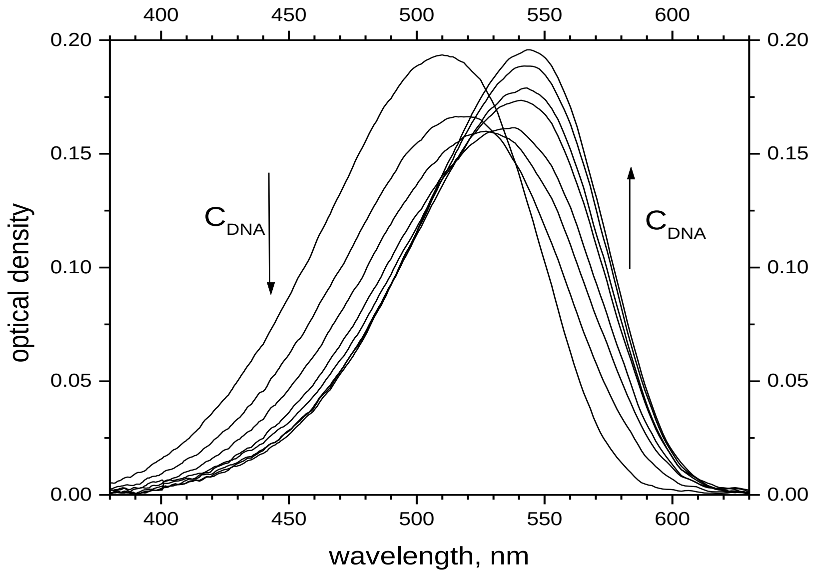

Figure 4.1. Absorption spectra of the dyes Sbt in Tris HCl buffer in the presence of 0-6.0×10^{-4} M DNA. The dye concentration used for the measurements was 5×10^{-6} M.

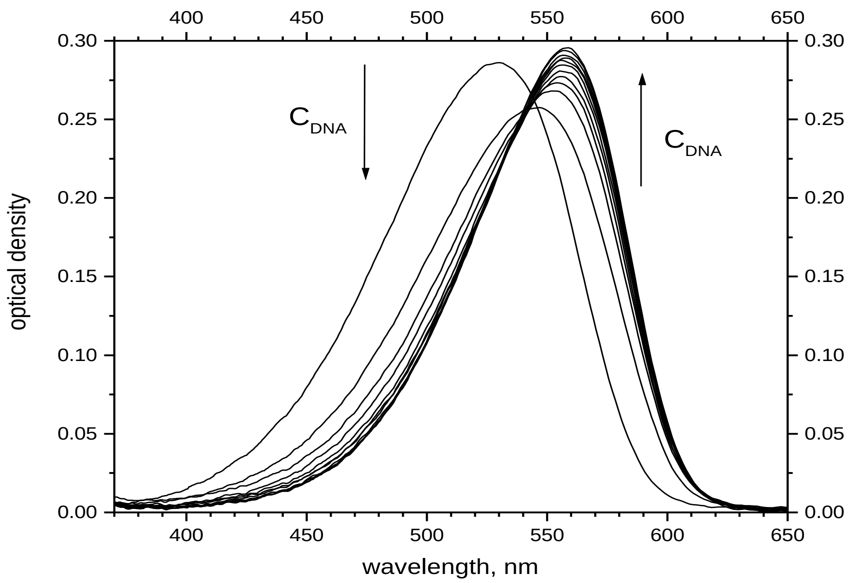

Figure 4.2. Absorption spectrum of the dye Bos-5 in Tris HCl buffer in the presence of 0-6.0×10^{-4} M DNA. The dye concentration was 5×10^{-6} M.

The binding constants (K_b) and the the number of DNA base pairs occupied by one bound dye molecule (n) for the dyes Sbt and Bos-5 were estimated by fluorimetric titrations. The approximation of the experimental results with the McGhee and von Hippel equation (Eq. 6; Figures 4.3 and 4.4) shows that for the both dimer dyes the mentioned equation generally correctly describes the obtained results. Binding constants (K_b) and the number of DNA base pairs occupied by one bound dye molecule (n) values are summarized for studied dyes in Table 4.2.

Table 4.2. Binding constant (K_b) and the numbers of DNA base pairs occupied by one bound dye molecule (n) values of investigated dyes.

Dye	K_b, 10^4 M^{-1}	n
Sbt	1.8 ± 0.3	3.4 ± 0.8
Bos-5	6.2 ± 0.9	2.3 ± 0.5
DBos-13	10.0 ± 1.4	4.9 ± 2.2
DBsu-10	2.7 ± 0.8	14.5 ± 3.2

The average K_b values obtained for dyes Sbt and Bos-5 were respectively 1.8×10^4 $M^{-1}$and 6.2×10^4 M^{-1}, the number of DNA base pairs occupied by one bound dye molecule (n) were 3.4 and 2.3. Such values of K_b show that Sbt and Bos-5 form stable complexes with DNA. It should be noted that K_b values for Bos-5 is four times higher for than that Sbt. Since the structures of these two monomer styryls differ from each other by N-alkyl ammonium substituent (spermine tail group) we can notify that incorporation of this substituent leads to the increase of dye affinity to DNA.

Binding constant (K_b) values for intercalators that bind to DNA usually do not exceed 10^7 M^{-1}. K_b values of acridine orange (AO), thiazole orange (TO), and ethidium bromide (EB) are equal to 5.03×10^4, 10^6 and 1.5×10^5 M^{-1}, respectively (Neidle, 1994; Rye, et.al., 1993; Rye, et.al., 1991). The n value for Bos-5 (2.3) implies that dye can interact with DNA by intercalation mode, since in the case of groove-binding this dye would occupy at least 3 base pairs. Meanwhile, the same value for Sbt (3.4) could be consistent with both intercalation and groove binding.

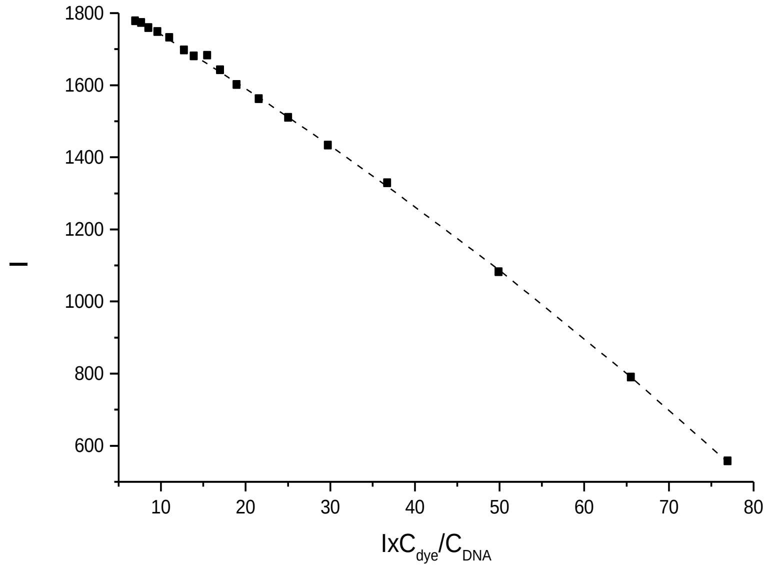

Figure 4.3. Plot of dependence of fluorescence intensity to C_{dye}/ C_{DNA} ratio versus fluorescence intensity of Sbt.

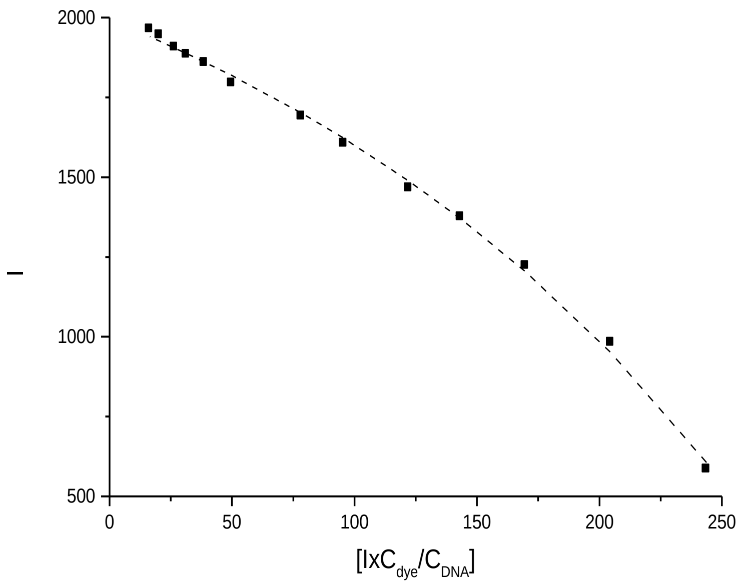

Figure 4.4. Plot of dependence of fluorescence intensity to C_{dye}/ C_{DNA} ratio versus fluorescence intensity of Bos-5.

At the same time, the binding constant values obtained for these dyes are typical for both intercalators and groove-binders as well. In order to obtain more information about the binding mechanism of Sbt and Bos-5, the dyes fluorescent properties of the dyes in the presence of AT- and GC-containing polynucleotides were studied (Table 4.3).

Table 4.3. Characteristics of fluorescence spectra of styrylcyanine dyes in complexes in the presence of poly(dA-dT)$_2$ and poly(dG-dC)$_2$ polynucleotides.

Dye	I_0	poly(dA-dT)-poly(dA-dT)				poly(dG-dC)-poly(dG-dC)			
		λ_{ex}(nm)	λ_{em}(nm)	I^{AT}	I^{AT}/I_0	λ_{ex}(nm)	λ_{em}(nm)	I^{GC}	I^{GC}/I_0
Sbt	19.1	548	601	658	34.5	562	607	756	39.6
Bos-5	24.8	566	608	1695	68.3	575	612	996	40.2
DBos-13	2.2	557	606	1455	661.4	562	608	1445	656.8
DBsu-10	6.1	551	596	729	119.5	574	614	82	13.4

Both dyes Sbt and Bos-5 showed large enhancement of fluorescence intensity in the presence of both poly(dA-dT)$_2$ and poly(dG-dC)$_2$ polynucleotides. Small preference to GC-containing DNA sequences over the AT-containing ones observed for Sbt could evidence for its binding with DNA *via* intercalation. At the same time, for Bos-5 the preference to AT-sequence was observed. Nevertheless, the fluorescence intensity of Bos-5 in the presence of poly(dA-dT)$_2$ (I^{AT}) is only in 1.7 times higher than the same value in the presence of poly(dG-dC)$_2$ (I^{GC}), while for the groove-binding dyes I^{AT} generally exceeds I^{GC} for an order of magnitude. Thus taking into account the n value for Bos-5, we could consider the intercalation mode of interaction to be more consistent with the experimental results as compared to the groove-binding one.

4.1.3. Homodimer dyes

Interaction of two benzothiazole styryl homodimers DBos-13 and DBsu-10 that differs from each other by the position of linkage group with DNA and synthetic polynucleotides poly(dA-dT)$_2$ and poly(dG-dC)$_2$ was studied.

Absorption spectra of the both dyes in the presence of different DNA concentrations are presented in the Figures 4.5 and 4.6.

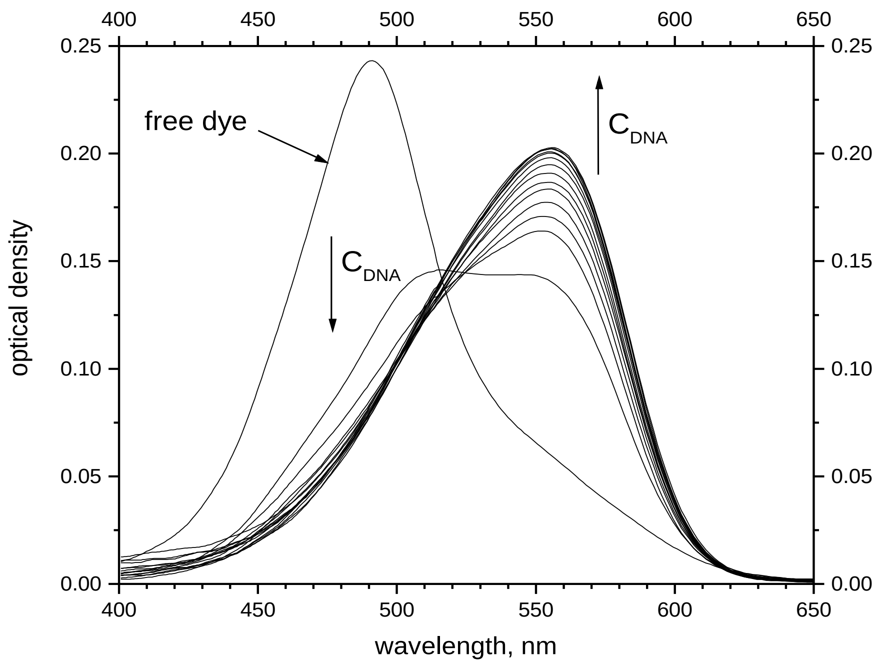

Figure 4.5. Absorption spectrum of the dye DBos-13 in Tris HCl buffer in the presence of 0-6.0×10^{-4} M DNA. The dye concentration was 2.5×10^{-6} M of dimer molecules.

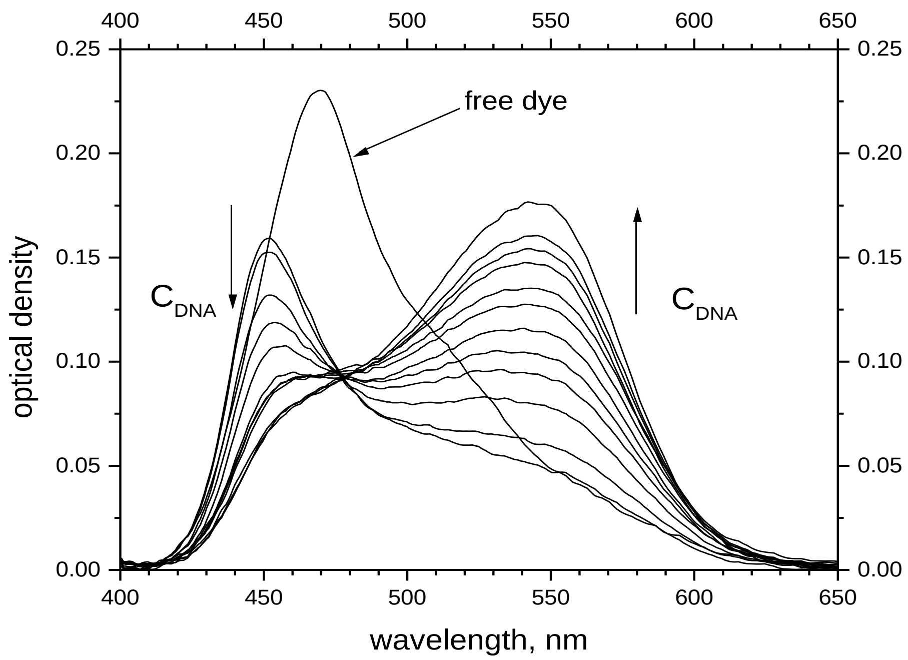

Figure 4.6. Absorption spectrum of the dye DBsu-10 in Tris HCl buffer in the presence of 0-6.0×10^{-4} M DNA. The dye concentration was 2.5×10^{-6} M of dimer molecules.

For the both DBos-13 and DBsu-10 in free form, the absorption spectrum belongs to the aggregates of the H-type (maxima at 491 and 470 nm respectively). The addition of the small DNA amount causes the appearing of new aggregate bands in absorption spectra of the both dyes, which could be attributed to the dye H-aggregates bound with the DNA. It should be mentioned that while in the case of DBsu-10 only one band (at 452 nm) corresponding to H-aggregates is observed, the behavior of the DBos-13 spectra is more complicated. Besides the maximum near 510 nm, in the absorption spectrum of DBos-13 in DNA presence one more aggregation band situated at about 460 nm and manifested as a shoulder could be observed. Further addition of DNA leads to the decrease of mentioned H-aggregate bands in the spectra of the both dyes and increase of the band corresponding to the dye monomers bound to DNA (556 nm for DBos-13 and 545 nm for DBsu-10).

Thus, in the studied solutions of the dimer dyes in presence of DNA, the equilibrium takes place between the dye H-aggregates formed on DNA and dye monomers bound to DNA, besides, in the case of DBos-13 at least two kinds of H-aggregates exist. Thus, the equilibrium equations should be much more difficult for both dimmer dyes as compared to the equation (1), and the McGhee and von Hippel equation cannot be correctly applied to the binding of DBos-13 and DBsu-10 with DNA. Nevertheless, the McGhee and von Hippel equation turned out to give adequate approximation of the dependence of I on $I \times C_{dye}/C_{DNA}$ (Figures 4.7 and 4.8). The values of K_b and n obtained as the approximation parameters are presented in the Table 4.2.

Significant difference in *n* values (Table 4.2) observed for DBos-13 and DBsu-10 dyes points that due to the distinctions of structures these homodimer dyes interact with DNA *via* different mechanisms. DBos-13 has a positively charged linkage which is bounded to the nitrogen atoms of benzothiazole ring. At the same time, in DBsu-10 the linkage group is attached in the 6-position of benzothiazole residues. The value of n for DBos-13 (4.9) points to the bis-intercalative DNA-binding mechanism for this dye, while the same value for DBsu-10 (n = 14.5) clearly demonstrates the groove-binding mechanism of the interaction of this dye with the DNA.

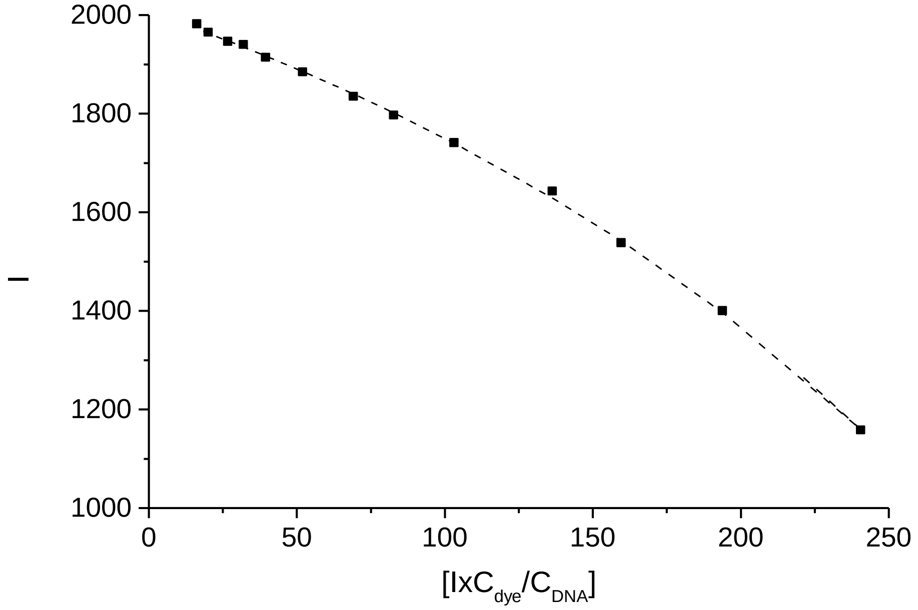

Figure 4.7. Plot of dependence of fluorescence intensity to C_{dye}/ C_{DNA} ratio versus fluorescence intensity of DBos-13.

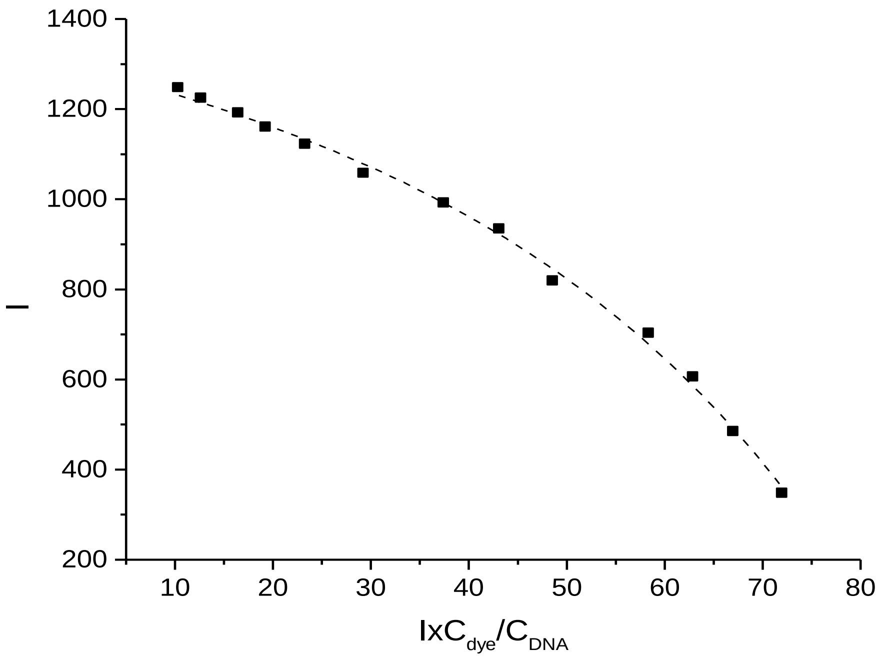

Figure 4.8. Plot of dependence of fluorescence intensity to C_{dye}/ C_{DNA} ratio versus fluorescence intensity of DBsu-10.

On the other hand, K_b values for the both dyes (10.0×10^4 M^{-1} for DBos-13 and 2.7×10^4 M^{-1} for DBsu-10) could be characteristic for both groove-binding and intercalation. Nevertheless, the high exceed of the K_b value for DBos-13 over this for DBsu-10 is consistent with the intercalation binding mode for the first dye and the groove-binding for the last one.

The study of the fluorescent properties of the dyes in the presence of AT- and GC-containing polynucleotides (Table 4.3) showed almost the same I^{AT} and I^{GC} values for DBos-13. This result evidences for the dye intercalation into the DNA supporting the supposition made before basing on the n value for this dye. The possible structure of DBos-13 intercalation complex with DNA is presented in the Figure 4.9a. This structure corresponds to the case when the dye molecule occupies 5 base pairs (accounting for the nearest neighbor exclusion principle). Nevertheless, the model of bis-intercalation provides the possibility for DBos-13 chromophores to be situated in the DNA on different distances one to another due to the flexible linking group.

At the same time, the dye DBsu-10 demonstrates the high specificity to AT-sequence (I^{AT} exceeds I^{GC} in almost 9 times) that points on the groove binding mode of DBsu-10 interaction with DNA. This result is consistent with the high *n* value for this dye. Besides, the intercalation seems to be spatially hindered for the structure with the linkage group attached in the 6-position of the benzothiazole residue. The possible structure of DBsu-10 complex with DNA formed by groove-binding mode is presented in the Figure 4.9b. It is seen from this figure that the DBsu-10 dye molecule occupies approximately 9-10 base pairs that is generally consistent with the *n* value obtained as the result of approximation. Higher value obtained in the experiment (n=14.5) could be explained by the preference of the groove-binding molecules to AT-rich sequences.

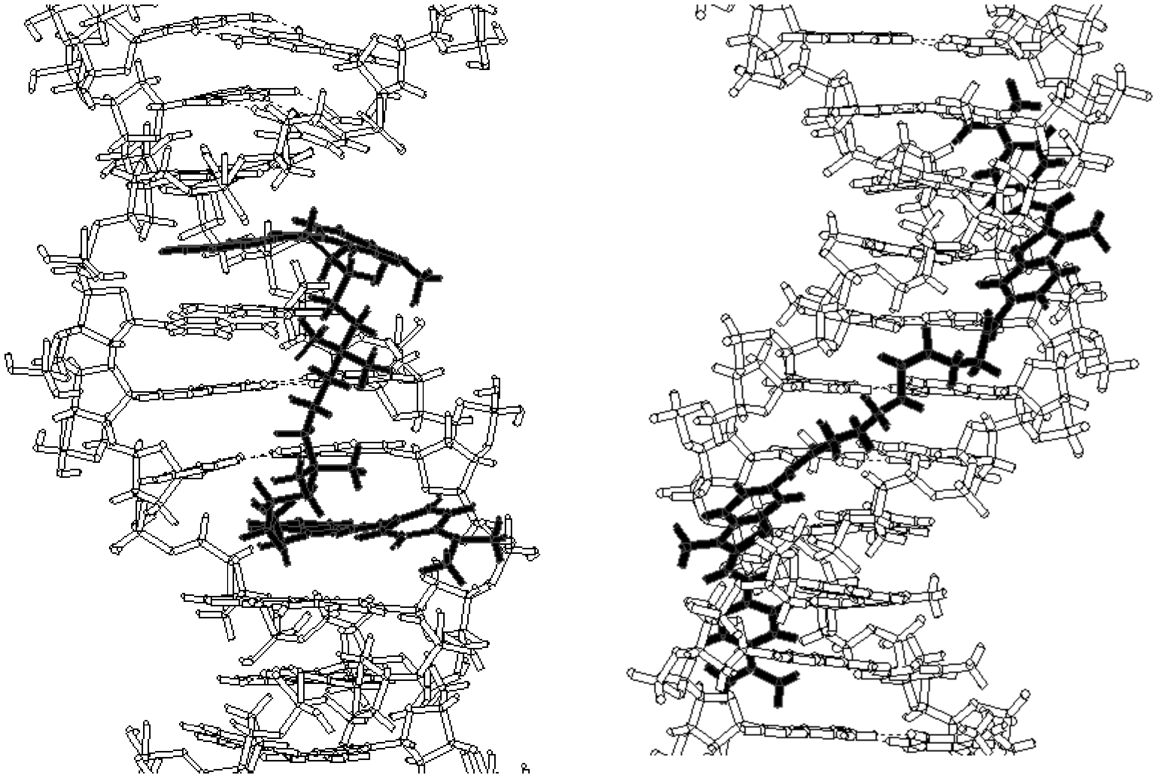

Figure 4.9. The possible structures of DBos-13 intercalation complex **(a)** and DBsu-10 groove-binding complex **(b)** with DNA.

4.1.4. Comparison of monomer and homodimer dyes

The study of the equilibrium parameters of dyes binding with DNA revealed several results.

- First of all, the presence of spermine-like tail group in the monomer molecule leads to the increase of K_b in about three times, thus to stabilization the dye-DNA complex.
- Second, for a dimer with the positively charged linkage which is bounded to nitrogen atoms of benzothiazole ring (DBos-13) the estimated binding constant increases in 5 times as compared to the parent monomer Sbt. It should be also noticed that for the both monomers and the DBos-13 dimer, the study of dyes sensitivity for AT- and GC-sequences of DNA point to the intercalative mechanism of dye-DNA binding, that is consistent with the obtained values of *n*.

  Finally, for the dimer dye with the linkage group containing quaternary nitrogen atoms and bound in 6, 6 positions of benzothiazole heterocycle

(DBsu-10), the value of K_b was close to this of the parent dye Sbt. It could be explained by groove binding mode of DBsu-10 interaction with DNA.

- The evidences for this mechanism are
    - the large value of binding site length (n=14 base pairs), and
    - the strong preference to the AT-containing DNA sequence over the GC-containing ones.

4.2. Studies of ethidium derivatives

The cationic dye ethidium bromide (EB) is used as major intercelation agent for DNA in many years (Alonso, et.al., 2006; Labieniec and Gabryelak, 2006). It emits intense fluorescence light in the presence of DNA. Its chemical structure is shown in Figure 4.10. It has been widely utilized in biochemical and biophysical applications as a fluorescent stain. In literature, novel ethidium derivatives have been proposed as DNA probes and compared their DNA affinity and toxicity with EB. They have been synthesized via exocyclic amines at 3- and 8-positions or 6-position of phenyl ring. Also, 5-substitued ethidium derivatives have also been synthesized recently (Rangarajan and Friedman, 2007). But some novel derivatives possess significantly lower or no DNA affinities when compared to EB.

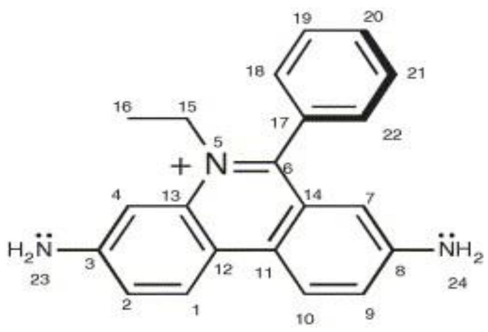

Figure 4.10. Chemical structure of EB showing numbering system.

The most derivatives of ethidium were synthesized via exocyclic amines (Luedtke, et.al., 2003; Garbett, et.al., 2004). The exocyclic amines of ethidium are poor nucleophiles and have weak basic properties. The lone pair on the 3-amine can easily delocalize onto the quaternary nitrogen atom. Hence, 8-amine has much more nucleophilic and basic properties than 3-amine. For this reason, it has more electron deficient and less reactivity against electrophiles (Figure 4.11). Therefore each of the ethidium's exocyclic amines cannot be protected easily via some protecting group. For protecting of exocyclic amines more stronger electrophiles or highly basic medium must be used. The exocyclic amines of ethidium are known to be important for DNA binding. Indeed modification of one or both, of these amines was affected electronic structure of ethidium as well as the nucleic acid affinity and specificity of the resulting derivatives. Although some ethidium's exocyclic amines derivatives have similar DNA affinity as ethidium.

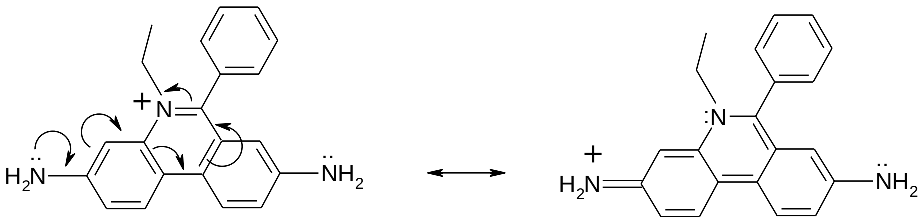

Figure 4.11. Resonans structures of exocyclic amines of EB at 3-position.

In this work, new ethidium derivatives synthesized, characterized and investigated to DNA affinities (Figure 3.2). The protecting of exocyclic can be formed regioisomers. Seperation and isolation of each regioisomers is very difficult because of similar retention time. In this experiment conditions, regioisomers of each compounds were not formed. In addition, this synthesis method was very simple, fast, effective and high yield to obtained ethidium derivatives. Each of the exocyclic amines can be protected easily in a one-pot reaction with benzoyl chloride, phenylacetyl chloride, ethyl chloroformate and methyl chloroformate. Then the main products were obtained as bis derivatives of ethidium (Luedtke et.al,2005).

4.2.2. The effect of interaction with DNA on the fluorescence of derivatives

The fluorescence emission spectra of 5.0×10^{-6} M *E2, E3, E4* and *E5* had been obtained in the presence of various concentrations of DNA (Figures 4.12, 13, 14 and 15). The results showed that the fluorescence intensities of derivatives decreased with the increasing concentration of DNA. But there was no each significant λ_{em} shift with the addition of DNA. These data indicated that DNA could interact with each derivative and quench its fluorescence.

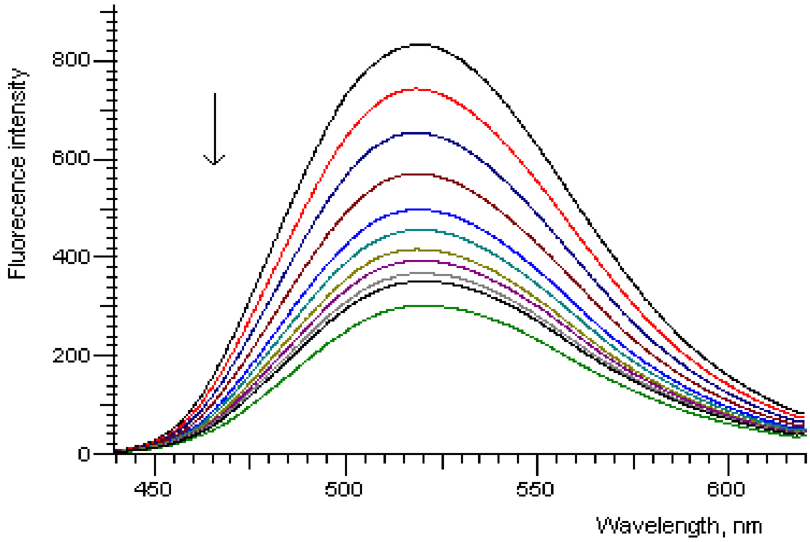

Figure 4.12. Fluorescence emission spectra of 5.0x10^{-6} M E2 in the presence of DNA. Conditions: λ_{ex} = 313 nm, the concentration of DNA from highest curve to lowest is 0, 1.5, 3.0, 4.5, 6.0, 7.5, 9.0, 10.5, 12, 13, 16.5, 19.5 (x10^{-7}) M

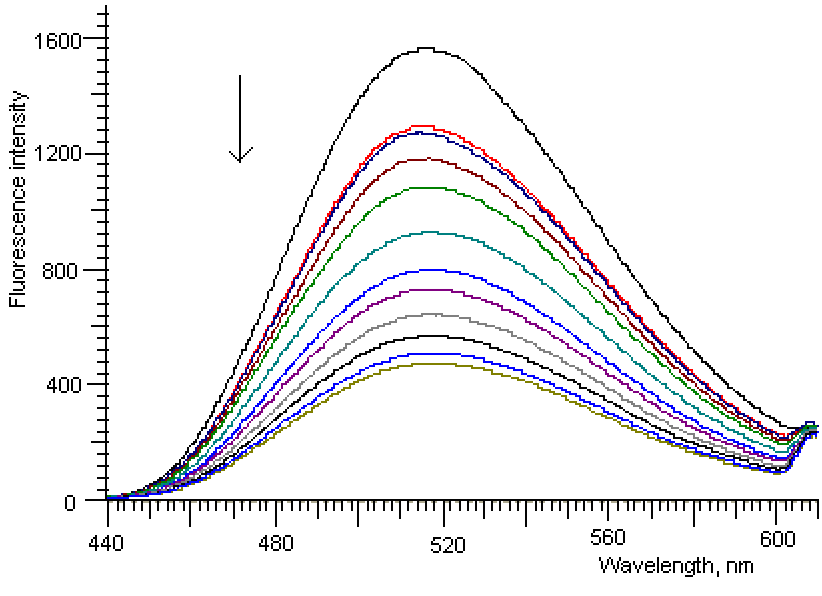

Figure 4.13. Fluorescence emission spectra of 5.0x10^{-6} M E3 in the presence of DNA. Conditions: λ_{ex} = 304 nm, the concentration of DNA from highest curve to lowest is 0, 7.5, 9.0, 10.5, 12, 13.5, 15,18, 21, 24, 27, 30, 31 (x10^{-8}) M.

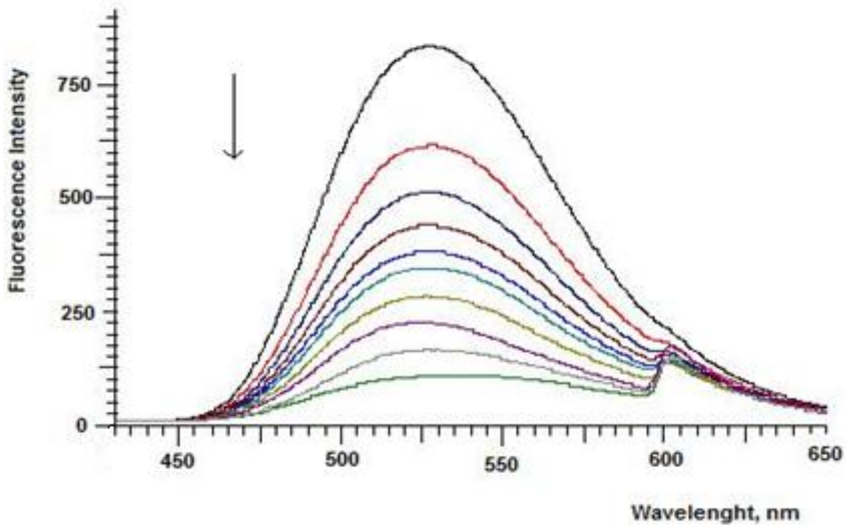

Figure 4.14. Fluorescence emission spectra of $5.0x10^{-6}$ M E4 in the presence of DNA. Conditions: λ_{ex} = 300 nm, the concentration of DNA from highest curve to lowest is 0, 1.2, 2.4, 3.6, 4.8, 6.0, 8.4, 10.8, 13.2, 18 ($x10^{-5}$) M.

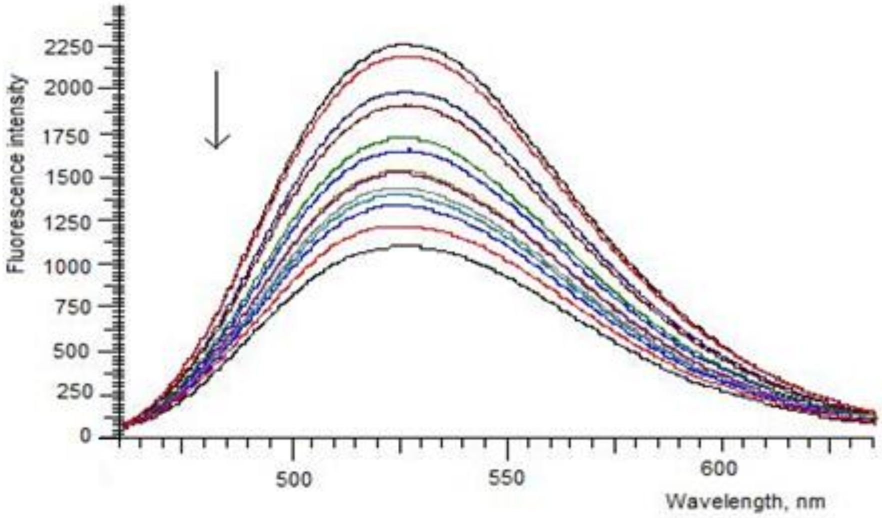

Figure 4.15. Fluorescence emission spectra of $5.0x10^{-6}$ M E5 in the presence of DNA. Conditions: λ_{ex} = 300 nm, the concentration of DNA from highest curve to lowest is 0, 3.0, 6.0, 9.0, 12, 15, 18, 21, 24, 27, 30, 36 ($x10^{-6}$) M

The fluorescence intensity of a compound can be decreased (called as *quenching*) by a variety of molecular interactions such as excited–state reactions, molecular rearrangements, energy transfer, ground state complex formation and collosional quenching. The mechanisms of these processes are usually classified as either dynamic or static quenching, and they can be distinguished by fluorescence measurements at different temperatures. Dynamic quenching depends on molecular diffusion; generally, larger diffusion coefficients are obtained at higher temperatures, and the bimolecular quenching constants are expected to increase with increasing temperature. In contrast, stability of complexes decreases with increasing temperature, and thus static quenching constants are obtained lower values. The fluorescence quenching data were analyzed according to the *Stern–Volmer* equation (Lakowicz, 2006),

$$F_0 / F = 1 + K_{SV}[Q] = 1 + \tau_0 k_q [Q]$$

where, F_0 and F are the fluorescence intensities of *E2, E3, E4* and *E5* before and after the addition of DNA, respectively. [Q] is concentration of DNA as quencher. K_{SV} is the Stern–Volmer quenching constant, k_q the quenching rate constant of biomolecule, τ_0 the average lifetime of the fluorescent molecule in the absence of quenching reagent and its value is about 10^{-8} s (Quiao, et.al., 2008), and $K_{SV} = \tau_0 k_q$.

Linear Stern-Volmer plots were obtained from the fluorescence titrations under different temperatures for the all derivatives with DNA (Figures 4.16 and 17). *Ksv* values were found from slopes of these graphs (Table 4.4). The results showed that *Ksv* decreased with increased temperature, suggesting that the probable quenching mechanism of fluorescence of all derivatives by DNA was *static quenching* procedure.

Also, the quenching rate constants k_q calculated from $K_{SV} = \tau_0 k_q$. The order of magnitude of k_q was calculated as $10^{12\text{-}14}$ $M^{-1}s^{-1}$ in this study. According to the literature (Sun, et.al., 2008) for dynamic quenching the upper limit of k_q expected for a diffusion-controlled bimolecular quenching rate constant of various quenchers with biomolecules is 10^{10} $M^{-1}s^{-1}$. Considering that in quenching experiments, the rate constants of all derivatives quenching procedure initiated by DNA were much greater than 10^{10} $M^{-1}s^{-1}$. It can be concluded that the quenching is not initiated by dynamic quenching, but probably by *static quenching* from the formation a complex between of each derivative and DNA.

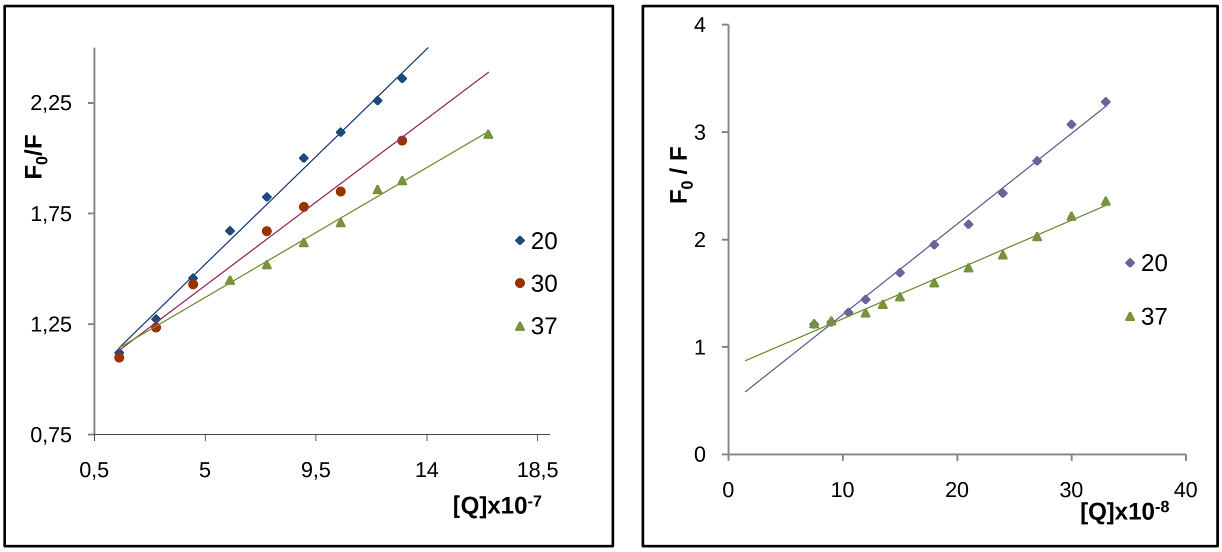

Figure 4.16. The Stern-Volmer plots for the interaction of E2 (left) and E3 (right) with DNA at different temperatures. [E2]= [E3]=5.0x10-6 M.

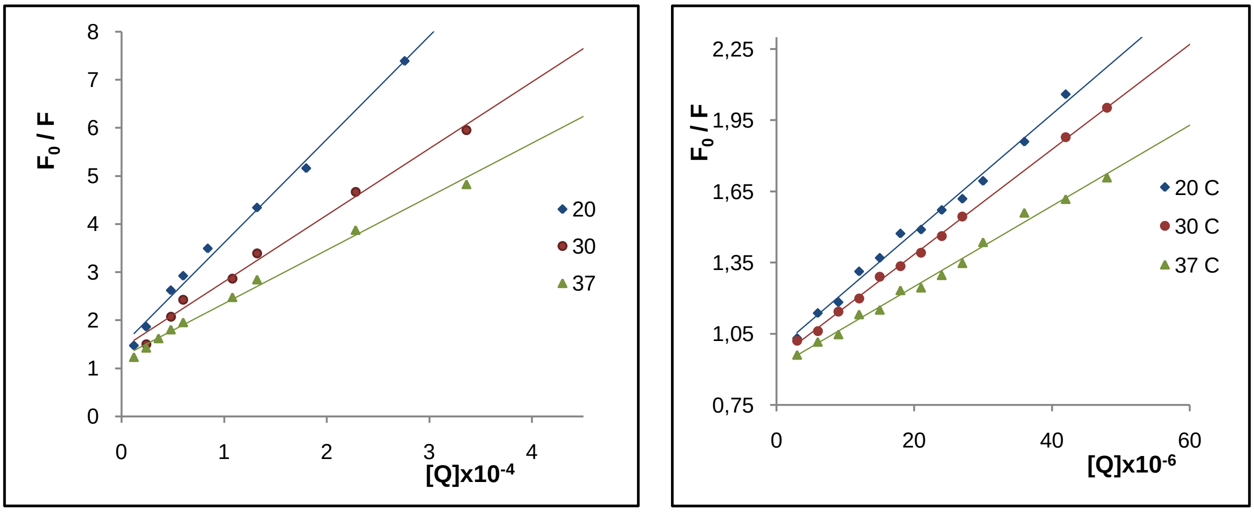

Figure 4.17. The Stern-Volmer plots for the interaction of E4 (left) and E5 (right) with DNA at different temperatures. [E4]= [E5]=5.0x10-6 M.

Table 4.4. Stern-Volmer data for ethidium derivatives-DNA.

Dye	˚C	Linear regression equation	K_{sv} (M^{-1})	R^2
E2	20	$F_o/F = 0.9802 + 1.082x10^6[Q]$	$1.082x10^6$	0.991
	30	$F_o/F = 1.005 + 8.380x10^5[Q$	$8.380x10^5$	0.993
	37	$F_o/F = 1.045 + 6.520x10^5[Q]]$	$6.520x10^5$	0.993
E3	20	$F_o/F = 0.4568 + 8.440x10^6 [Q]$	$8.440x10^6$	0.994
	37	$F_o/F = 0.8025 + 4.590x10^6 [Q]$	$4.590x10^6$	0.990
E4	20	$F_o/F = 1.462 + 2.151x10^4 [Q]$	$2.151x10^4$	0.992
	30	$F_o/F = 1.416 + 1.385x10^4[Q]$	$1.385x10^4$	0.990
	37	$F_o/F = 1.238 + 1.111x10^4 [Q]$	$1.111x10^4$	0.993
E5	20	$F_o/F = 0.9797 + 2.49x10^4 [Q]$	$2.49x10^4$	0.992
	30	$F_o/F = 0.9075 + 2.21x10^4 [Q]$	$2.21x10^4$	0.999
	37	$F_o/F = 0.9407 + 1.70x10^4 [Q]$	$1.70x10^4$	0.993

4.2.3. Analysis of binding equilibria

For the static quenching, if it is assumed that there are similiar and independent binding sites in the biomolecule, the binding constant can be got from the double logarithm regression curve of log $(F_0–F) / F$ versus log[Q] based on the following equation (Sun, et.al., 2008),

$$\log (F_0–F) / F = \log K_b + n \log[Q]$$

where K_b is the binding constant and site number n can be determined by the slope of double logarithm regression curve based on the equation. Linear double logarithm regression curves were obtained from the fluorescence titrations under three different temperatures for *E2, E4, E5* and two different temperatures for *E3*.

Figures 4.18 and 4.19 show the plots of log $(F_0–F)/F$ versus log[*Q*] of *E2, E3, E4* and *E5* in the presence of DNA under studied temperatures.

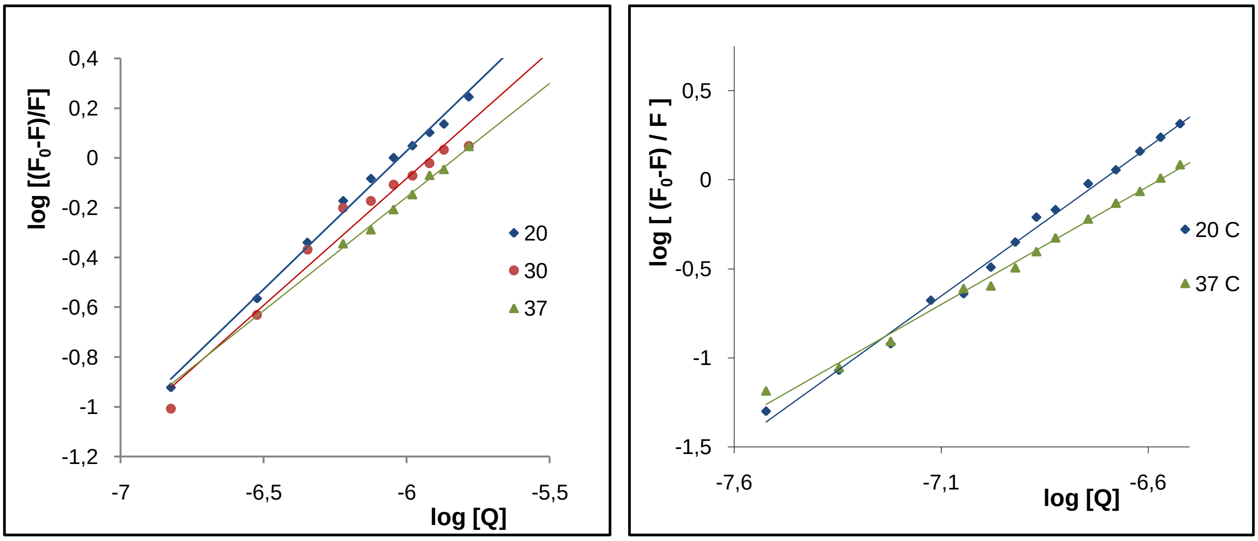

Figure 4.18. Double-log plots of DNA quenching effect on *E2* (left) and *E3* (right) fluorescence at different temperatures.

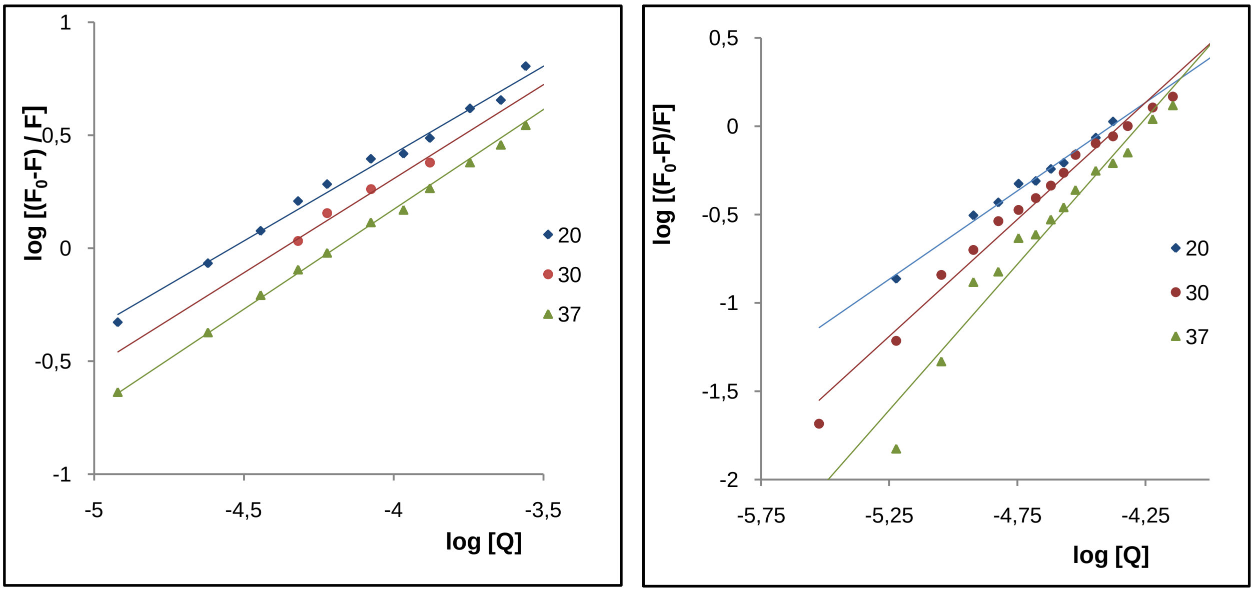

Figure 4.19. Double-log plots of DNA quenching effect on *E4* (left) and *E5* (right) fluorescence at different temperatures.

Table 4.5 gives the calculated K_b and n for *ethidium derivatives*-DNA. It was found that the binding constants decreased with the increasing of temperature, resulting in a reduction of the stabilities of *E2* and *E3*-DNA complexes. But comparing the binding constants and binding site numbers of two groups, *E3* has greater binding affinity to DNA than *E2*. It can be seen that this property increases with increasing nucleophilic characters of functional groups. When *E4* and *E5* were checked against to each other, we encountered unexpected result. In spite of the *E4*'s larger –R groups bounded to ester groups, *E5* showed the larger binding affinity to DNA. Our expectance was to obtain the similar results with *E2* and *E3*, but we observed that molecules which have ester groups beside amide groups exhibited inverse effect with amides. In amides larger functional group which has higher nucleophilic character showed the larger affinity but in esters a smaller group which has lower nucleophilic character showed larger affinity. And also stability of ester-DNA complexes and binding site numbers were increased at higher temperatures.

Table 4.5. Binding constant Kb and the number of binding sites n for ethidium derivatives-DNA.

Dye	˚C	Equation	K_b (M^{-1})	n	R^2
E2	20	log $(F_0–F)/F$=log 6.6936 +1.1112 log [Q]	4.939×10^6	1.1112	0.994
	30	log $(F_0–F)/F$=log 6.0329+1.0193 log [Q]	1.079×10^6	1.0193	0.966
	37	log $(F_0–F)/F$=log 5.3225+0.9134 log [Q]	2.101×10^5	0.9134	0.992
E3	20	log $(F_0–F)/F$=log 11.228 +1.6732 log [Q]	1.690×10^{11}	1.6732	0.994
	37	log $(F_0–F)/F$ =log 8.7197 +1.3267 log[Q]	5.240×10^8	1.3267	0.994
E4	20	log $(F_0–F)/F$=log 3.5106+0.7728 log [Q]	3.24×10^3	0.772	0.994
	30	log $(F_0–F)/F$ =log 3.6369+0.8322 log [Q]	4.14×10^3	0.839	0.993
	37	log $(F_0–F)/F$ =log 3.7051+0.8833 log [Q]	5.07×10^3	0.883	0.997
E5	20	log $(F_0–F)/F$=log 4.3847+1.0003 log [Q]	2.425×10^4	1.0003	0.992
	30	log $(F_0–F)/F$ =log 5.7556+1.3230 log [Q]	5.696×10^5	1.3230	0.982
	37	log $(F_0–F)/F$ =log 7.0598+1.6511 log [Q]	1.147×10^7	1.6511	0.955

We proposed a series of following studies that characterize and distinguish interactions of *E2, E3, E4* and *E5* with DNA in terms of surface binding, intercalation and groove binding.

4.2.4. Iodide ion quenching investigation

Anionic quencher, base pairs below and above the intercalator would hinder the accessibility of fluorescent probe to quencher. In addition electrostatic repelling between DNA phosphate backbone and anionic quenchers will support the protection of intercalated species (Qui, et.al., 2007). The groove binders are influenced from the solvent surrounding of helix much more than intercalators. Iodide ion is a dynamic, or collision, fluorescence quencher for the small fluorescent molecules. It can effectively quench the fluorescence of a small molecule. Steady-state quenching experiments using iodide ion as anionic quencher may provide further information about the binding of probe molecule with DNA.

In this group study, when KI solution ranged from 0.01 to 3 mM was added in the presence of DNA, particular quenching was observed in *E2* and *E3*-DNA systems (Figure 4.20). But increasing KI concentration did not change the quenching amount. The quenching by the addition KI at the beginning was thought as quenching effect of KI on free probe. These are consistent with intercalation rather than groove binding into the DNA helix.

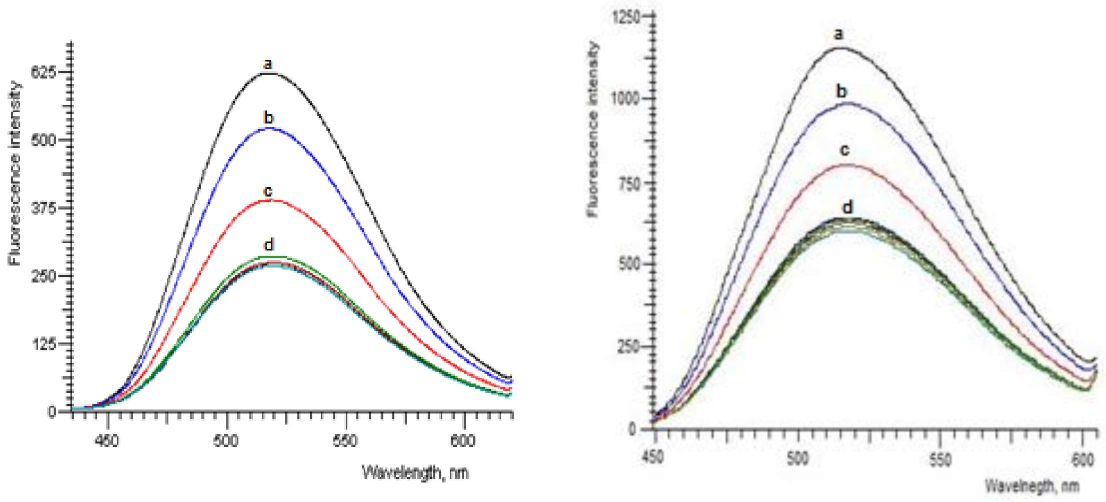

Figure 4.20. Fluorescence emission spectra of *E2*-DNA (left) and *E3*-DNA (right) system in the presence of KI.

(a)*E2* (black line)
(b)*E2* in the presence of 1mM KI (blue line)
(c)*E2*-DNA system (red line)
(d)System in the presence of 0.0125-1 mM KI

(a) *E3* (black line)
(b) *E3* in the presence of 0.25 mM KI (blue line)
(c) *E3*-DNA (red line)
(d) System in the presence of 0.98 μM-0.25 mM KI

The KI quenching experiments had been also performed to further deduce the interaction mode of the fluorescence probe *E4* and *E5* with DNA. The quenching behaviors of KI in the *E4*-DNA and *E5*-DNA systems were shown in Figure 4.21. In these studies, quenching of fluorescence yield of *E4* and *E5* were increased by the increasing KI concentration. We concluded that the KI ripped off E4 and E5 molecules from DNA helix. These can be evidence that *E4* and *E5* interact with DNA on groove binding mode.

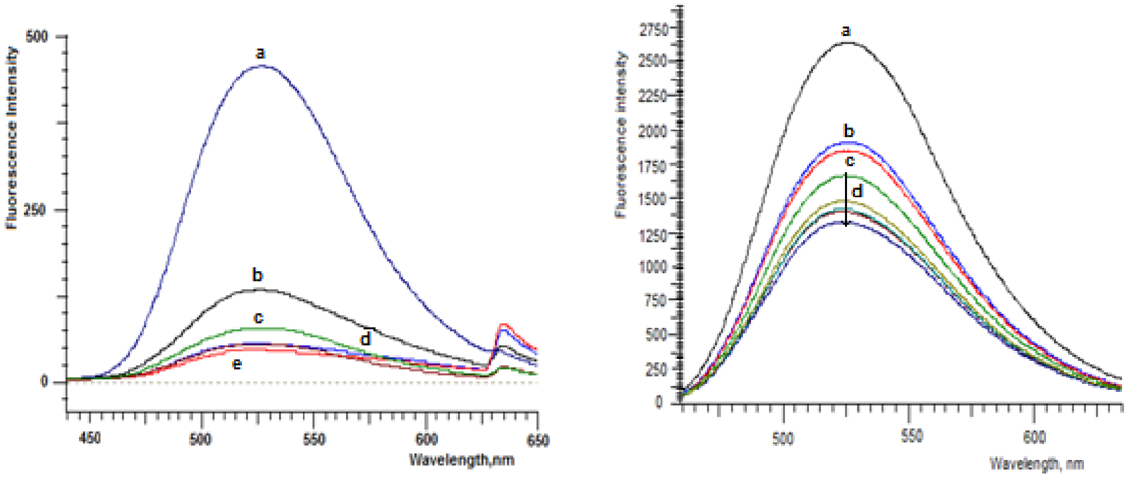

Figure 4.21. Fluorescence emission spectra of *E4*-DNA (left) and *E5*-DNA (right) system in the presence of KI.

(a) *E4* (dark blue line)
(b) *E4*-DNA system (black line)
(c) System in the presence of 0.01 M KI (green line)
(d) System in the presence of 0.02 M KI (blue line)
(e) System in the presence of 0.06 M KI (red line)

(a) *E5* (black line)
(b) *E5* in the presence of 3 mM KI (blue line)
(c) *E5*-DNA system (red line)
(d) System in the presence of 0.012-3 mM KI

4.2.5. Effect of ionic strength

The change of ionic strength is an efficient method for distinguishing the binding modes between small molecules and DNA. Increasing the cation concentration will increase the combination probability between cation and DNA phosphate backbone. Due to a competition for phosphate anion, the addition of cations will weaken the surface-binding mode of interaction between a molecule and DNA. The effect of the ionic strength on the binding modes between the four derivatives and DNA was also studied with different concentrations of NaCl ranged from 0.04 to 12.5 mM. The addition of NaCl, in the presence of DNA, had no significant effect on the fluorescence yields of *E2* and *E3* derivatives (Figure 4.22). At the same time the addition of NaCl to the *E2* and *E3* solutions, free from DNA, did not affect the fluorescence yields of the *E2* and *E3*. These results can be explained by the protection of fluorescent probes from solvent surrounding, and indicate that the interaction between derivatives and DNA was not surface-binding mode (Hu and Tong, 2007). These results can be evaluated as a sample for classical intercalative behavior.

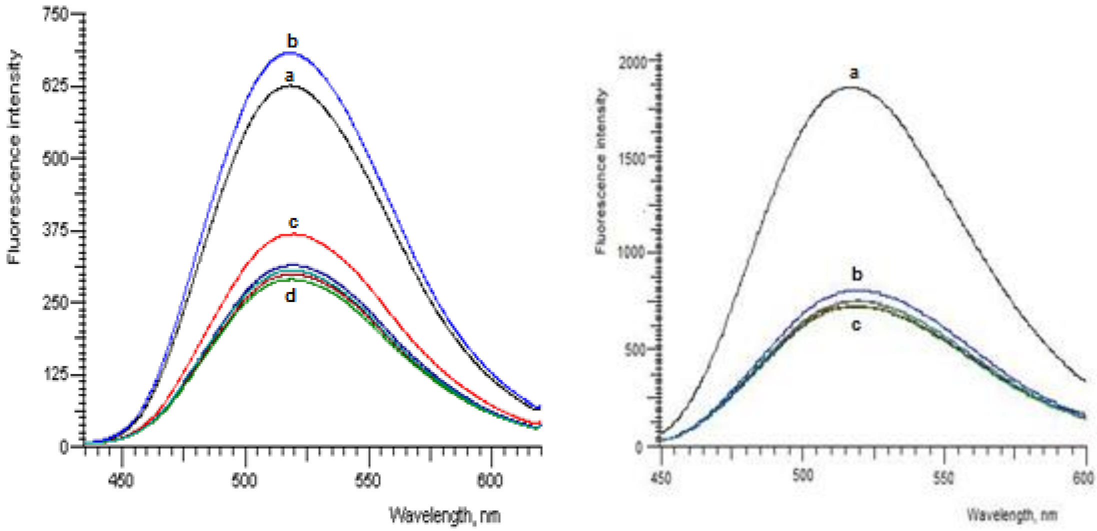

Figure 4.22. Fluorescence emission spectra of *E2*-DNA and *E3*-DNA systems in the presence of NaCl.

(a) *E2* (black line)
(b) *E2* in the presence of 10 mM NaCl (blue line)
(c) System (red line)
(d) System in the precence of 0.063-10 mM NaCl

(a) *E3* (black line)
(b) *E3*-DNA system (blue line)
(c) System in the presence of 0.16-5 mM NaCl

The addition of NaCl to the free probes *E4* and *E5*, in the absence of DNA, had little or no effect on the fluorescence yields of the dyes (Figure 4.23). However, in the presence of DNA, fluorescence yields increased by increasing salt concentration. Since the fluorescence from the free *E4* and *E5* were not enhanced by salt, it was evident that the enhancements in the presence of DNA were due to the release of the dye from the DNA grooves into the solution. The strong dependence of the binding on the ionic strength clearly indicates that *E4* and *E5* binding to DNA is predominantly controlled by electrostatic interactions and these observations are consistent with groove binding rather than intercalation into the helix.

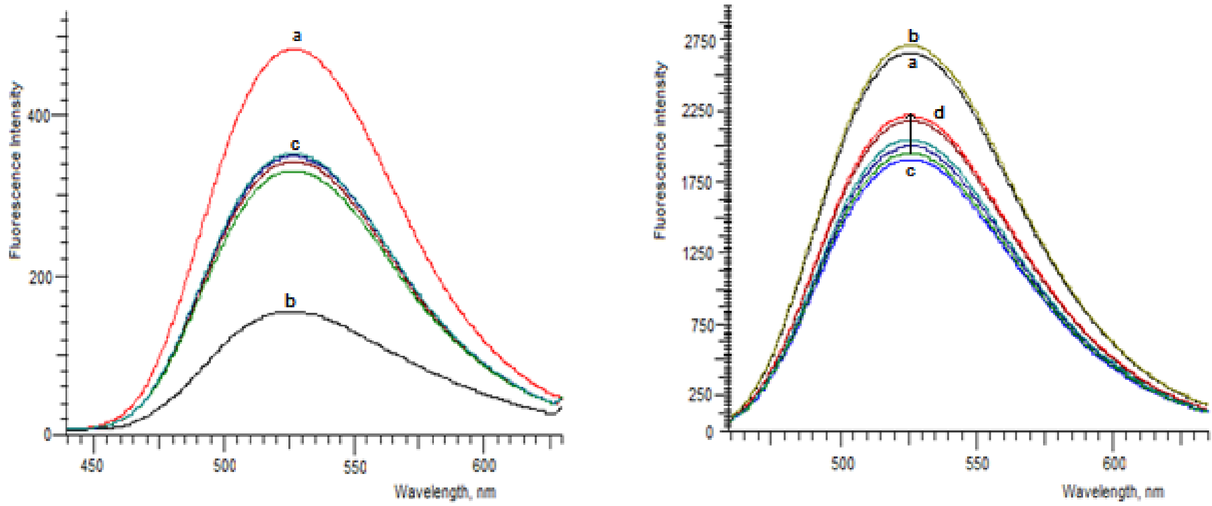

Figure 4.23. Fluorescence emission spectra of *E4*-DNA and *E5*-DNA systems in the presence of NaCl.

a)*E4* (red line)
b)*E4*-DNA system (black line)
c) System in the presence of 0.049 – 12.5 mM NaCl

a) *E5* (black line)
b) *E5* in the presence of 12.5 mM NaCl (green line)
c) *E5*-DNA system (blue line)
d)System in the presence of 0.049 – 12.5 mM NaCl

4.2.6. Characterization of binding properties with polynucleotides

Binding properties of ethidium dyes were studied in the presence of AT- and GC-containing polynucleotides. Derivatives including ester groups (*E4*, *E5*) showed large preference for poly(dG-dC)-poly(dG-dC) over poly(dA-dT)-poly(dA-dT), whereas the other two derivatives showed no preference. Obtained K_{sv} values in the presence of poly(dA-dT)-poly(dA-dT) and poly(dG-dC)-poly(dG-dC) for ethidium derivatives were listed in Table 4.6. The Stern-Volmer quenching constant of *E4* with poly(dA-dT)$_2$ is nearly 12 times, Stern-Volmer quenching constant of *E5* with poly(dA-dT)$_2$ is nearly 24 times less than with poly(dG-dC)$_2$, which indicate high selectivity. The ester groups provide the strong discrimination between AT and GC sites. This selectivity is due to the high preference of *E4* and *E5* for groove binding (Tan, et.al., 2006).

Table 4.6. *Stern-Volmer* data for dyes in presence of polynucleotides.

Dye	K_{sv} in the presence poly(dA-dT)-poly(dA-dT)	K_{sv} in the presence poly(dG-dC)-poly(dG-dC)	Ratio of K_{sv}*	Binding Type
E2	$1.57 x 10^5$	$1.84 x 10^5$	1.17	Intercalation
E3	$6.00 x 10^4$	$7.43 x 10^4$	1.24	Intercalation
E4	$1.23 x 10^5$	$1.53 x 10^6$	12.44	Groove binding
E5	$3.73 x 10^4$	$8.99 x 10^5$	24.10	Groove binding

* Ratio of K_{sv} value in the presence of poly(dG-dC)-poly(dG-dC) over in the presence of poly(dA-dT)-poly(dA-dT) were used.

4.2.7. Absorption spectrum investigation

The mode of the interaction of EB with DNA was studied by many research reports (Bi, et.al., 2008; Li and Dong, 2009). It is generally recognized that the strong mode of binding of EB to DNA result in the intercalation of the planar phenanthridinium ring between adjacent base pairs on the double helix. It is well known that intercalation binding commonly results in hypochromic and bathochromic effect of the transition of the intercalated chromophore; generally external groove binding causes a spectral shift and a hyperchromic effect.

The results of UV-vis spectra analyses about the interaction of DNA with four ethidium derivatives are shown in Figures 4.25 and 4.26. They compared with the typical intercalation figure of EB and DNA (Figure 4.24). It showed UV-vis spectra of EB, DNA and EB-DNA complex. Adding DNA into EB solution, spectrum (b) changed to spectrum (c). The maximum absorption wavelength showed batochromic shift, and absorbance decreased with the increasing concentration of DNA.

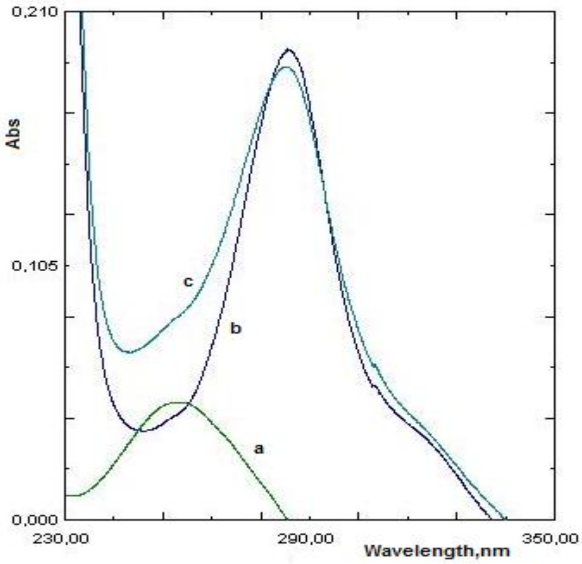

Figure 4.24. Absorption spectra of *EB*-DNA system
a) 7.5×10^{-6} M DNA, b) 5×10^{-6} *EB*, c) *EB*-DNA complex.

Figure 4.25 shows the increasing amounts of *DNA* decreased peak intensities of *E2* and *E3* in the presence of DNA. It can be seen clearly from absorption spectra that on addition of *DNA* to *E2* and *E3* a hypochromicity was observed without any band shift. Therefore, the results indicated that it could be the indication of intercalative binding of the two derivatives between the base pairs of DNA.

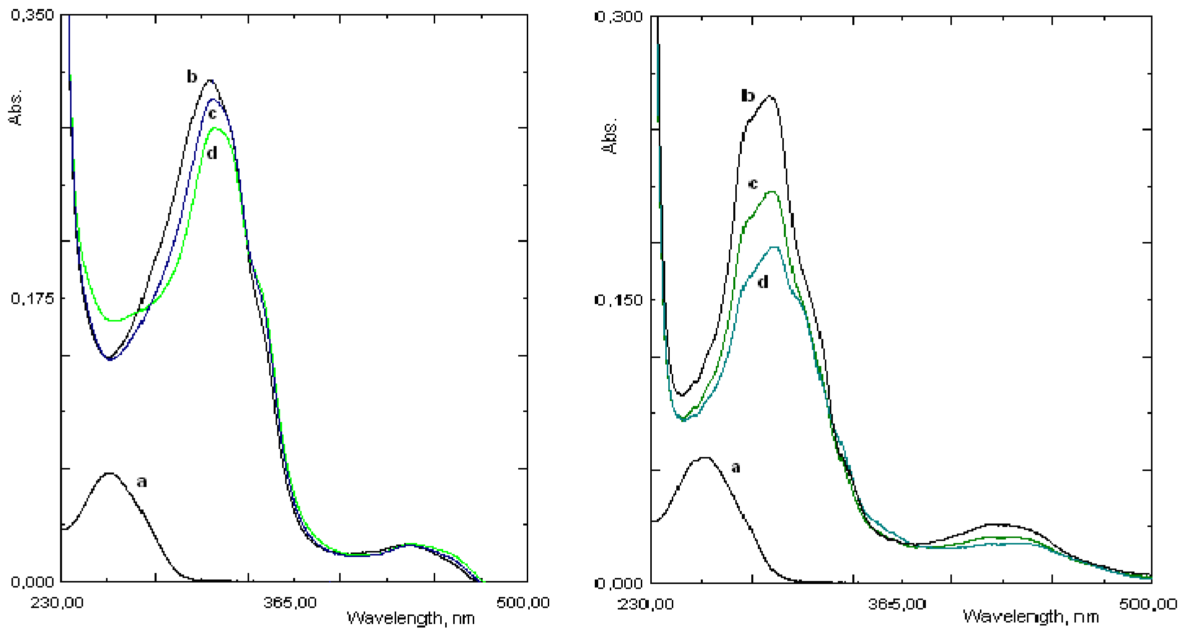

Figure 4.25. Absorption spectra of *E2*-DNA and *E3*-DNA systems.
a) 1.2×10^{-5} M DNA, b) 5×10^{-6} *E2* (left) and *E3* (right), c,d) *E2*-DNA (right) and *E3*-DNA (left) systems

Figure 4.26 shows absorption maxima for *E4* and *E5* in the presence of DNA remain unchanged even in the presence of an excess of DNA. While the absorption intensity of two dyes were increasing with the increasing DNA concentration, shape of the absorption band were observed similar. The behavior of the systems clearly showed that interaction mode of *E4* and *E5* with DNA were not intercalation (Wu, et.al., 2008).

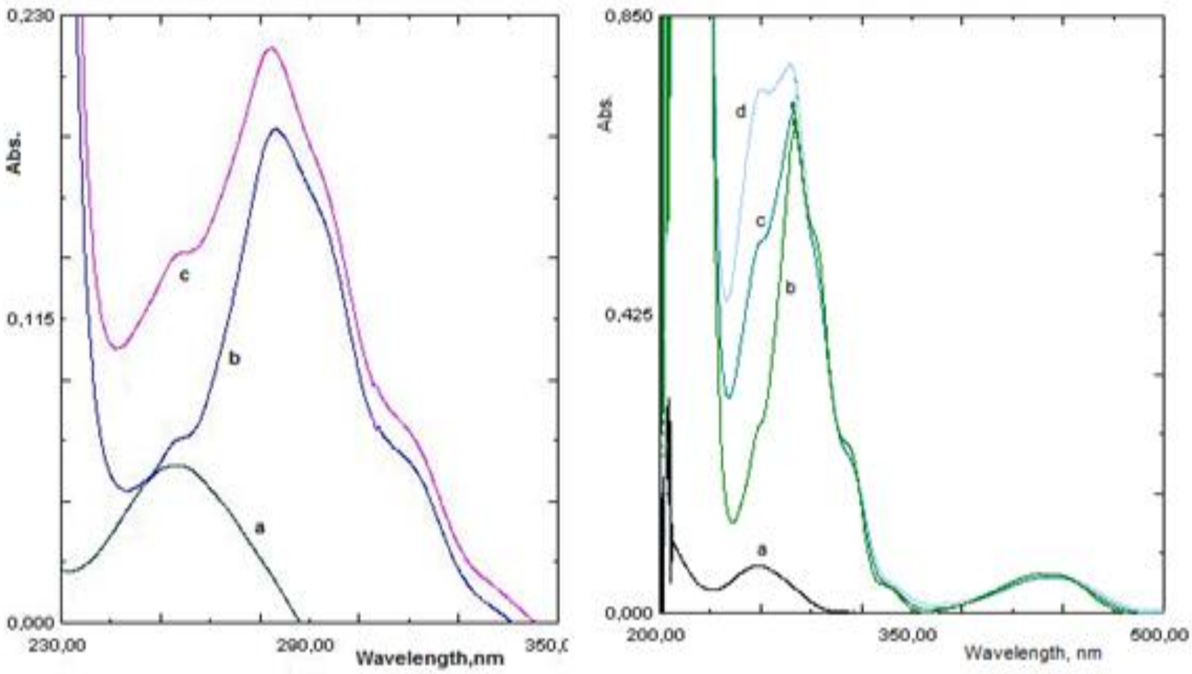

Figure 4.26. Absorption spectra of E4-DNA and E5-DNA systems.
a) $7.5x10^{-6}$ M DNA, b) $5x10^{-6}$ *E4* (left) and *E5* (right), c, d) *E4*-DNA(right) and *E5*-DNA (left) systems

4.2.8. Thermodynamic parameters and binding modes between ethidium derivatives and DNA

The interaction between a small molecule and biomolecule may involve hydrogen bond, van der Waals force, electro static force, hydrofobic interaction force, and so on. The thermodynamic parameters (ΔG, ΔH and ΔS) are very important for confirming binding modes of them. The log K (binding constant) values obtained at three different temperatures (20, 30 and 37^{o}C) for *E2*-DNA, E4-DNA and E5-DNA systems are plotted against the reciprocal of temperature (Figure 4.27) according to the van’t Hoff equation.

$$\log K = - \Delta H / 2.303 RT + \Delta S / 2.303 R$$

The values of ΔH and ΔS were obtained from the slopes and intercepts of linear van't Hoff graphs.

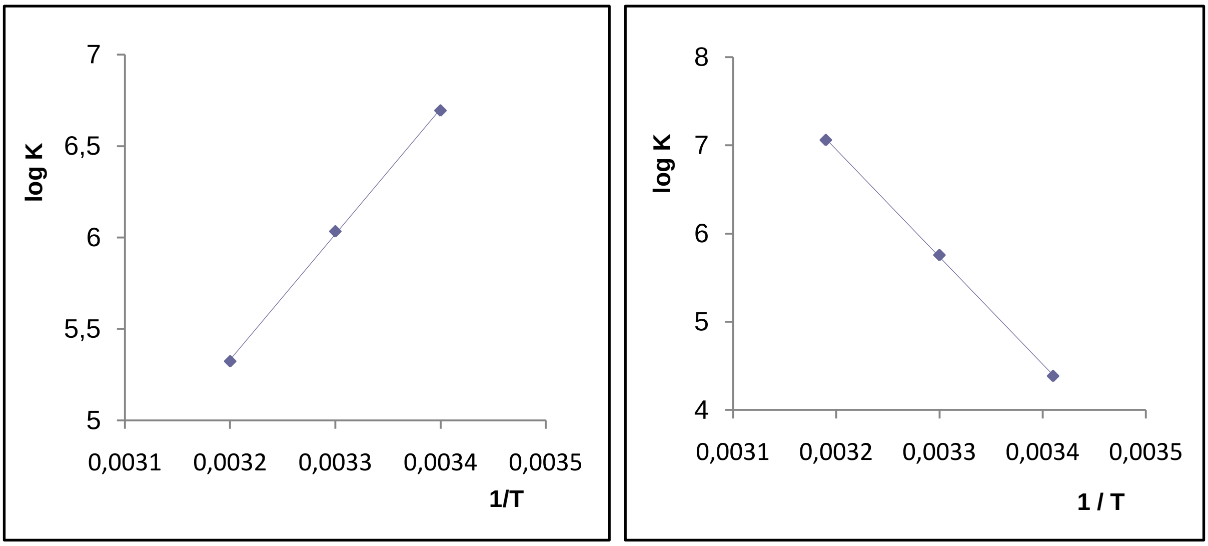

Figure 4.27. Log K versus 1/T for *E2*-DNA (left) and *E5*-DNA (right) systems.

The following formulas were used for *E3*-DNA system at two different temperatures (20 and 37^{o}C).

$$\ln K_2 / K_1 = \Delta H / R [1 / T_1 - 1 / T_2]$$

$$\Delta G = \Delta H - T \Delta S = - R T \ln K$$

K_1 and K_2 are binding constants at 20 and 37^{o}C, respectively. Thermodynamic parameters for the interactions of *E2, E3, E4* and *E5* with DNA are calculated and listed in Table 4.7.

The distinct variations in binding enthalpies are evident for the functional groups at 3- and 8- positions of ethidium compounds are playing major role in the DNA binding interactions of ethidium derivatives. Modification of ethidium bromide from 3- and 8- amino positions changes the characteristic behaviour of EB against to DNA from enhancement to quenching. In our study we also examined the effect of similar functional groups on binding affinity of ethidium compounds. We observed that the using phenylacetyl instead of benzoyl as functional group largely increased the affinity of compound to DNA. One can be concluded that being far away of aromatic ring from carbonyl group may increase the contribution of delocalized electrons of aromatic ring system to affinity of DNA.

The negative values of ∆G reveal that the interaction processes are spontaneous. Negative values of ∆H and ∆S mark the van der Waals interactions and hydrogen bonds in the binding mechanism of molecules to DNA (Ross and Subramanian, 1981). Because of the incapability of forming hydrogen bonds of aromatic ring systems, we eliminate the contribution of hydrogen bonds to negative values of ∆H and ∆S in these ethidium derivatives. We proposed the van der Waals interactions as only interaction type of the *E2* and *E3* with DNA.

Table 4.7. The thermodynamic parameters of the binding *E2*, *E3, E4* and *E5* to DNA*

Dye	∆H (kJ/mol)	T∆S (j/molK)	∆G (kJ/mol)	Interaction mode
E2	-131.3	-93.22	-36.5	van der Waals interaction
E3	-256. 8	-193.95	-62.984	van der Waals interaction
E4	16.97	36.68	-19.69	hydrophobic association
E5	232.8	257.4	-24.45	hydrophobic association

* Values were calculated from data at 20 ^{o}C.

On the other hand, results showed that if the functional groups at 3- and 8-positions of ethidium compounds comprise ester groups, smaller alkyl groups bounded to ester oxygen raised the binding affinity of molecules to DNA. And also obtained ∆H values for these esters contained two derivatives showed the vast difference to each other. Obtained positive ∆H and ∆S values sign the hydrophobic association and ionic interactions. But ionic interactions are generally faced at slight positive ∆H values. Obtained large positive ∆H values for *E4*-DNA and *E5*-DNA systems provide chance to eliminate this interaction type for these systems. So we can suggest the hydrophobic association for two ethidium derivatives.

4.2.8. Calibration graphs and determination of DNA

The fluorescence quenching of four ethidium derivatives had a good relationship with the concentration of DNA. The calibration graphs were used for the determination of DNA in the presence of *E2, E3, E4* and *E5* under the experimental conditions above described. Calibration graphs were plotted by the changes in emission intensities against *DNA* concentrations. The linear equations were,

$F_0/F = 0.9802 + 1.082x10^6$ [Q], R^2=0.991 (n=4) for *E2,*
$F_0/F = 0.4568 + 8.440x10^6$ [Q], R^2=0.994 (n=7) for *E3,*
$F_o/F = 1.4620 + 2.151x10^4$ [Q], R^2=0.992 (n=5) for *E4*,
$F_o/F = 0.9797 + 2.490x10^4$ [Q], R^2=0.992 (n=6) for *E5* at 20^{o}C.

The detection and quantification limits of DNA were calculated as $3S_b/m$ and $10S_b/m$. S_b is the standard deviation of the intercept and m is the slope of the calibration graph (Deepa and Mishra, 2005) The analytical results are given in Table 4.8.

Table 4.8. The analytical results of *DNA* determination in presence *E2*, *E3, E4* and *E5*.

Name	**Dynamic range of DNA (M)**	**S_b standard deviation of the intercept**	**Limit of detection (LOD) (M)**	**Limit of quantification (LOQ) (M)**
E2	$1.50\text{-}16.5x10^{-7}$	0.027	$7.49x10^{-8}$	$2.50x10^{-7}$
E3	$7.50\text{-}33.0x10^{-8}$	0.118	$4.18x10^{-8}$	$1.39x10^{-7}$
E4	$1.20\text{-}18.0x10^{-5}$	0.206	$2.87x10^{-5}$	$9.58x10^{-5}$
E5	$3.00\text{-}36.0x10^{-6}$	0.06	$7.23x10^{-6}$	$2.41x10^{-5}$

From the dynamic range and detection limit for *DNA*, it can be seen that *E3* has more sensitive for this method. When four ethidium derivatives compared, amides showed the affinity with an increase of three orders of magnitude and two orders of magnitude for *E4* and *E5*, respectively.

4.3. Study on the interactions of serum albumins with ethidium derivatives

Serum albumins are major proteins in plasma. The fluorescence *quenching* characteristics of the serum albumins provide a sensitive spectroscopic method to study their interactions with various dye molecules. The changes in the fluorescence intensity of these spectra can be used to probe the nature of the binding reactions of serum albumins and dye molecules.

In this group study, the interactions of serum albumins such as BSA and HSA with four ethidium derivatives were assessed employing fluorescence quenching and absorption spectroscopic methods. BSA and HSA display approximately 76% sequence homology. The structure of BSA is believed to be similar to that of HSA. From the spectroscopic point of view one of the major difference between the two proteins is that HSA has one tryptophan (Trp214), whereas BSA has two tryptophan residues (Trp134 and Trp212).

Procedure: BSA and HSA were obtained from Sigma. They were dissolved in Tris HCl buffer at pH 7.4. The interactions of BSA and HSA with four ethidium derivatives were investigated by fluorimetric titration at three temperatures (20, 30 and 37^{o}C). Florimeter cell (1 cm) was filled with 2 mL 1.09x10^{-5} M BSA and HSA in buffer solution. To investigate effect of derivatives on the fluorescence intensity of serum albumins, 5-150 μL of stock solutions of derivatives were added to 2 mL 1.09x10^{-5} M of protein solutions. Then fluorescence intensities and spectra of proteins in the presence or absence of derivatives were recorded in the range of 300-650 nm with 294 nm.

4.3.1. Fluorescence quenching

The fluorescence spectra of BSA and HSA in presence of increasing amounts of *E1, E2, E3* and *E4* were recorded their characteristic emission fluorescence at 358 nm (λ_{ex} = 294 nm) due to Trp residues**.** Figure 4.28 and 4.29 show that E4 causes a concentration dependent quenching of the intrinsic fluorescence of BSA and HSA without changing the emission maximum and shape of the peaks. In the interactions of other derivatives with BSA and HSA (data not shown), almost same effects were observed with E4. Thus, apparently, on binding to BSA and HSA, *E1,* *E2, E3* and *E4* quenched the spectral intensity of albumins, and had their own fluorescence intensities increased simultaneously.

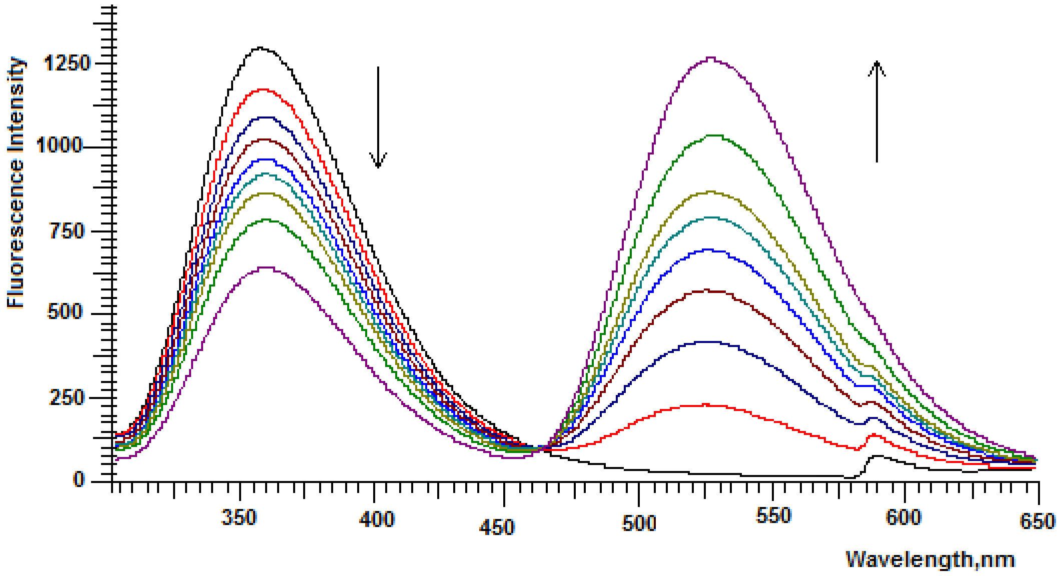

Figure 4.28. Fluorescence emission spectra of BSA in the presence of E4. BSA concentration was $1.09 x 10^{-5}$ M. Conditions: $\lambda_{ex} = 294$, the concentration of E4 from highest curve to lowest is 0, 1.0, 2.0, 3.0, 4.0, 5.0, 6.0, 8.0, 10, 12 ($x10^{-6}$) M.

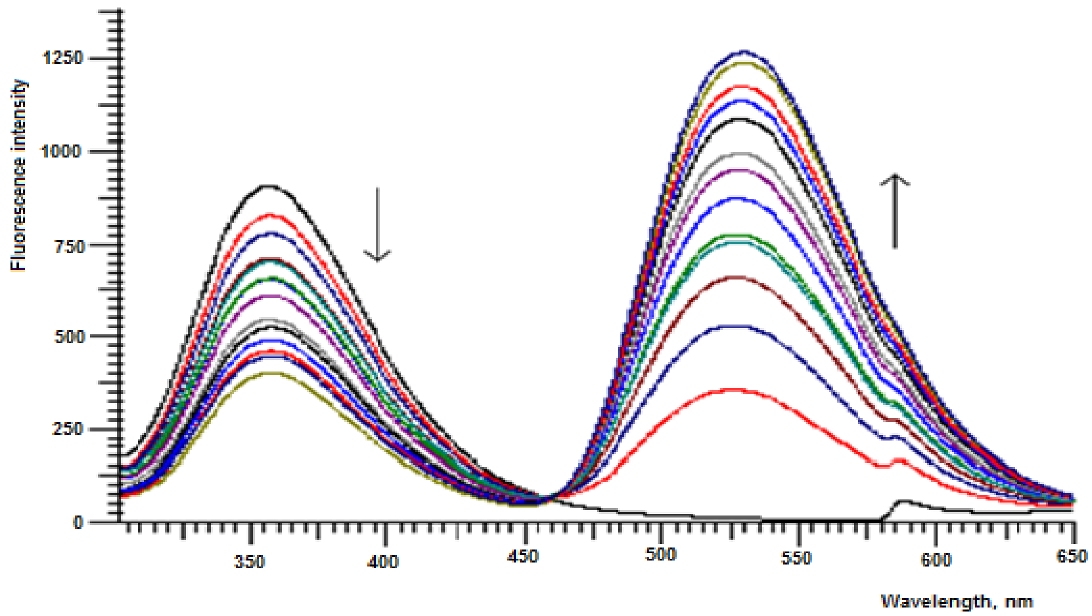

Figure 4.29. Fluorescence emission spectra of HSA in the presence of E4. HSA concentration was $1.09 x 10^{-5}$ M. Conditions: $\lambda_{ex} = 294$, the concentration of E4 from highest curve to lowest is 0, 1.5, 2.5, 3.5, 4.0, 4,5, 5.0, 6.0, 7.0, 8.0, 9.0, 10, 11, 12 ($x10^{-6}$) M.

All fluorescence quenching data are analyzed by the Stern–Volmer equation at studied temperatures,

$$F_0 / F = 1 + K_{SV}[Q] = 1 + \tau_0 k_q [Q]$$

where τ_0 is the lifetime of the protein without the quencher. The τ_0 value for BSA is known to be approximately 5 ns (Wei, et.al., 2006). The maximum scatter collision quenching constant, k_q of various quenchers with the biopolymer is $2x10^{10}$ $M^{-1}s^{-1}$. Thus, the rate constant of protein quenching procedure initiated by ethidium derivatives are greater than k_q of scatter procedure. This indicates that a *static quenching* mechanism is operative with the formation of derivatives-BSA complexes. Table 4.9 shows that linear regression equations**,** K_{sv} and quenching rate constants (k_q) for each derivatives at given temperatures. These results indicate that probable quenching mechanism of fluorescence of BSA by the derivatives is static queching procedure, because K_{sv} and k_q are decreased with increase in temperature.

Table 4.9. Stern-Volmer data for *ethidium derivatives*-BSA.

Dye	**˚C**	**Linear regression equation**	**K_{sv} (M^{-1})**	**R^2**	k_q
E2	20	$F_o/F = 0.6748 + 2.755x10^5[Q]$	$2.755x10^5$	0.993	$5.51x10^{13}$
	30	$F_o/F = 0.7042 + 2.554x10^5[Q]$	$2.554x10^5$	0.995	$5.11x10^{13}$
	37	$F_o/F = 0.7278 + 2.181x10^5[Q]]$	$2.181x10^5$	0.995	$4.36x10^{13}$
E3	20	$F_o/F = 0.6328 + 2.525x10^5 [Q]$	$2.525x10^5$	0.983	$5.05x10^{13}$
	30	$F_o/F = 0.8543 + 1.793x10^5 [Q]$	$1.793x10^5$	0.986	$5.59x10^{13}$
	37	$F_o/F = 0.9202 + 1.421x10^5 [Q]$	$1.421x10^5$	0.995	$2.84x10^{13}$
E4	20	$F_o/F = 1.0135 + 8.400x10^4 [Q]$	$8.40x10^4$	0.998	$1.68x10^{13}$
	30	$F_o/F = 0.9824 + 8.330x10^4[Q]$	$8.330x10^4$	0.997	$1.67x10^{13}$
	37	$F_o/F = 0.9477 + 7.770x10^4 [Q]$	$7.770x10^4$	0.990	$1.55x10^{13}$
E5	20	$F_o/F = 0.7222 + 2.679x10^5 [Q]$	$2.679x10^4$	0.987	$5.36x10^{12}$
	37	$F_o/F = 0.8794 + 2.158x10^5 [Q]$	$2.158x10^5$	0.993	$4.32x10^{13}$

On the other hand, fluorimetric titrations were performed at two different temperatures for dye-HSA complex systems. When we looked at the K_{sv} values of these complexes we see that the values are nearly same for two temperatures. And quenching rate constants (k_q) were calculated by using, τ_0 of the biomolecule without quencher is known to be 10^{-8} s (Wang, et.al., 2006). Obtained K_{sv}, and k_q values of dye-HSA complexes were listed in table 4.10.

Table 4.10. Stern-Volmer data for ethidium derivatives-HSA.

Dye	˚C	Equation	K_{sv} (M^{-1})	R^2	k_q
E2	20	$F_o/F = 0.758 + 2.685 \times 10^5$ [Q]	2.685×10^5	0.995	2.685×10^{13}
	37	$F_o/F = 0.672 + 2.471 \times 10^5$ [Q]	2.471×10^5	0.992	2.471×10^{13}
E3	20	$F_o/F = 0.977 + 1.787 \times 10^5$ [Q]	1.787×10^5	0.997	1.787×10^{13}
	37	$F_o/F = 0.074 + 5.418 \times 10^5$ [Q]	5.418×10^5	0.988	5.418×10^{14}
E4	20	$F_o/F = 0.904 + 1.041 \times 10^5$ [Q]	1.041×10^5	0.993	1.041×10^{13}
	37	$F_o/F = 0.962 + 1.092 \times 10^5$ [Q]	1.092×10^5	0.997	1.092×10^{13}
E5	20	$F_o/F = 0.658 + 2.618 \times 10^5$ [Q]	2.618×10^5	0.996	2.618×10^{13}
	37	$F_o/F = 0.743 + 2.705 \times 10^5$ [Q]	2.705×10^5	0.990	2.705×10^{13}

The fluorescence data was further examined using modified Stern–Volmer equation,

$$F_0 / (F_0 - F) = 1 / f_a + 1 / [Q]\, f_a K_{sv}$$

where f_a is the fraction of the initial fluorescence, which is accessible to quencher. The values of f_a refer to the fraction of fluorescence accessible to quenching, which need not be the same as the fraction of tryptophan residues, i.e. accessible to quenching. From the plot of $F_0/(F_0-F)$ versus $1/[Q]$, the values of f_a and K_{SV} were obtained from the values of intercept and slope, respectively. The value of f_a (%) were found to be 77.8%, 72.7%, 59.5% and 98.3% of the total fluorescence of BSA is accessible to quenchers as *E2, E3, E4* and *E5* at 20˚C, respectively. In the same manner f_a (%) values for *E2, E3* and *E4* were found 97.4, 96.1, and 96.3 from fluorimetric titration of HSA, respectively.

4.3.2. Binding constant and binding sites

The equilibrium constants and binding sites number of dye-BSA and dye-HSA were evaluated by using the following double logarithm regression equation:

$$\log (F_0–F) / F = \log K_b + n \log[Q]$$

The binding studies were carried out at three different temperatures for BSA and two different temperatures for HSA. The obtained K_b and n values at these temperatures were listed in Table 4.11 and Table 4.12.

Table 4.11. Binding constant K_b and the number of binding sites n for e*thidium derivatives*-BSA.

Dye	˚C	Equation	K_b (M^{-1})	n	R^2
E2	20	$\log (F_0–F)/F=\log 5.862 +1.1004 \log [Q]$	$7.278x10^5$	1.1004	0.980
	30	$\log (F_0–F)/F=\log 6.1025+1.1537 \log [Q]$	$1.266x10^6$	1.1537	0.993
	37	$\log (F_0–F)/F=\log 6.2477+1.1945 \log [Q]$	$1.769x10^6$	0.9134	0.998
E3	20	$\log (F_0–F)/F=\log 6.3207 +1.1989 \log [Q]$	$2.093x10^6$	1.1989	0.997
	30	$\log (F_0–F)/F=\log 5.8599 +1.1295 \log [Q]$	$7.243x10^5$	1.1295	0.991
	37	$\log (F_0–F)/F =\log 5.7093 +1.1159 \log[Q]$	$5.120x10^5$	1.1159	0.997
E4	20	$\log (F_0–F)/F=\log 4.7437+0.9614 \log [Q]$	$5.542x10^4$	0.9614	0.996
	30	$\log (F_0–F)/F =\log 4.9307+1.0052 \log [Q]$	$8.525x10^4$	1.0052	0.996
	37	$\log (F_0–F)/F =\log 5.165+1.0655\log [Q]$	$1.46x10^5$	1.0655	0.987
E5	20	$\log (F_0–F)/F=\log 5.8431+1.0967 \log [Q]$	$6.968x10^5$	1.0967	0.991
	37	$\log (F_0–F)/F =\log 6.0227+1.1434 \log [Q]$	$1.054x10^6$	1.1434	0.997

The values of n are approximately equal to 1 that indicates the existence of just a single binding site in albumins for ethidium derivatives. The binding constants increase with increasing temperature, resulting in increase of the stability of the dye-albumin complexes.

Table 4.12. Binding constant K_b and the number of binding sites n for e*thidium derivatives*-HSA.

Dye	˚C	Equation	K_b (M^{-1})	n	R^2
E2	20	log (F_0–F)/F=log 6.1024+1.1477 log [Q]	1.266×10^6	1.1477	0.988
	37	log (F_0–F)/F=log 6.2348+1.1832 log [Q]	1.717×10^6	1.1832	0.995
E3	20	log (F_0–F)/F=log 5.3264+1.0152 log [Q]	2.120×10^5	1.0152	0.997
	37	log (F_0–F)/F=log 8.1026+1.4875 log [Q]	1.266×10^8	1.4875	0.995
E4	20	log (F_0–F)/F=log 5.495+1.1106 log [Q]	3.126×10^5	1.1106	0.988
	37	log (F_0–F)/F=log 5.4766+1.094 log [Q]	2.996×10^5	1.094	0.996
E5	20	log (F_0–F)/F=log 6.6989+1.2671 log [Q]	4.999×10^6	1.2671	0.987
	37	log (F_0–F)/F =log 6.4956+1.2271 log [Q]	3.130×10^6	1.2271	0.996

4.3.3. Absorption measurements

UV absorption spectra of BSA and HSA were recorded in the presence of derivatives. Figure 4.29 and 4.30 show that absorption intensity of BSA at 294 nm was enhanced with addition *E2*, *E3* and *E4*, *E5*, respectively. Absorption spectra of BSA were changed due to form ground state complexes of derivatives-BSA.

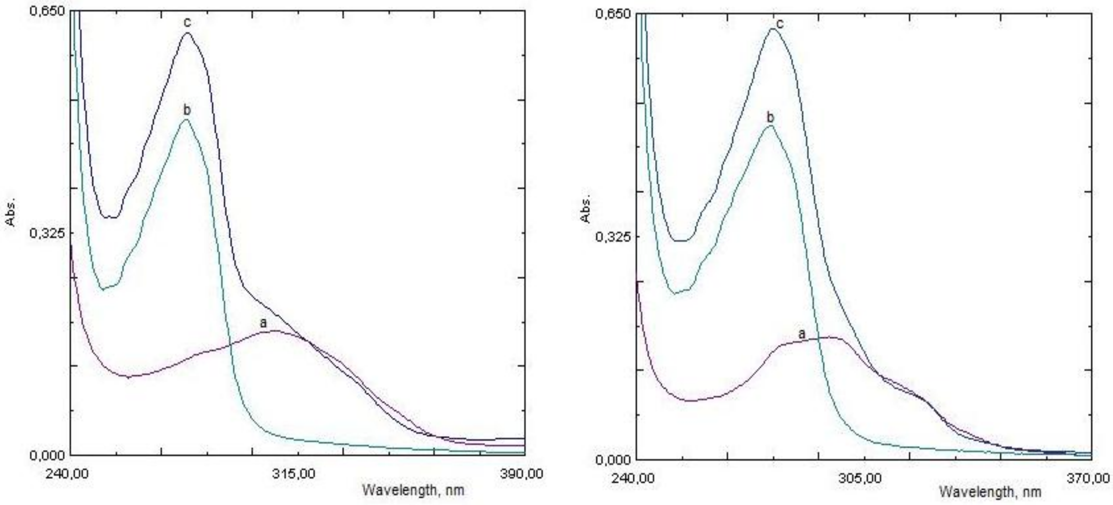

Figure 4.30. Absorbance spectra of

a) 4.0x10^{-6} M *E2*
b) 1.09x10^{-5} M BSA
c) BSA – *E2* system

a) 4.0x10^{-6} M *E3*
b) 1.09x10^{-5} M BSA
c) BSA – *E3* system

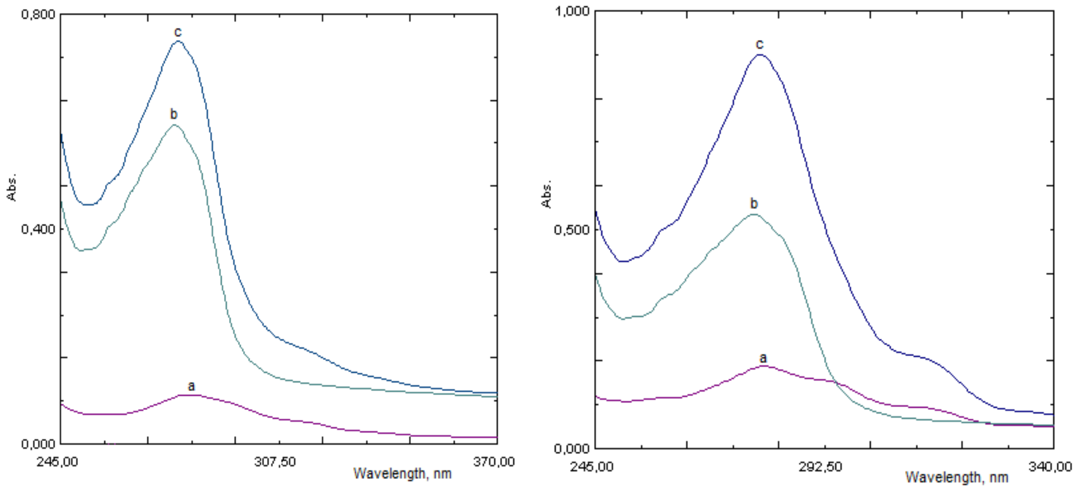

Figure 4.31. Absorbance spectra of

a) 4.0x10^{-6} M *E4*
b) 1.09x10^{-5} M BSA
c) BSA-*E4* system

a) 4.0x10^{-6} M *E4*
b) 1.09x10^{-5} M BSA
c) BSA-*E4* system

Same behavior was observed in the absorption spectra of HSA in the presence of ethidium dyes. Figure 4.31 and 4.32 show the *E2*, *E3* and *E4*, *E5* complex systems with HSA, respectively. Absorption intensities were enhanced at absorption maxima of HSA in the presence of dyes.

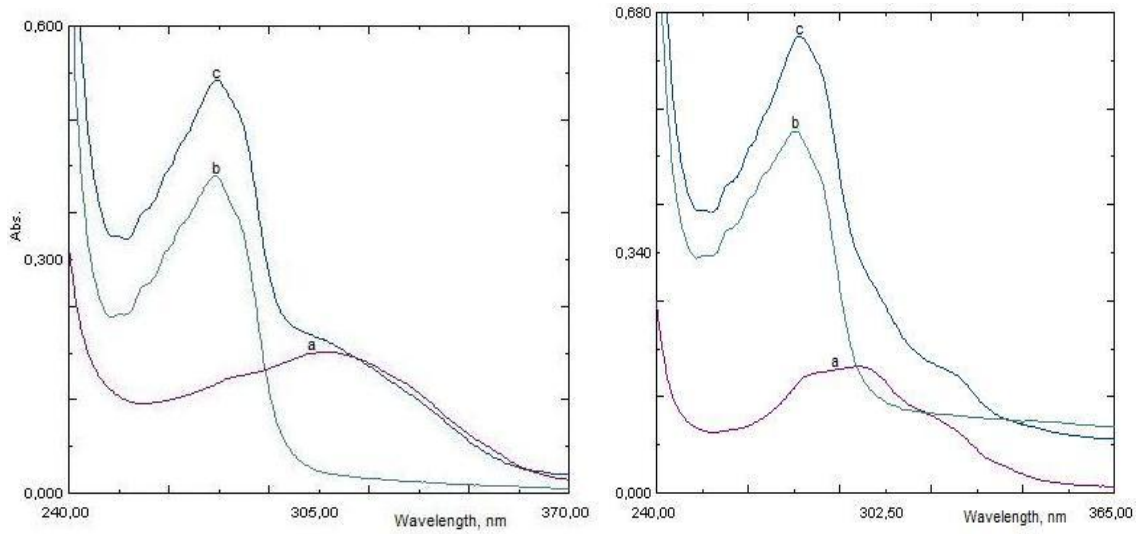

Figure 4.32. Absorbance spectra of
a) 4.0×10^{-6} M *E2*
b) 1.09×10^{-5} M HSA
c) HSA – *E2* system

a) 4.0×10^{-6} M *E3*
b) 1.09×10^{-5} M HSA
c) HSA – *E3* system.

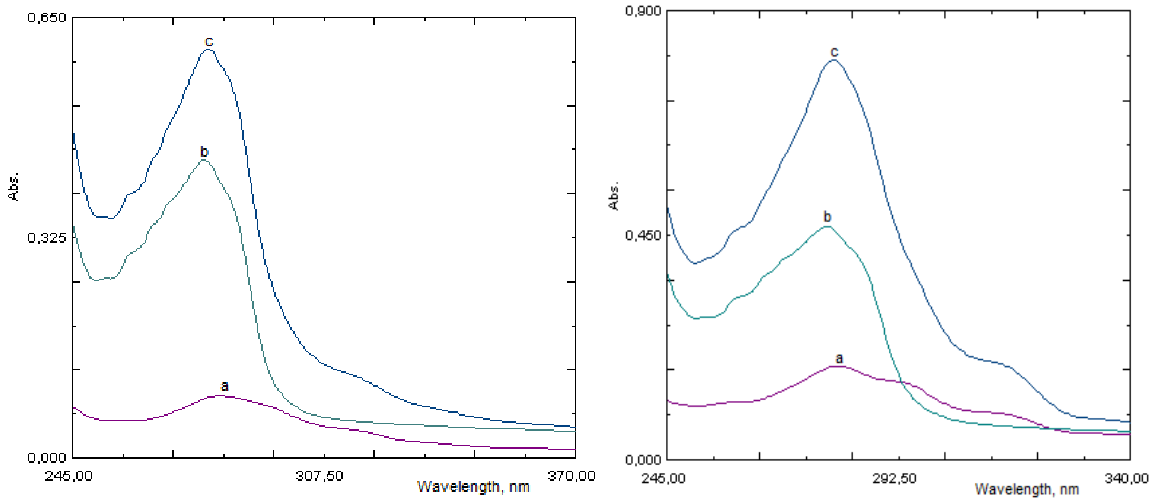

Figure 4.33. Absorbance spectra of
a) 4.0×10^{-6} M *E4*
b) 1.09×10^{-5} M HSA
c) HSA-*E4* system

a) 4.0×10^{-6} M *E4*
b) 1.09×10^{-5} M HSA
c) HSA-*E5* system

4.3.4. Thermodynamic parameters and nature of the interaction modes

The thermodynamic parameters, ΔH and entropy change ΔS were used to confirm the interaction modes between the four derivatives and protein. The temperature-dependence of the binding constants was studied for *E2, E3* and *E4* at 20, 30 and

37°C and for E5 at 10 and 37°C in the titration of BSA. HSA investigations were carried out at 20 and 37°C for studied ethidium dyes. At these temperatures the albumins do not undergo any structural degradation. From Section 4.2.7, using Equations (1), (2) and (3), ΔH, ΔS and ΔG were calculated and presented in Table 4.13 and 4.14. Interaction modes of dye-albumin systems were evaluated according to these data.

The sign and magnitude of the thermodynamic parameters have characterized various individual kinds of interaction that may take place in protein association processes.

Table 4.13. Thermodynamic parameters of the dye-BSA systems.

Dye	ΔH (kJ/mol)	TΔS (kJ/mol)	ΔG (kJ/mol)	Interaction mode
E2	39.60	72.53	-32.93	hydrophobic interaction
E3	-61.73	-26.51	-35.22	van der Waals interaction
E4	41.25	67.59	-26.34	hydrophobic interaction
E5	18.40	51.19	-32.79	hydrophobic interaction

Table 4.14. Thermodynamic parameters of the dye-HSA systems.

Dye	ΔH (kJ/mol)	TΔS (kJ/mol)	ΔG (kJ/mol)	Interaction mode
E2	-13.55	20.70	-34.25	Ionic interaction
E3	-49.29	-16.77	-32.52	van der Waals interaction
E4	-1.89	28.95	-30.84	Ionic interaction
E5	20.82	58.41	-37.59	hydrophobic interaction

From the point of view of water structure, a positive ΔS value is frequently taken as evidence for hydrophobic interaction. The negative ΔH and ΔS point the van der Waals interactions. The negative value of ΔG reveals that the interaction process is spontaneous. The positive ΔH and ΔS values suggest that the hydrophobic forces play major role in the binding of *E2*, *E4* and *E5* with BSA. Negative ΔH and ΔS values make sign to van der Waals forces. On the other hand negative ΔH and positive ΔS values suggest the ionic interaction in the medium.

5. CONCLUSIONS

- It was shown that presence of spermine-like linkage / tail group leads to the increasing of dye-DNA binding constant values. This value was 1.8×10^4 M^{-1} for parent dye Sbt; 6.2×10^4 M^{-1} for monomer Bos-5 and 10.0×10^4 M^{-1} for homodimer DBos-13. Despite the presence of linkage group for homodimer dye DBsu-10 value of binding constant (2.7×10^4) was close to that for dye Sbt. Value of binding constants recorded for the studied dyes are consistent with both groove binding and intercalation mechanisms.

- Values of DNA base pairs number occupied by one bound dye molecule calculated for monomer Bos-5 ($n = 2.3$) and homodimer DBos-13 ($n = 4.9$) point on existing of intercalation binding mode, while for homodimer DBsu-10 this value ($n = 14.5$) is the evidence of groove binding mechanism. The value obtained for Sbt ($n = 3.4$) does not point unambiguously on one of these mechanisms.

- Studies of dyes interaction with synthetic polynucleotides poly(dA-dT)$_2$ and poly(dG-dC)$_2$ has shown that parent dye Sbt, monomer Bos-5 and homodimer DBos-13 gave the comparable fluorescent response on the presence of both type of polynucleotides. That could be an evidence of intercalation binding mode. Strong AT-binding preference demonstrated by homodimer DBsu-10 points on groove binding mode.

- For homodimer dyes it was shown that position of linkage group could significantly affect on the mode of dye interaction with DNA. Thus for a dimer DBos-13 having linkage group which is bounded to nitrogen atoms of benzothiazole ring intercalation is proposed as binding mode. At the same time homodimer DBsu-10 with linkage bound in 6-positions of benzothiazole heterocycle is considered to be groove binder.

- It was clearly shown that binding type of ethidium derivatives to DNA was determined by substituents at 3-and 8- amino positions. Amide containing derivatives (*E2* and *E3*) preferred the intercalation which is the same behavior with parent dye EB. On the other hand ester containing derivatives (*E4* and *E5*) exhibited preference for groove binding.

- Ester containing and amide containing derivatives gave opposite binding behavior to DNA according to containing functional groups. In amide derivatives (*E2* and *E3*), large functional group showed larger binding affinity to DNA. But in ester containing derivatives (*E4* and *E5*) smaller one showed more affinity to DNA. Binding constants for *dye*-DNA complexes are $4.939x10^{6}$, $1.690x10^{11}$, $3.24x10^{3}$ and $2.425x10^{4}$ for *E2*, *E3*, *E4* and *E5*, respectively.

- Presence of KI in the medium showed same effect on *E2*-DNA and *E3*-DNA complex systems. Increasing amount of KI doesn't proportional with the quenching amount. This indicates the protection of dye molecules by DNA helix and also classical intercalation status. On the other hand, *E4*-DNA and *E5*-DNA complex systems showed larger quenching in the higher KI presence. This action points groove binding.

- Ionic strength effect on studied medium was controlled by strong electrolyte NaCl. Obtained results support the binding type propositions. *E2* and *E3* behaved like intercalators and chancing ionic strength didn't have significant effect on their complex systems. Like previous paragraph variations in ionic strength of medium changed the behavior of *E4* and *E5* complex systems. Increasing of ionic strength lowered the quenching amount of their complex systems.

- Investigation of dyes interaction with synthetic polynucleotides poly(dA-dT)$_2$ and poly(dG-dC)$_2$ presents strong discriminations between amide and ester dyes. Amide containing dyes *E2* and *E3* didn't select any of these polynucleotides. But ester containing dyes *E4* and *E5* preferred the GC containing one and GC affinity of *E4* is nearly 12 times, GC affinity of *E5* is nearly 24 times higher than the AT preference of these dyes.

- Thermodynamic parameters such as ΔG, ΔH and ΔS were calculated dye-DNA complex systems. Obtained values marked van der Waals interactions to *E2* and *E3* systems and hydrophobic association to *E4* and *E5* systems.

- From the calibration studies detection limit of DNA were obtained as 7.49×10^{-8} (n=4), 4.18×10^{-8} (n=7), 2.87×10^{-5} (n=5) and 7.23×10^{-6} M (n=6) in the presence of *E2, E3, E4* and *E5*, respectively.

- Also Interaction type of four ethidium derivatives with serum proteins (BSA and HSA) were investigated and obtained thermodynamic parameters at different temperatures. The obtained all results are given in below.

Dye	DNA-Binding type	DNA-interaction mode	BSA- interaction mode	HSA- interaction mode
E2	intercalation	van der Waals interactions	hydrophobic association	ionic interactions
E3	intercalation	van der Waals interactions	van der Waals interactions	van der Waals interactions
E4	groove binding	hydrophobic association	hydrophobic association	ionic interactions
E5	groove binding	hydrophobic association	hydrophobic association	hydrophobic association

6. REFERENCES

Akbay, N., Losytskyy, M.Yu., Kovalska, V.B., Balanda, A.O., Yarmoluk, S.M., 2008, The mechanism of benzothiazole styrylcyanine dyes binding with dsDNA: Studies by spectral-luminescent methods, *Journal of Fluoresc*ence, 18, 1, 139-147.

Akbay, N., Seferoğlu, Z., Gök, E., 2009, Fluorescence interaction and determination of calf thymus DNA with two ethidium derivatives, *Journal of Fluoresc*ence, (in press).

Akbay, N., Topkaya, D., Ergün, Y., Alp, S., Gök, E., 2009, Fluorescence study on the interaction of bovine serum albumin with two coumarin derivatives, *Journal of Analytical Chemistry,* (in press).

Alonso A., Almendral M.J., Curto Y., Criado J.J., Rodriguez, Manzano J.L. 2006, Determination of the DNA-binding characteristics of ethidium bromide, proflavine ,and cisplatin by flow injection analysis: Usefulness in studies on antitumor drugs, *Analytical Biochemistry*, 355, 157-164.

Balanda, A.O., Volkova, K.D., Kovalska, V.B., Losytskyy, M.Yu., Lukashov, S.S., Yarmoluk, S.M., 2006, Novel styrylcyanines and their dimers as fluorescent dyes for nucleic acids detection: Synthesis and spectral-luminescent studies, *Ukrainica Bioorganica Acta,* 4, 1, 17-29.

Bi, S., Zhang, H., Chunyu Qiao, C., Sun, Y., Liu, C., 2008, Studies of interaction of emodin and DNA in the presence of ethidium bromide by spectroscopic method, *Spectrochimica Acta Part A,*69, 123-129.

Deepa, S., Mishra A.K, 2005, Fluorescence spectroscopic study of serum albumin-bromadiolone interaction: Fluorimetric determination of bromadiolone. *Journal of Pharmaceutical and Biomedical Analysis*, 38, 556-563.

Garbett N.C., Hammond N.B., Graves D.E., 2004, Influence of the amino substituents in the interaction of ethidium bromide with DNA, *Biophysical Journal*, 87, 3954-3981.

Göransson E., Karlsson I., Oxblad C., 2005, Asymmetric Cyanine Dyes, DNA-technology, Chalmers University of Technology, 4-14.

Guo, L., Qui, B., Chen, G., 2007, Synthesis and investigation on the interaction with calf thymus deoxyribonucleic acid of a novel fluorescent probe 7-oxobenzo[b][1,10]phenanthroline-12(7H)-sulfonic acid, *Analytica Chimica Acta*, 588, 123-130.

Hu, Z., Tong, C., 2007, Synchronous fluorescence determination of DNA based on the interaction between methylene blue and DNA. *Analytica Chimica Acta*, 587, 2, 187-193.

Kovalska, V.B., Kryvorotenko, D.V., Balanda, A.O., Losytskyy, M.Yu., Tokar, V.P., Yarmoluk S.M., 2005, Fluorescent homodimer styrylcyanines: synthesis and spectral-luminescent studies in nucleic acids and protein complex, *Dyes and Pigments,* 67, 1, 47-54.

Kovalska, V.B., Volkova, K.D., Losytskyy M.Y., Tolmachev, O.I., Balanda A.O., Yarmoluk, S.M., 2006, 6,6'-Disubstituted benzothiazole trimethine cyanines – new fluorescent dyes for DNA detection, Spectrochimica Acta Part A, 65, 271–277.

Kumar, C.V., Turner, R.S., Asuncion, E.H., 1993, Groove binding of a styrylcyanine dye to the DNA double helix: the salt effect, Journal of *Photochemistry* and *Photobiology* C: *Chemistry, 74, 231-238.*

Labieniec M., Gabryelak T., 2006, Interactions of tannic acid and its derivatives (ellagic and gallic acid) with calf thymus DNA and bovine serum albumin using spectroscopic method, *Journal Photochemistry Photobiology B: Biology,* 82, 72-78.

Lakowicz, J.R., 2006**,** Principles of Fluorescence Spectroscopy, 3rd edn. Springer, New York.

Li, J.F., Dong, C., 2009, Study on the interaction of morphine chloride with deoxyribonucleic acid by fluorescence method. *Spectrochimica Acta Part A,* 71, 1938–1943.

Luedtke, N.W., Liu, Q., Tor, Y., 2003, Synthesis, photophysical properties, and nucleic acid binding of phenanthridinium derivatives based on ethidium, *Bioorganic Medicinal Chemistry* 11, 5235-5247.

Luedtke, N.W., Liu, Q., Tor, Y., 2003, On the electronic structure of ethidium, Chemical Europan Journal 11, 495-508.

McGhee, J.D., von Hippel, P.H., 1974, Theoretical aspects of DNA-protein interactions: Cooperative and non-cooperative binding of large ligands to a one-dimensional homogeneous lattice, *Journal of Molecular Biology,* 86, 2, 469-489.

Neidle, S., 2002, Nucleic Acid Structure and Recognition, Oxford University Press, New York.

Petrucci, R.H., Harwood, W.S., Herring, F.G., 2002, General Chemistry Principles and Modern Applications, 8th Edition, Prentice Hall, New Jersey.

Qui B., Guo L., Wang W., Chen G., 2007, Synthesis of a novel fluorescent probe useful for DNA detection. *Biosensors and Bioelectronics*, 22, 2629-2635.

Quiao C., Bi S., Sun Y., Song D., Zhang H., Zhou W., 2008, Study of interactions of anthraquinones with DNA using ethidium bromide as a fluorescence probe, *Spectrochimica Acta Part A,* 70, 1, 136-143.

Rangarajan S., Friedman S.H., 2007, Design, synthesis, and evaluation of phenanthridine derivatives targeting the telomerase RNA/DNA heteroduplex, *Bioorganic Medicinal Chemistry Letters*, 17, 2267-2273.

Ross, P.D., Subramanian, S., 1981, Thermodynamics of protein association reactions: Forces contributing to stability, *Biochemistry,* 20, 3096-3102.

Rosenzweig, Z., Yeung, E.S., 1994, Laser-based particle-counting microimmunoassay for the analysis of single human erythrocytes, *Analytical Chemistry*, 66,1771-1776.

Rye, H.S., Dabora, J.M., Quesada, M.A., Mathies, R.A., Glazer, A.N., 1993, Fluorometric assay using dimeric dyes for double- and single-stranded DNA and RNA with picogram sensitivity, *Analytical Biochemistry,* 208, 1, 144-150.

Rye, H.S., Quesada, M.A., Peck, K., Mathies, R.A., Glazer, A.N., 1991, High-sensitivity two-color detection of double-stranded DNA with a confocal fluorescence gel scanner using ethidium homodimer and thiazole orange, *Nucleic Acids Research,* 19, 2, 327-333.

Shaikh, S.M.T., Seetharamappa, J., Kandagal, P.B., Manjunatha, D.H., Ashoka, S., 2007, Spectroscopic investigations on the mechanism of interaction of bioactive dye with bovine serum albumin, *Dyes and Pigments,* 74, 665-671.

Sun Y., Bi S., Song D., Qiao C., Mu D., Zhang H., 2008, Study on the interaction mechanism between DNA and the main active components in *Scutellaria baicalensis* Georgi, *Sensors Actuators B*, 129, 799–810.

Tan, W. B., Bhambhani, A., Duff, M.R., Rodger, A., Kumar, C.V., 2006, Spectroscopic identification of binding modes of anthracene probes and DNA sequence recognition, *Photochemistry and Photobiology,* 82,20-30.

Tokar, V.P., Losytskyy, M.Yu., Kovalska, V.B., Kryvorotenko, D.V., Balanda, A.O., Prokopets, V.M., Galak, M.P., Dmytruk, I.M., Yashchuk, V.M., Yarmoluk, S.M., 2006, Fluorescence of styryl dyes-DNA complexes induced by single- and two-photon excitation, *Journal of Fluoresc*ence*,* 16, 6, 783-791.

Wu, M., Wu, W., Lian, X., Lin, X., Xie, Z., 2008, Synthesis of a novel fluorescent probe and investigation on its interaction with nucleic acid and analytical application, *Spectrochimica Acta Part A,* 71, 1333-1340.

Zeena, S., George Thomas, K., 2001, Conformational switching and exciton interactions in hemicyanine-based bichromophores, *Journal of American Chemical Society,* 123, 32, 7859-7865.

Zhou, B., Qi, Z-D., Xiao, Q., Jia-Xin Dong, J-X., Zhang, Y-Z., Liu, Y., 2007, Interaction of loratadine with serum albumins studied by fluorescence quenching method, *J. Biochem. Biophys. Methods, 70, 743–74*

APPENDIX 1

^1H NMR of E2

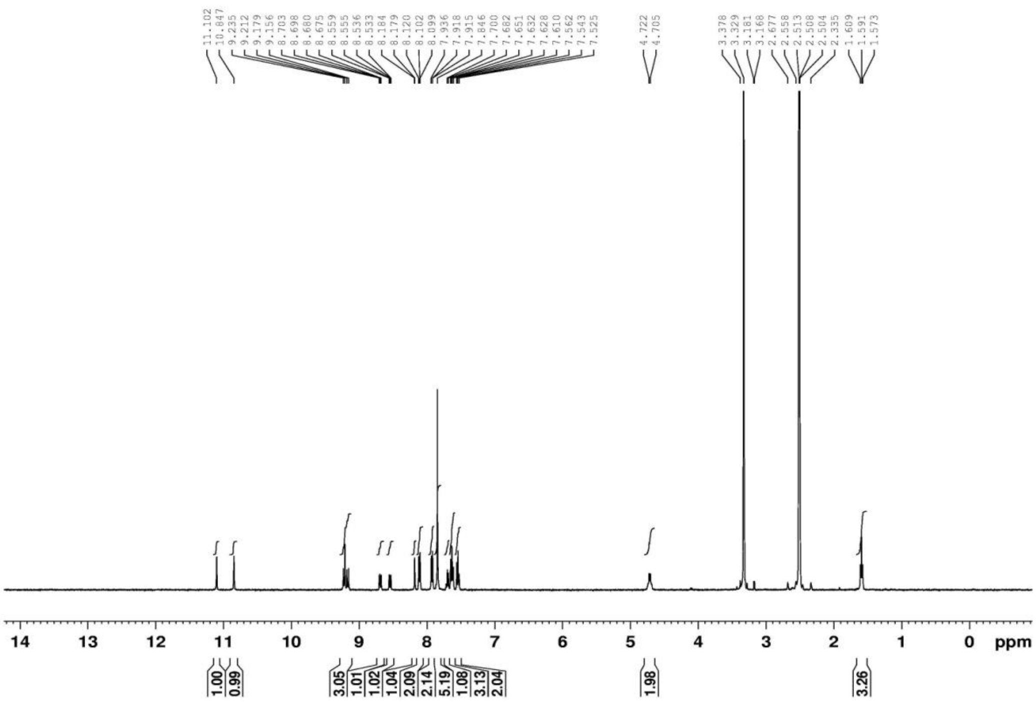

^{13}C NMR of E2

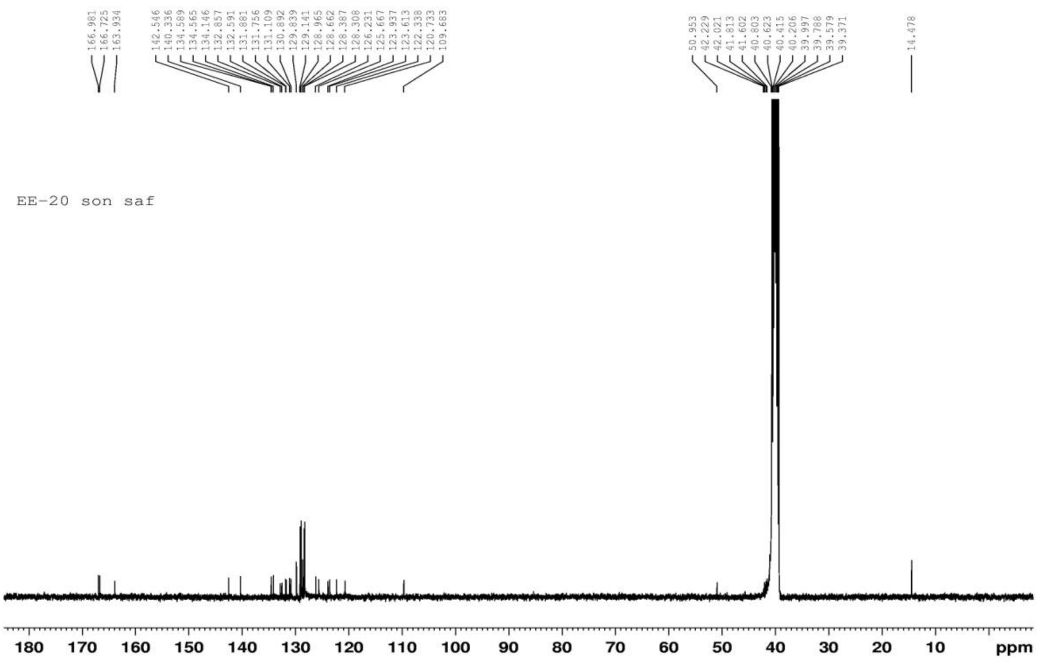

APPENDIX 2

^1H NMR of E3

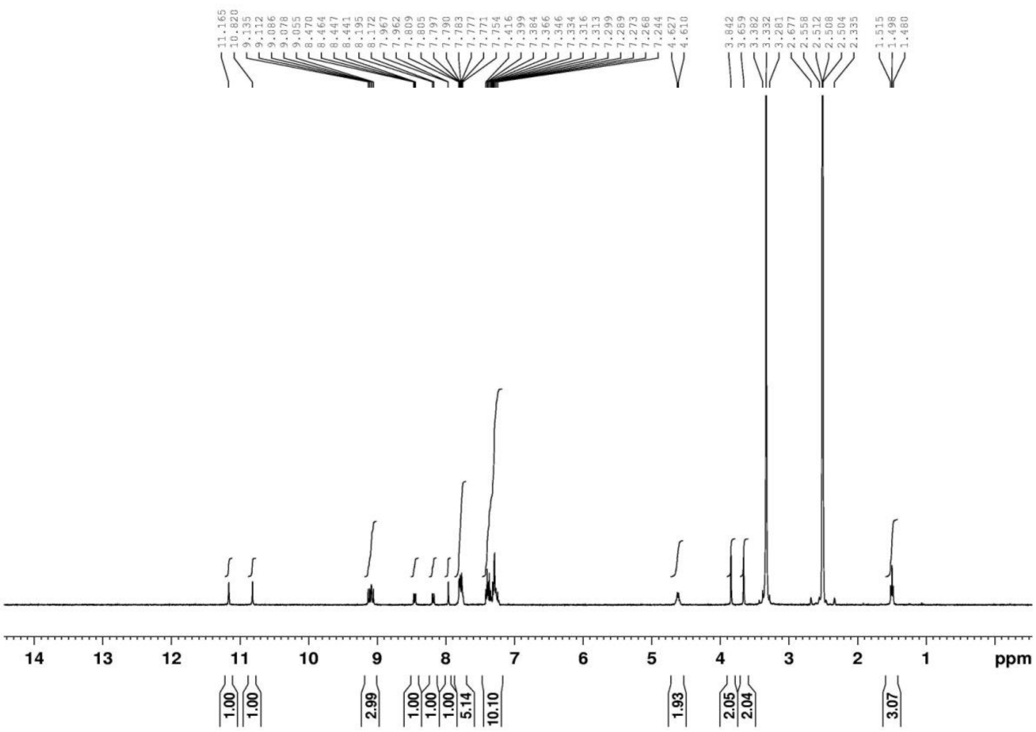

^{13}C NMR of E3

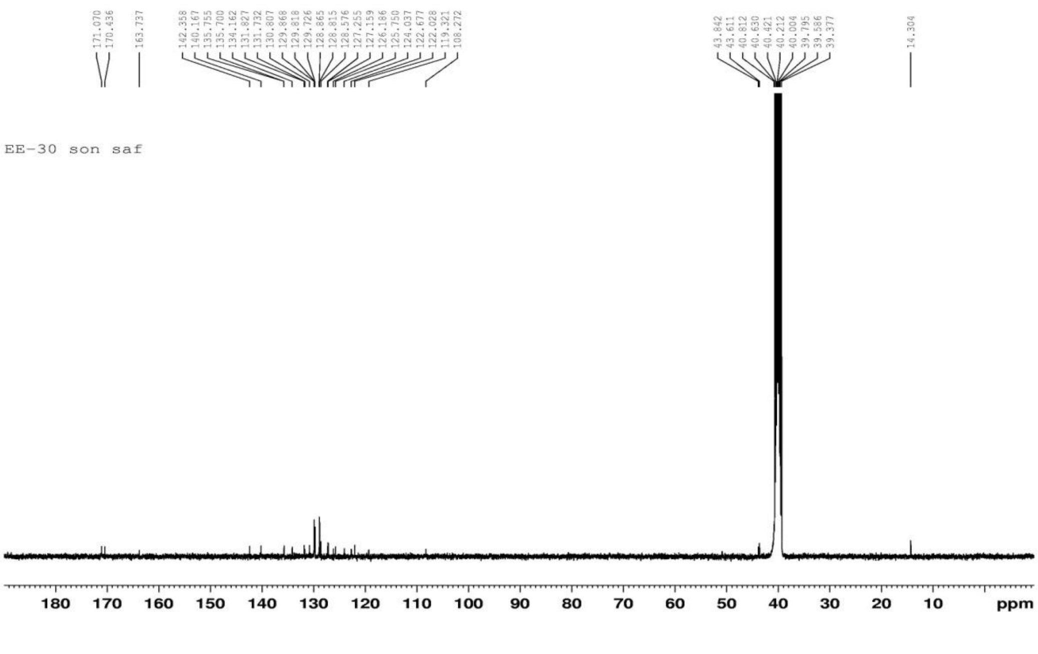

APPENDIX 3

^{1}H NMR of E4

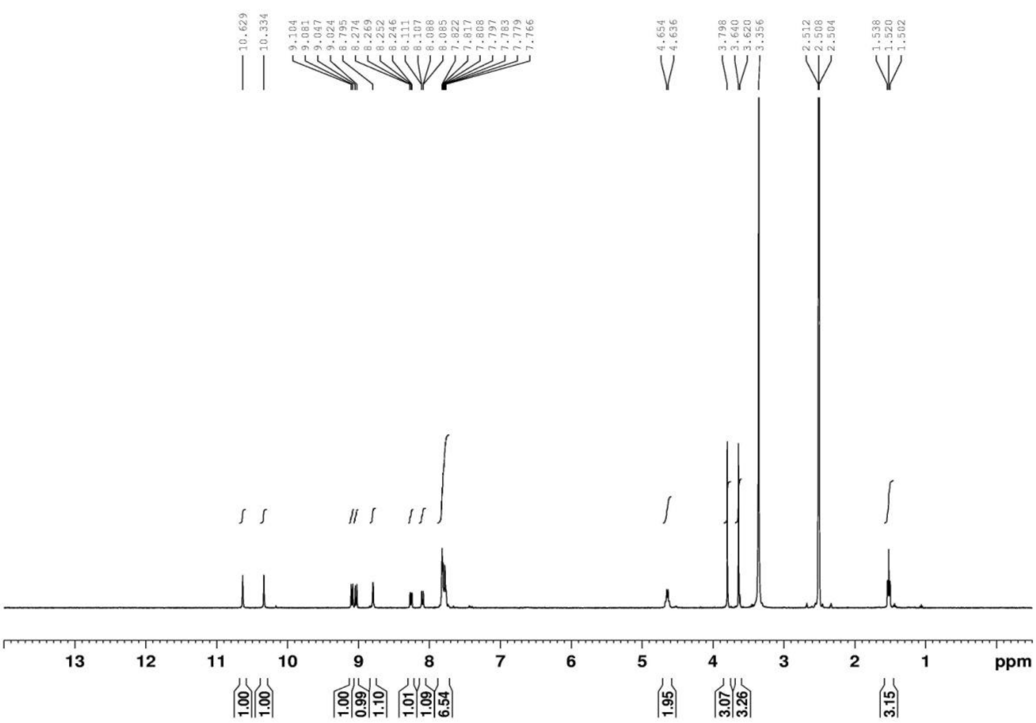

^{13}C NMR of E4

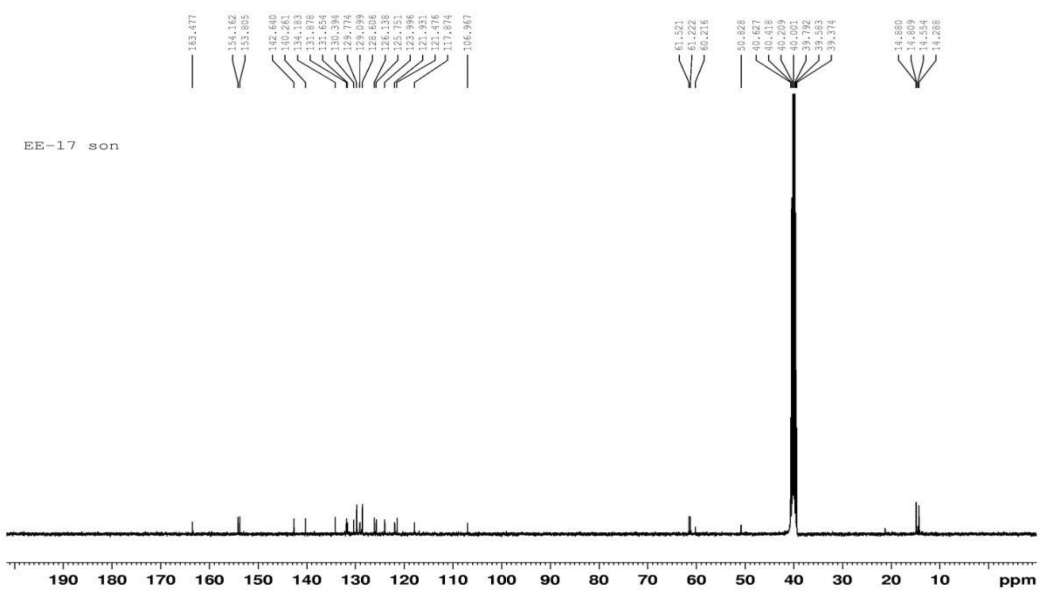

APPENDIX 4

^{1}H NMR of E5

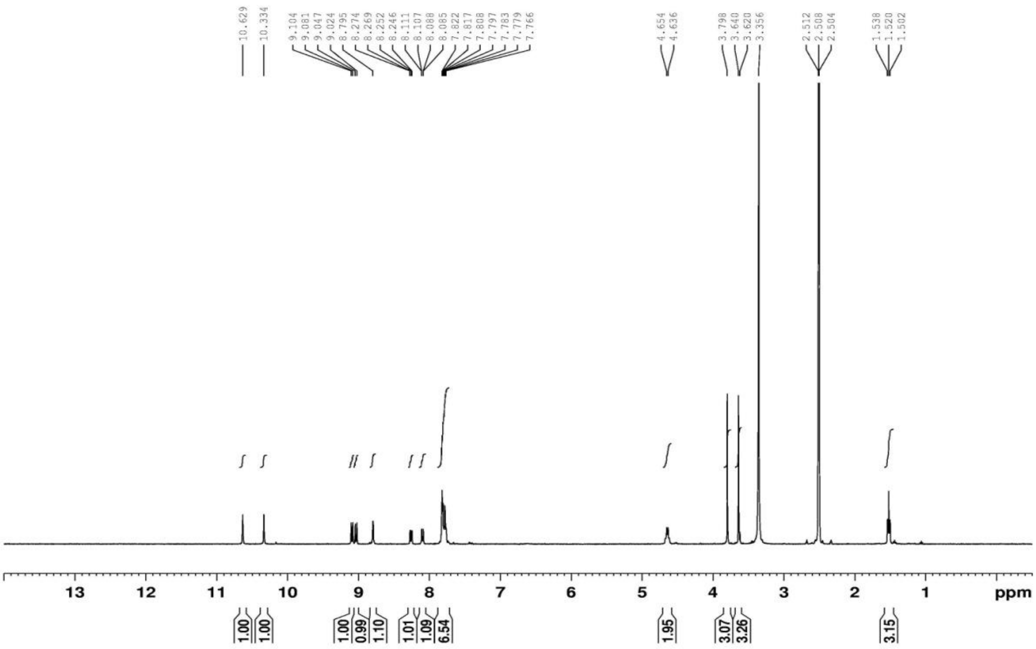

^{13}C NMR of E5

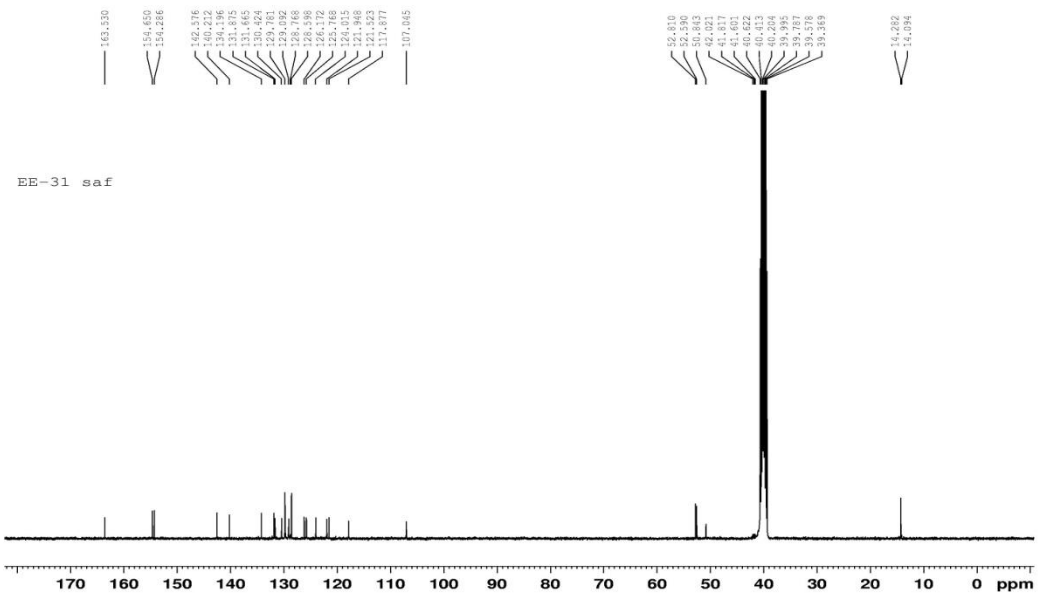

CURRICULUM VITAE

Name & Surname : NURİYE AKBAY
Place of Birth : TOKAT
Date of Birth : 10.12.1980
Marital Status : Single

Education and Academic Carrier

High School : 1993-1995 Niksar Danişment Gazi Lisesi
Under Graduate : 1995 2000 Hacettepe University, Department of Chemistry
MSc. : 2000-2003 Hacettepe University, Department of Chemistry, Analytical Chemistry Division
PhD. : 2003-2009 Hacettepe University, Department of Chemistry, Analytical Chemistry Division

Foreign Language

English

Experience at Work

1999 : Summer training, TPAO
2001- : Research Assistant, Hacettepe University, Department of Chemistry, Analytical Chemistry Division
2006 : Molecular Biology and Genetic Institute of National Academy of Sciences of Ukraine (NAS)